A MOBILE GROUND TEST RIG FOR EVALUATING SMALL-SCALE TURBOJET IN-FLIGHT PERFORMANCE AND START RELIABILITY

By

COLTON RAY SWART

Bachelor of Science in Aerospace Engineering

Bachelor of Science in Mechanical Engineering

Oklahoma State University

Stillwater, Oklahoma

2020

Submitted to the Faculty of the
Graduate College of the
Oklahoma State University
in partial fulfillment of
the requirements for
the Degree of
MASTER OF SCIENCE
May 2021

A MOBILE GROUND TEST RIG FOR EVALUATING SMALL-SCALE TURBOJET IN-FLIGHT PERFORMANCE AND START RELIABILITY

Thesis Approved:

Dr. Kurt P. Rouser

Thesis Adviser

Dr. Richard J. Gaeta

Dr. Jamey D. Jacob

ACKNOWLEDGEMENTS

First, I would like to thank God for allowing me to attend a University I have dreamt of since I was a child. I would also like to thank my wonderful mother, Patty, for representing an example of hard work, perseverance, patience, and determination, showing me what can be achieved when all are combined. Without her, this journey would have been much more difficult. I would like to thank my father, Coulter, who started teaching me at a young age how to operate tools and familiarize myself with hands-on work to help develop my use of practical knowledge. These skills were essential throughout college and paved the way for my need to understand how more things worked in this world. I would also like to thank my two sisters, Morgan, and Kaley, for motivating me and understanding my time was extremely limited while this project was being completed. I would also like to thank my Aunt, Pam, for helping me develop an attitude of gratitude and making sure I give thanks for everything that happened to me, knowing that every step was a step forward towards achieving something much larger. I would also like to thank my advisor, Dr. Kurt Rouser, for guiding me in a direction where I could thoroughly utilize my skillset in an area of engineering that I found particularly interesting. I would also like to thank my committee members, Dr. Jamey Jacob and Dr. Richard Gaeta, for providing their time and knowledge throughout this project. I want to thank the members of my senior capstone team, Lauren Jones, Thomas Coulon, Grant Schumacher, Riley Johnson, and Michael Mines, for creating such a great initial atmosphere while working around small-scale turbojet engines and helping me narrow in my field of interest. I would also like to thank Austin Stottlemyre and Kathryn Stewart for their contribution to the preliminary work with the combustion research that ultimately led to this project. Lastly, I would like to thank the Mechanical and Aerospace Engineering department for providing the facilities and resources for this project.

Acknowledgements reflect the views of the author and are not endorsed by committee members or Oklahoma State University.

Name: COLTON RAY SWART

Date of Degree: MAY 2021

Title of Study: A MOBILE GROUND TEST RIG FOR EVALUATING SMALL-SCALE TURBOJET IN-FLIGHT PERFORMANCE AND START RELIABILITY

Major Field: MECHANICAL AND AEROSPACE ENGINEERING

Abstract: This paper presents the design and analysis of a mobile ground test rig for small-scale turbojet engines to simulate in-flight start reliability for design changes aimed at increasing the performance of the engine. One of the primary goals of these efforts was focused on the desired capabilities of the test rig, such as affordability, mobility, the capability of simulating a range of conditions such as total pressure, mass flow rate, and Mach number, whilst testing the effect of different fuels and equivalence ratios. Successful engine ignition can be a difficult task when operating at flight speed and higher altitudes. Developing an engine ignition envelope for the best chance of ignition would allow pilots to know what flight speed and altitude to fly at for best operability. To understand the influence of combustion characteristics on combustor ignition, a test rig was needed to analyze these attributes. This rig utilizes the fuel distribution system and engine control unit readily available from a KingTech K-160 turbojet to reduce complexity, although the test stand is adaptable to different engines. The ground test rig incorporates a portable compressor attached to a pressure chamber to simulate a range of operating conditions by altering the total pressure and mass flow rate into the engine. While simulating these conditions, combustion was then tested with different fuels to show their effect on start reliability, fuel consumption, exhaust gas temperature, and other performance parameters. Diesel required less fuel than Jet-A and consistently produced more thrust over a range of throttle conditions. This resulted in the engine having a thermal efficiency of 12% using Diesel and 11% using Jet-A. Successful ignition occurred more frequently and most notable at leaner equivalence ratios using Diesel.

TABLE OF CONTENTS

Chapter Page

LIST OF TABLES

Table Page

LIST OF FIGURES

Figure Page

Figure Page

CHAPTER I

INTRODUCTION AND RESEARCH QUESTIONS

Introduction and Motivation

In-flight performance and start reliability of small-scale turbojet engines are limited. This paper has been written to analyze the start reliability and performance parameters of small-scale turbojets by simulating combustion operating conditions and testing different fuels and equivalence ratios. This paper will also introduce a general ground test rig design to try and adapt to a wide range of engine manufacturers for ease of simplicity and replicating the experiment. Small gas-driven engines typically have small compression pressure ratios, which negatively affect the combustion characteristics of the engine. Furthermore, a decrease in the overall performance of the engine also negatively affects the start reliability.

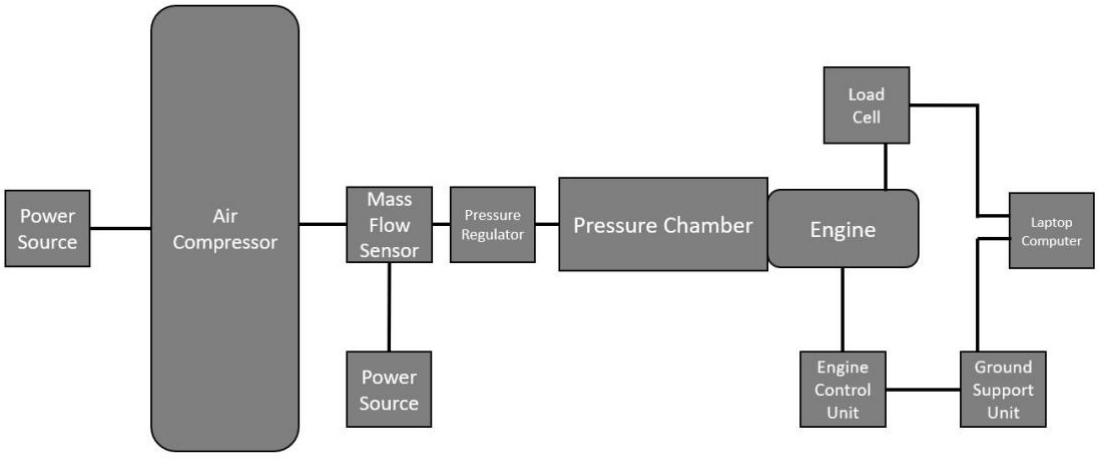

Figure 1: Ground Test Rig Component Block Diagram

This loss in performance and power from the turbine engine because of degradation of the combustor can lead to dangerous conditions like combustor blow-out, which is most likely to happen at higher altitudes during extreme maneuvers. A ground test rig, as shown by the block diagram in Fig. 1, can be created to simulate in-flight start reliability for design changes aimed at increasing the performance and durability of the engine by analyzing the changes in combustion characteristics when different fuels and fuel-air-ratios are used. These key parameters that affect combustion performance can be controlled individually to determine which elements should be altered or combined to optimize burner efficiency. Also, all airflow conditions can be controlled independently of how the combustion process might affect the turbine and subsequently the compressor. To reduce complexity and maintain a consistent measurement throughout the experiments, a ground test rig that utilized the fuel distribution system and engine control unit readily available from a small turbine engine manufacturer, as shown in Fig. 2, would be most practical. Therefore, the design of the test rig presented in this paper will specifically incorporate the use of a KingTech K-160 turbojet engine.

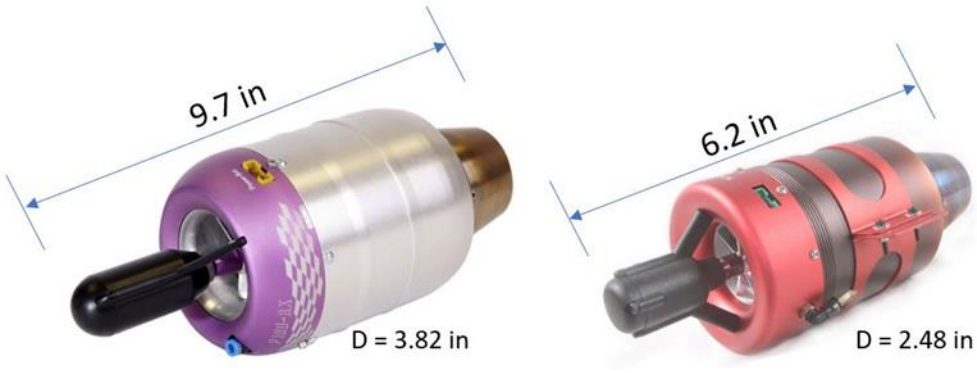

Figure 2: JetCat P100 RX (left) and KingTech K-45 (right) [5]

Although this design uses a specific make and model, the general concept of integrating a small turbine engine into a ground test rig still applies to other turbines of similar size, regardless of manufacturer. Turbine engines on this scale typically have compressor pressure ratios ranging from 1.5 to 4, with the compression ratio of the K-160 at 3.4. To understand how airflow is

affected through the different components of an engine, a parametric cycle analysis (PCA) is commonly used in aircraft engine design to study the thermodynamic changes of the air as it moves through these components. The inputs of a PCA analysis, which will be performed in this paper, include engine specifications given by the manufacturer, gaseous properties of air, and assumptions about component efficiencies, which are based on similar engines and level of technology (LOT). Understanding combustion theory is also critical to know which key parameters affect combustion characteristics and how they influence the data obtained from any numerical or analytical analysis. Many factors contribute to how well the combustion process takes place, such as the type of fuel injection used, how well the fuel atomizes and vaporizes, and the execution of the mixing of fuel and air. This ratio impacts how well the flame holds in the combustion chamber. Based on this equivalence ratio and the temperature of the atmosphere, there are three significant regions of flammability, which are flammable mist, flammable vapor, and spontaneous ignition, the last area, being the lowest temperature at which visible or audible evidence of combustion is observed. When the combustion process can sustain itself, it is considered stable. There are also additional parameters that affect this combustion stability; these are lumped into what is called the combustor loading parameter (CLP). The magnitude of the effect these parameters implore is also determined by the type of burner used in the engine. For most small-scale turbojet engines, an annular combustor is used, which is true of that of the K-160.

To evaluate the start reliability given different combustion operating conditions, a system needs to be designed to simulate in-flight speeds to adjust the total pressure. This can be done by placing a device on the exit of the engine to essentially suck air through the turbojet or by connecting a pressurized device to the inlet of the engine to push air through it. Each option has unique advantages and disadvantages, and these will be discussed later. Figure 3 illustrates a

mobile test rig setup that incorporates a pressurized device to push air through the engine, like what is presented in this paper.

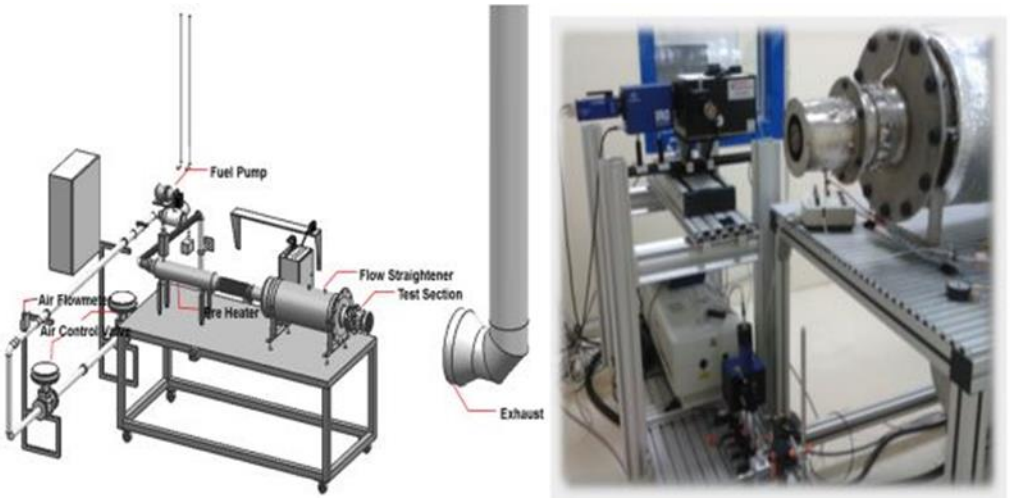

Figure 3: Combustor Test Rig Set-up [3]

A dimensional analysis identifies correlating parameters that allow data taken under one set of conditions to be extended to other conditions. With aircraft gas turbine engines, these correlating parameters result in what is commonly known as corrected performance and are derived in a manner that makes sense physically [6]. This will be particularly important for the analysis performed in this paper to ensure any irregularities or changes in data are not due to the procedure in the study itself but instead resulting from the changes in the operating conditions. Finally, utilizing this system to simulate operating conditions, combustion would then be tested with several fuels and different fuel-air ratios to show their effect on start reliability, fuel consumption, thrust specific fuel consumption, exhaust gas temperature, and specific thrust. Combustor loading parameter can be obtained from the collection of data to effectively map the start reliability and operability of the small turbine engine.

Research Questions and Objectives

The research questions are as follow:

1. What is a practical method to simulate in-flight operating conditions for combustion research?
2. Given a range of operating conditions, what effect do different fuels and equivalence ratios have on the in-flight start reliability of the turbine engine?
3. Given a range of operating conditions, what effect do different fuels have on the performance of the turbine engine?

***Objective 1:* Design and evaluate a ground test rig to simulate in-flight operating conditions.** This objective will be critical to complete to even attempt the following two objectives. Although this paper is not focused on the design and analysis of the ground test rig itself, the apparatus serves as a critical tool to simulate in-flight and ground speed operating conditions and evaluating the performance of the turbine. To do this, previous research will be studied to determine an effective and efficient way of implementing a small-scale turbine engine into the ground test rig. The test rig will focus on a design that is feasible, mobile, and convenient to use with similar gas-powered turbine engines.

***Objective 2:* Evaluate the effect of fuel-to-air ratio and fuel type on in-flight start reliability of a turbine engine.** While the turbine engine is plumbed to the ground test rig to simulate operating conditions, different fuels and equivalence ratios will be tested independently and analyzed to determine how the design changes affect the in-flight start reliability of the engine. By plotting and analyzing this data, an optimized ignition map can be determined for a range of in-flight operating conditions, fuel type, and ignition fuel-to-air ratio.

***Objective 3:* Evaluate the effect of fuel type on the in-flight performance of a turbine engine.** Again, with the turbine engine plumbed to the ground test rig to simulate operating conditions, different fuels will be tested and analyzed to evaluate how they affect the performance of the

turbine engine. One of the main benefits of using a small-scale turbine engine to analyze combustion characteristics is the ability to use the current instrument devices within the engine, like pitot tubes and thermal couples, to measure pressures and temperatures, respectively. Furthermore, these engines also come with user-friendly software that simplifies the operation of the engine, provides accessibility and ease of modification to the fuel consumption delivery system, and displays functional and precise readings of the data obtained from the instrumentation.

CHAPTER II

BACKGROUND AND THEORY, REVIEW OF LITERATURE, AND PRELIMINARY STUDIES

Background and Theory

Aircraft Gas Turbine Engines

It is vital to discuss airbreathing engines to understand the benefits of using a turbojet engine for combustion research. Fundamentally, the thrust produced from any gas turbine engine (turbojet, turbofan, turboprop, or turboshaft) or a ramjet/scramjet is the result of accelerating an air mass as efficiently as possible to meet the aircraft-engine system mission needs [6]. An ideal Brayton Cycle can be used to illustrate how pressure changes as a function of temperature and entropy as the air flows through the components of the engine, shown by Fig. 4. The central portion of a gas turbine engine is the gas generator, also known as the core. The primary purpose of the core of the engine is to supply high-temperature and high-pressure gas. Three major components of the engine are located in the core, the compressor, combustor, and turbine. As air flows into the inlet of the engine, it passes through the compressor, where the temperature and pressure are increased significantly to prepare the flow for combustion. Following the compressor, the air enters the combustor and undergoes a chemical reaction with a hydrocarbon fuel. This reaction causes a substantial increase in energy in the form of temperature while maintaining a constant total pressure. Finally, this high-energy gas is expanded through the turbine, which supplies power to drive the engine compressor and other auxiliary units on the

aircraft. How the engine cycles differentiate is determined by what the remaining energy is used for.

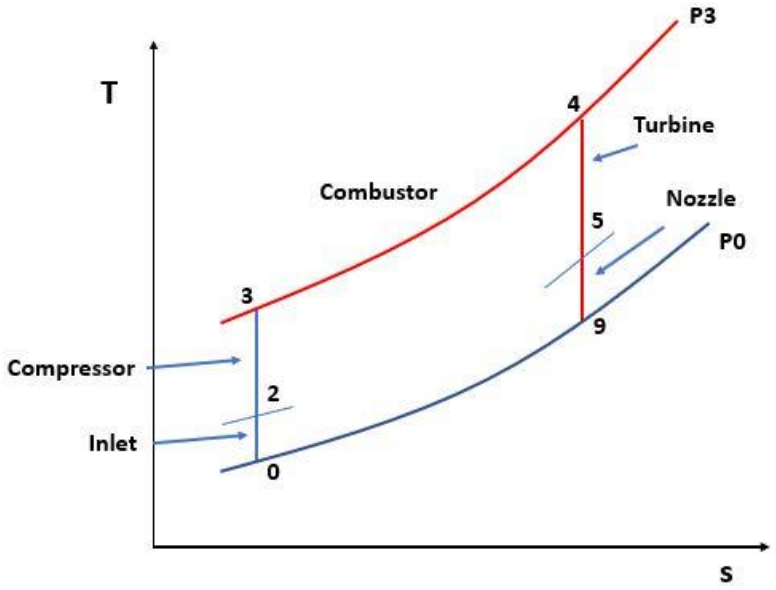

Figure 4: Ideal Brayton Cycle

A turbojet is most commonly recognized for its capability of producing large amounts of thrust, which is done by adding an inlet and nozzle to the gas generator. The excess energy that was expanded through the turbine is now accelerated through a nozzle to achieve high exhaust gas velocities. Furthermore, if even larger amounts of the thrust are needed, an afterburner (essentially a second combustor) can be added between the core turbine and the nozzle to reheat the exhaust gases and produce more energy. The first operational turbojet to be used as a means of aircraft propulsion was patented in 1936 by Sir Frank Whittle [10]. These engines are typically compact in size and simple in their overall layout, creating a high thrust-to-weight ratio. Because of this, small-size turbojet engines are becoming attractive for their ability to be incorporated into remote-control airplanes and unmanned aerial vehicles [9]. A turbofan engine takes some of the excess gas energy exiting the core turbine (HPT) and further expands it against a low-pressure turbine to drive a fan and often a low-pressure compressor (LPC) or booster [6]. A large amount of air is moved through the fan, which increases the propulsive efficiency; however, due to the

large inlet enclosure, this efficiency is partially offset by drag [12]. The ratio of air pushed through the fan and the core is called the bypass ratio. A low-bypass turbofan takes on performance characteristics more similar to those of a turbojet, whereas a high-bypass turbofan takes on performance characteristics more similar to those of a turboprop [6]. A turboprop engine has a power turbine instead of a nozzle, which typically drives a propeller [13]. This propeller provides most of the propulsive thrust needed by the aircraft. Very similar to the turboprop is the turboshaft, but instead, a shaft is powered by the turbine rather than a propeller. Advantages of the turboprop and turboshaft are their ability to produce a lot of thrust efficiently at low-speed conditions but are limited to high flight speeds. Finally, ramjet and scramjet engines contain an inlet, combustor, and nozzle. These engines do not have a compressor or turbine and rely on high flight speeds to compress the incoming air. The air is then mixed with fuel, burned, and the exhaust gas is accelerated through the nozzle. To study combustion characteristics, not only would the most straightforward engine cycle be beneficial, but the engine should have the capability of operating in many flight conditions, characterized by an extensive range of flight speeds and altitudes, which is why a turbojet is the most practical engine cycle to use.

Combustion Theory

The purpose of the combustion systems of aircraft gas turbine engines is to increase the thermal energy of a flowing gas stream by combustion [7]. Most of the reaction takes place in what is known as the primary zone of the combustor. In this zone, the injected fuel is atomized, partially or entirely vaporized, and then mixed into the primary air that enters through the diffuser; this process is shown in Fig. 5. As these gases burn, some of the excess gas is recirculated into the fresh reactants, which allows for a continuous self-ignition process called flame holding [7]. Typically, a spark plug or some external device is used to initiate the flame holding process; however, once the self-ignition process has started, this external ignition device is no longer needed. These high temperatures dictate how much energy the turbine can extract

from the combustion process but also determines the design of the combustor due to limitations in material properties. The increased operating temperatures and the increased compression ratios have provided jet engines with improved performance and specific fuel consumption figures [14]. This mixture of partially mixed and actively burned gas continues into the secondary or intermediate zone. Two main processes must happen in this zone for the combustion process to be complete by the time it enters the dilution zone. The primary zone effluent gasses must continue to burn out, and the in-mixing secondary air must reduce the fuel-air ratio of the liner gas stream [7]. Finally, to avoid hot spots forming on the first-stage high-pressure turbine stator, the remaining annulus airflow is dumped through the dilution holes into the liner hot gas stream to promote more stirring. These gases are accelerated through a converging transition duct until they reach the first-stage high-pressure turbine stator.

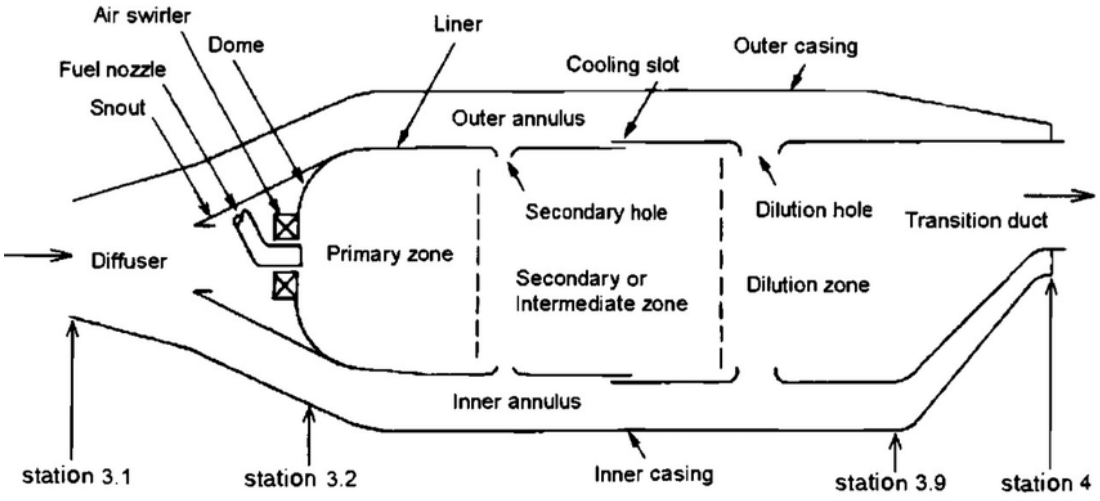

Figure 5: Main Features and Flow Patterns of the Main Burner [6]

Under most operating conditions, the rate of combustion is limited by the rate at which the fuel is vaporized and mixed with air [6]. Equivalence ratio, ø is defined as the actual fuel/air ratio (f) divided by the theoretical fuel/air ratio (f_{stoich}) required for complete combustion [15]. This term is calculated using Eq. (1). The equivalence ratio ø is greater than 1.0 for a rich fuel/air ratio and less than 1.0 for a lean fuel/air mixture [6]. For combustion to maintain a stationary flame within

a high-velocity airstream, the flame velocity needs to propagate around the same speed as the combustible mixture. If the velocity of the flame is too high, the flame will "blow out," ending the combustion process. If the flame velocity is too slow, the flame will travel upstream and be extinguished. Flame holders, which are typically located at the front of the main burner or afterburner, are used to establish recirculation to hold the combustion flame. These regions of recirculation create areas of local low velocity that "hold" the flame, and at the same time, the resulting turbulence gently increases the rate of energy transfer from these regions [6].

$$ø = \frac{f}{f_{stoich}} \tag{1}$$

Before the combustion process can take place, a source of ignition needs to be initiated. The flammability characteristics of the fuel type used are a function of the temperature in the combustor and the equivalence ratio. Generally, three main zones dictate the type of flame present in the combustor, which is: a flammable mist, flammable vapor, and spontaneous ignition. The spontaneous ignition temperature (SIT) is the lowest temperature at which visible or audible evidence of combustion is observed [6]. When the temperature in the combustion system is below the SIT, an ignition source is required to bring the local temperature above the spontaneous ignition temperature [16, 17].

If the fuel-to-air ratio becomes too lean or rich, causing the temperatures and reaction rates to drop below the level necessary to heat and vaporize effectively, the flame will not remain stable. The ability of the combustion process to sustain itself continuously is called combustion stability [6]. The volume of the combustion zones, the mass flow rate of the fuel/air mixture, and pressure directly affect the stability of the combustion process. These effects are combined into a term called the combustor loading parameter (CLP), defined by Eq. (2), where n is an experimentally calculated value of 1.8 based on a complex set of reactions occurring when a hydrocarbon is burned in air.

$$CLP = \frac{\dot{m}}{P^n(combustion\ volume)} \tag{2}$$

Figure 6 illustrates the combustion stability characteristics as a function of the combustor loading parameter and equivalence ratio and shows the unstable and stable operational regions. The method of presenting the stability characteristics of a combustion process for a gas turbine engine is based on stirred reactor theory [6, 17, 18, 19, 20].

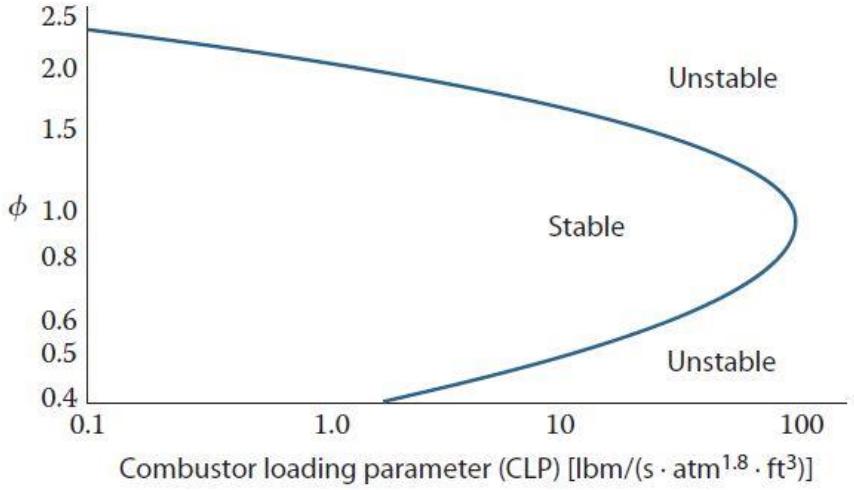

Figure 6: Combustion Stability Characteristics [16]

The main burner design is generally classified into three types: can, cannular, or annular. Most modern main burner systems employ the annular design where there is a single burner or combustion zone [6]. A can system utilizes several cylindrical burners, each in its own casing. A cannular design uses cylindrical burners, but they are arranged with a common annulus. An annular system can provide high combustion efficiency at a high combustion loading parameter while incorporating a shorter burner, reduced linear surface area, and simpler design. These characteristics make it very dominant in maximizing the thrust-to-weight ratio of propulsion systems [22].

Finally, the combustion process also has a direct effect on the performance of the aircraft. Combustion efficiency η_b is related to the propulsion system fuel consumption, which determines

the aircraft system range, payload, and operating cost [6]. Optimizing this metric to reach as close as possible to 100% is essential to minimize fuel consumption and adhere to chemical emission controls and limitations. Combustion efficiency is only slightly dependent on fuel chemistry but is strongly influenced by the physical fuel properties that govern atomization quality and spray evaporation rates [23]. An empirical model can be used for combustion efficiency based on the reaction rate parameter θ, shown by Fig. 7.

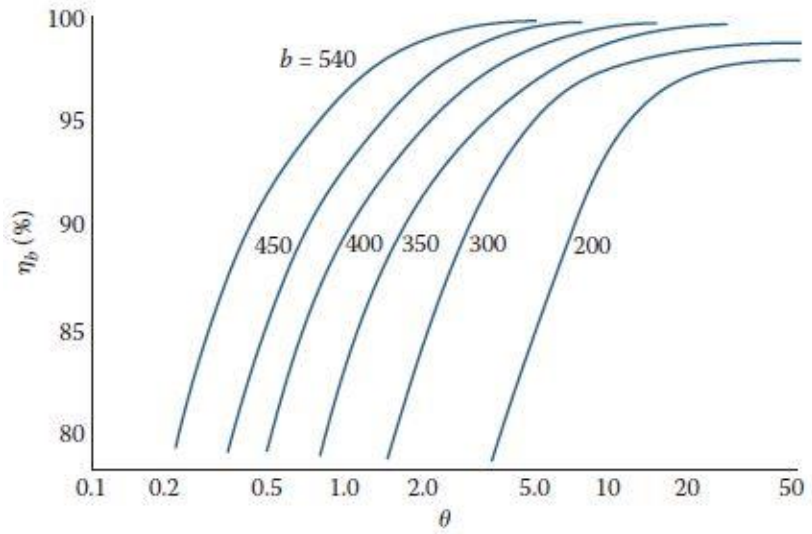

Figure 7: Combustion Efficiency vs. Reaction Rate Parameter [6]

This reaction rate is shown by Eq. (3), where P_{t3} is the main burner inlet pressure in psi, A_{ref} is the main burner reference area in in.^{2}, H is the height of the main burner in inches, T_{t3} is the main burner inlet temperature in °R, m_3 is the main burner inlet airflow in lbm/s, and b is a function of local equivalence ratio and b [6], given by Herbert [24] as Eq. (4).

$$\theta = \frac{{P_{t3}}^{1.75} A_{ref} H \exp\left(\frac{T_{t3}}{b}\right)}{\dot{m}_3} \times 10^{-5} \tag{3}$$

$$b = 382\left(\sqrt{2} \pm \ln\frac{\emptyset}{1.03}\right) \tag{4}$$

Where plus is used when ø < 1.03 and minus when ø > 1.03.

Simulating Engine Operating Conditions

To determine which parameters have the most effect on combustion performance, it is important to understand the influence that flight speed and altitude can have on these parameters as well. Engine performance varies depending on the location and operating conditions present. These changes are almost always due to differences in total pressure from the incoming air that the engine receives. This is caused by either static pressure that is directly related to the atmospheric conditions or from the dynamic pressure, which is related to the flight speed the aircraft is experiencing. Figure 8 illustrates a plot of atmospheric pressure vs. altitude.

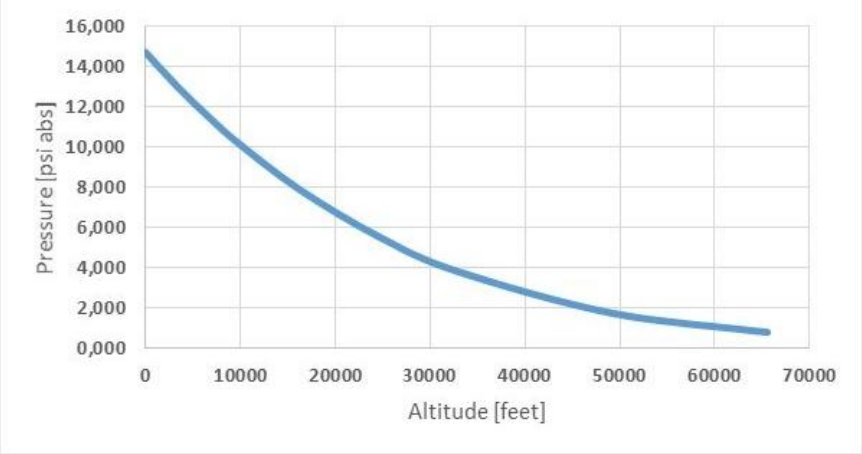

Figure 8: Atmospheric Pressure Given Altitude

Based on these operating conditions, a total pressure value is perceived by the inlet of the engine. Therefore, the total pressure entering the combustor is a function of the freestream Mach number and the ambient static pressure given an assumption about gamma or the ratio of specific heats. Compressible flow point relationships [25] give total to static property ratios based on the Mach number. Combined with US Standard Atmosphere data, the total properties can be determined [1], given by Eq. (5).

$$P_t = P_{atm}\left(1 + \frac{\gamma-1}{2}M^2\right)^{\frac{\gamma}{\gamma-1}} \tag{5}$$

Equation 5 can be used to develop operating conditions to test combustion performance. The Korea Aerospace Research Institute's (KARI) [26] Altitude Engine Test Facility features air supply and exhaust systems along with data acquisition systems to test total pressures both above and below ambient conditions. For simulated total pressures above ambient conditions, compressors would supply air, and for simulated total pressures below ambient conditions, a scavenging system would be used to create a negative pressure gradient through the engine. KARI's system also implemented equipment to dry the air, cool and heat the air, and flow straightening devices to prepare the flow for testing. Although these devices are important, they are costly and reduce the mobility of the testing apparatus. The most cost-effective design must be able to simulate flight conditions without requiring excessive equipment or power [1, 27].

Since many different operating conditions will be tested throughout this experiment, a dimensional analysis will need to be used to identify correlating parameters and validate experimental data. For gas turbine engines, these correlating parameters are commonly known as corrected performance and are derived in a manner that makes physical sense [6]. The quantities of pressure and temperature are normally made dimensionless by dividing each of its respective standard sea-level static conditions. The dimensionless pressure and temperature are represented by δ and θ, respectively, and given in Equations 6 and 7.

$$\delta_i \equiv \frac{P_{ti}}{P_{ref}} \tag{6}$$

$$\theta_i \equiv \frac{T_{ti}}{T_{ref}} \tag{7}$$

Where P_{ref} = 14.696 psia and T_{ref} = 518.69°R

Finally, the corrected mass flow rate at the engine station *i* used in this analysis is defined as

$$\dot{m}_{ci} \equiv \frac{\dot{m}_i\sqrt{\theta_i}}{\delta_i} \tag{8}$$

For example, if an operating condition of an altitude of 20,000 feet and a flight speed of Mach 0.8 wanted to be simulated, Eq. (5) could be used to calculate the total pressure from those conditions. Then, while keeping total pressure constant, given the desired location that would govern the static pressure, this condition could be tested with the correct Mach number. Furthermore, experimental data received from the performance parameters could be checked against standard corrected parameters for those conditions to analyze how they compare.

Variables That Affect Combustion Start Reliability

It is often necessary to start turbojet engines at altitude after combustion blow-out has occurred or when some of the engines of a multiengine aircraft have been inoperative during cruise [28]. It is more difficult to start a turbojet engine at a high altitude due to having lower pressures and temperatures in the combustor and a poor fuel spray, which makes ignition and flame propagation more difficult to achieve. Furthermore, as altitude increases, air density decreases. This means after an engine blow-out has occurred, there is less energy from the incoming air to accelerate the engine and counter the constant inertia of the accelerating components. The three main factors controlling the rate of acceleration are compressor surge and stall, combustion blow-out, and the maximum allowable turbine-inlet temperature. Successful acceleration is accomplished by adding fuel in such a manner that the compressor-turbine combination speeds up in a minimum time without exceeding the maximum allowable turbine temperature [29]. Since this process now requires a higher mass flow rate of fuel, it has a direct negative effect on the thrust specific fuel consumption. Once the engine has lost thrust, the aircraft substantially decreases in-flight speed due to drag. This scenario could be simulated by having a chamber in front of the engine that is pressurized to a desired total pressure while the engine is operating and then shutting off the engine to analyze the decrease in total pressure from the reduction in dynamic pressure. The reduction in the dynamic pressure would simulate the loss in flight speed.

The reliability of an ignition system can be evaluated at a particular flight condition by consideration of the time required to obtain initial ignition and the number of successful starts obtained with respect to the total number of attempts made [28]. In the early development of gas turbines, it was widely believed that these engines could operate using any type of fuel, with the assumption that higher volatility fuels would ignite more quickly. Although true in theory, modern turbojets today have high fuel flow rates with wide temperature and pressure variations, which require specific characteristics in the fuel [6]. The rate of evaporation of a fuel spray increases with an increase in fuel volatility. Hence, it would be expected that lower starting fuel flows and ignition energies would be required for fuels of high volatility [29]. On the contrary, the volatility of a multicomponent fuel of the type used commercially is not easily defined; consequently, the fuel properties most frequently used to define volatility have not produced completely satisfactory correlations of engine starting data. JP-8 is the most commonly used fuel for U.S. Air Force jet engines due to its high volatility. The U.S. Navy uses JP-5, a denser, less volatile fuel than JP-8. The most common commercial aircraft fuels are Jet-A and Jet A-1 [7]. Each of these fuels also incorporates additives to inhibit fuel system icing, prevent corrosion and improve lubricity, and avoid a buildup of static charge [6]. Some data also establishes the importance of fuel atomization in the combustion process. This data indicates that the vaporization of the fuel may play a rate-determining role. The differences in fuel atomization resulting from the use of different injection nozzles may serve primarily to altering the combustor volume zone [30]. This statement is important because a major assumption in combustion theory regarding parameters that affect combustion start reliability is that the volume of the reaction zone does not change with a change in operating conditions.

Engine Performance Parameters

A parametric cycle analysis (PCA) determines the performance of engines at different values of design choice (e.g., compressor pressure ratio), component performance (e.g., turbine

efficiency), and design limit (e.g., combustor exit temperature) parameters [6]. It is commonly used in aircraft engine design to study the thermodynamic changes of air as it moves between each component within the engine. The main goal of performing a PCA is to evaluate how changes in design choices and design limitations relate to engine performance parameters like specific thrust and thrust specific fuel consumption for a given operating condition. A PCA can be performed for ideal and real situations, with a real analysis incorporating component losses and a variety of specific heats in the engine cycle. For purposes of this study, a PCA for a real engine will be performed. The station numbering for a single-spool turbojet cycle analysis with no afterburner is in accordance with Aerospace Recommended Practice (ARP) 755A [31] and is given in Fig. 9.

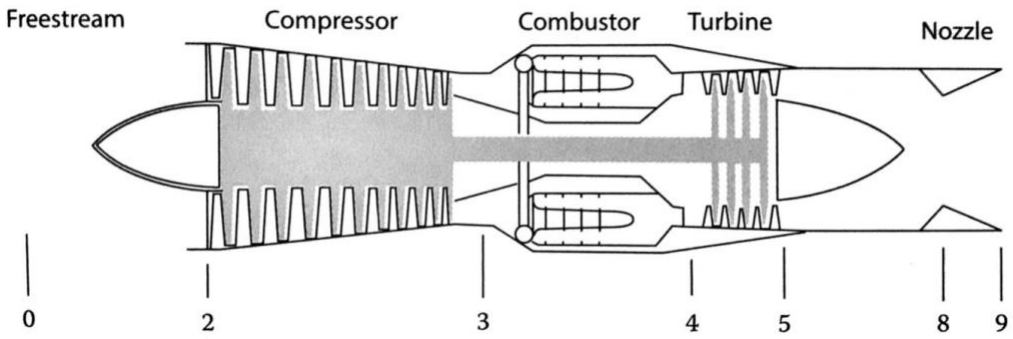

Figure 9: Turbojet Engine Station Numbering [6]

Assumptions of a parametric cycle analysis are as follows [6, 32]:

1. Perfect gas upstream of the main burner with constant properties γ_c, R_c, c_{pc}, and so on.
2. Perfect gas downstream of the main burner with constant properties γ_t, R_t, c_{pt}, and so on.
3. All components are adiabatic.
4. The efficiencies of the turbomachinery-compressor(s), turbine(s), fan- are described through the use of constant polytropic efficiencies e_c, e_t, and e_f, respectively.
5. No cooling or bleed flows.

The analysis assumes 1-D steady flow at the entrance and exit of each component. The steps of the cycle analysis follow closely as described in Mattingly [6].

Step 1: For uninstalled thrust, which means a static thrust test is performed, mitigating the effects of the engine inlet,

$$\frac{F}{\dot{m}_0} = \frac{a_0}{g_c}\left(\frac{\dot{m}_9}{\dot{m}_0}\frac{V_9}{a_0} - M_0\right) + \frac{A_9 P_9}{\dot{m}_9}\left(1 - \frac{P_0}{P_9}\right) \tag{9}$$

$$\frac{\dot{m}_9}{\dot{m}_0} = 1 + f \tag{9.1}$$

After applying gas property relationships with their appropriate subscripts for engine stations 0 to 9, Eq. (9) becomes

$$\frac{F}{\dot{m}_0} = \frac{a_0}{g_c}\left((1+f)\frac{V_9}{a_0} - M_0\right) + (1+f)\frac{R_t}{R_c}\frac{T_9/T_0}{V_9/a_0}\frac{1 - P_0/P_9}{\gamma_c} \tag{9.2}$$

Step 2: For the turbojet cycle,

$$\left(\frac{V_9}{a_0}\right)^2 = \frac{\gamma_t R_t T_9}{\gamma_c R_c T_0} {M_9}^2 \tag{9.3}$$

Step 3: We have

$${M_9}^2 = \frac{2}{\gamma_t}\left[\left(\frac{P_{t9}}{P_9}\right)^{(\gamma_t - 1)/\gamma_t} - 1\right] \tag{9.4}$$

Step 4: We have

$$\frac{T_9}{T_0} = \frac{T_{t9}/T_0}{(P_{t9}/P_9)^{(\gamma t - 1)/\gamma t}} \tag{9.5}$$

Step 5: Application of the first law of thermodynamics to the burner solves for fuel/air ratio and gives

$$f = \frac{h_{t4} - h_{t3}}{\eta_b h_{PR} - h_{t4}} \tag{9.6}$$

Step 6: Using a power balance, power into compressor = net power from the turbine

$$\dot{m}_0 c_{pc}(T_{t3} - T_{t2}) = \eta_m \dot{m}_4 c_{pt}(T_{t4} - T_{t5}) \tag{9.7}$$

Step 7: The equation for thrust specific fuel consumption is

$$S = \frac{f}{F/\dot{m}_0} \tag{9.8}$$

Step 8: Propulsive efficiency η_P is the ratio of the aircraft power to the power out of the engine. Thermal efficiency η_{Th} is the net rate of organized energy out of the engine divided by the rate of

thermal energy available from the fuel in the engine. From the definitions of propulsive and thermal efficiency, one can show that for the turbojet engine,

$$\eta_P = \frac{2g_c V_0 (F/\dot{m}_0)}{{a_0}^2[(1+f)\left(\frac{V_0}{a_0}\right)^2 - {M_0}^2]} \tag{9.9}$$

and

$$\eta_{TH} = \frac{{a_0}^2[(1+f)\left(\frac{V_9}{a_0}\right)^2 - {M_0}^2]}{2g_c f h_{PR}} \tag{9.10}$$

Given design choices and solving these equations with the correct assumptions, engine performance parameters can be analyzed. Furthermore, an optimized exit velocity can be obtained from the analysis to determine physical dimensions like exit area by using mass flow parameter (MFP). MFP is a function of total temperature, total pressure, Mach number, the ratio of specific heats, and the mass flow per unit area in the flow of a calorically perfect gas. Eq. (10) gives the equation for MFP. Given the exit velocity and an assumption for the ratio of specific heats, one could solve this parameter. Then, one way of simulating a range of altitudes would be to keep the total temperature and mass flow rate constant and varying the exit area to change the total pressure.

$$MFP(M) = \frac{\dot{m}}{A}\frac{\sqrt{T_t}}{P_t} = \sqrt{\frac{\gamma g_c}{R}} M \left(1 + \frac{\gamma - 1}{2} M^2\right)^{-\frac{\gamma+1}{2(\gamma-1)}} \tag{10}$$

Review of Literature

N. Lucido et al. [1] designed a system to simulate flight conditions with a total pressure of less than 14.7 psi. This was done by using a second turbojet engine to suck the air through the main engine essentially. By doing this, it created an adverse pressure gradient through the system, simulating flight conditions below standard atmospheric pressure. The values of the pressures tested could be varied by changing the RPM of the second engine, with higher values sucking larger quantities of air through the system, causing a larger delta in pressure. However, the design was limited to conditions less than standard atmospheric pressure. It was noted that to simulate flight conditions higher than 14.7 psi, the system would need to incorporate a device to pressurize

the inlet of the engine to push air through the system. Figure 10 illustrates how these flight conditions could be simulated. This figure shows a plot of constant total pressures with varying dynamic pressures as shown in the legend, with the y-axis referencing altitude and the x-axis referencing the flight speed, or Mach number. The equation projected on the plot represents total pressure as a function of the Mach number. Given the desired altitude and Mach number, one could find the corresponding total pressure for that condition. This device could be transported to locations with different atmospheric conditions to simulate flight speeds and altitudes, with these conditions changing at the inlet of the main engine.

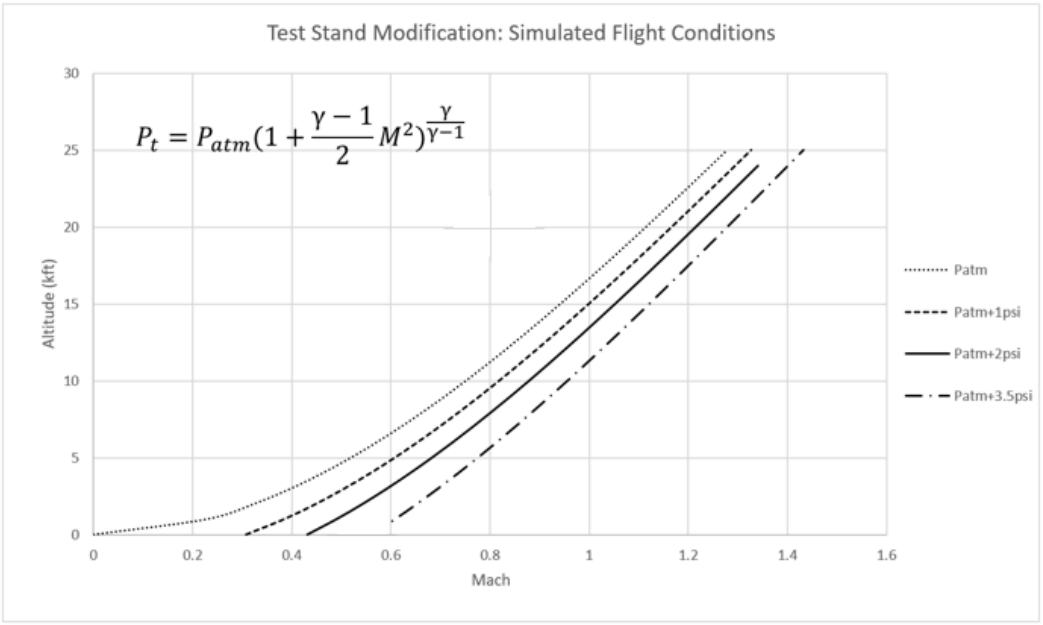

Figure 10: Simulated Flight Conditions [4]

Cooper and Dingle [2] analyzed and designed an afterburner for a small-scale turbine engine. Using flame holder stability parameters and blockage ratio, they determined what a stable flame would be for their system. Then, having already decided to use a hypodermic needle for injection, they utilized a customized form of Bernoulli's equation to determine adequate fuel pressure. Their result showed that although they achieved stable combustion, it did not have an even fuel distribution or even atomization, and their system tended to eject unspent fuel when operated wet, illustrated by Fig. 11. They conclude that while their initial design was not what

they desired it to be, they had the tools to progress with their research. Additionally, they stated that while they had some success with using necessary analyses to determine their system parameters, there was a certain amount of uncertainty in those estimations such that they did not adequately reflect the system once assembled. While burner design was the focus of their work, it shows the complexity surrounding combustion design itself and why integrating a fully working combustor from a small-scale turbojet can be beneficial to combustion research by saving a lot of time and cost. It was also noted in the paper that they mentioned that a key feature that might have improved their design was having the ability to control the preheat of the fuel before the atomization stage started, which, again, current small-scale turbines are capable of.

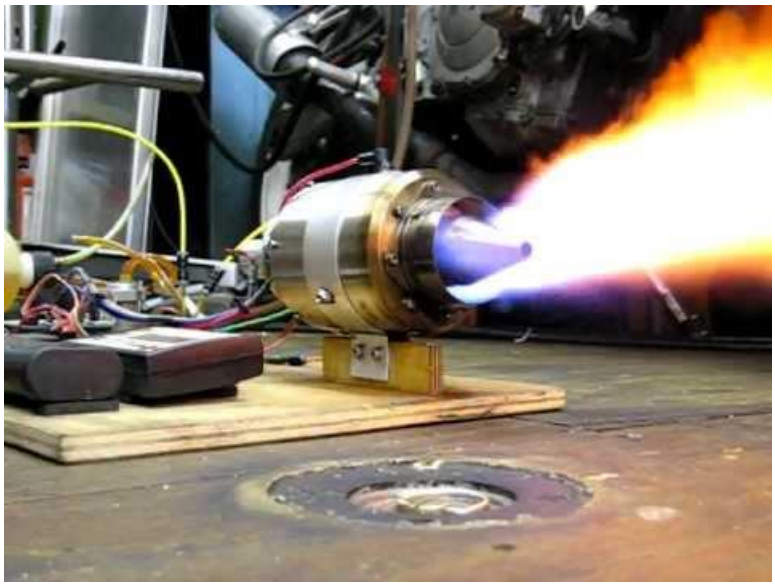

Figure 11: Combustion with Rich Fuel Mixture [3]

J. Armstrong et al. [3] investigated the altitude starting limits of turbojet engines. It was found that three main phases were needed for a successful start of a gas-turbine engine. First, there needs to be ignition in the combustor using an ignition device. Next, the flame would need to propagate from the ignited combustor to the other combustors if those are present. Finally, the engine would need to accelerate to full speed without exceeding the allowable temperature of the engine parts while also avoiding compressor surges or stalls. Each of these phases can limit the altitude-starting limits of the engine, which became a motivation in the research to identify the

effects of some aspects of the combustion stage on the altitude-start limits of the engine. Specifically, a reduction in fuel temperature from 30° to -2 °F generally reduced the altitude-ignition limit less than 5000 feet; but when the fuel temperature was decreased from -30 °F, a very abrupt lowering of the altitude limit was found with engine inlet-air temperature lower than 0 °F. Essentially, when simulated at a flight velocity of 0.6 Mach number, ignition was borderline, and at the lower fuel and air temperatures, the high air velocities through the combustor swept the vaporized fuel from the combustor before an ignitable fuel-vapor and air mixture could be established. For sea-level static conditions, the lower air velocity in the combustion chamber at engine cranking speeds allowed the establishment of a combustible fuel-vapor and air mixture, which is ignitable at the current pressure level in the chamber [3].

The Korea Aerospace Research Institute began operating the Altitude Engine Test Facility (AETF) for small gas turbine engines in 1999 [26]. The AETF is capable of simulating altitudes up to 30,000 ft. at Mach numbers up to roughly 1.0. The facility has a maximum mass flow rate of approximately 52 lbm/s and can accommodate engines that produce up to 3,000-lbf thrust. Although it is among the smallest altitude engine test facility in the world, the AETF size is significantly larger than what is desired in this study. The AETF features air supply and exhaust systems, facility control systems, and data acquisition systems. Air supply and exhaust are driven by two compressors of 3.500 hp and 3,750 hp, respectively. For conditioning supply airflow, AETF utilizes a desiccant dryer, water-cooled heat exchangers, and a liquid-air system allowing for simulated temperatures as low as -103 °F. Depending on the test conditions, the compressors can supply and/or exhaust air in series or parallel. For simulated total pressures above ambient conditions, the compressors supply air to the test cell. However, for simulated total pressures below ambient conditions, the compressors are only used in the scavenge system [1]. The small engine altitude test stand proposed in this study will incorporate a compressor on the feed side and rely on taking the ground test rig to different altitudes to simulate ambient conditions.

Preliminary Studies

Baseline Analytical Combustion Testing

To determine the stability range of the KingTech K-160 combustor that will be studied, it is necessary to calculate the theoretical combustor loading parameter and equivalence ratio. The fuel KingTech recommends to operate their engines is Jet Fuel A, which has a spontaneous ignition temperature of 501 °K; according to Kumar et al., the proper equivalence ratio for Jet-A is approximately 1.12 [33]. Because of the complex set of reactions occurring when a hydrocarbon is burned in air, the pressure component n has been experimentally determined to be 1.8 [6]. Then, the pressure was calculated from the compression ratio of the K-160, which is published as 3.4 [38]. The mass flow rate of the air at max throttle and diameter of the engine is also given by KingTech; those values are 0.77 lbm/s and 4.1 inches, respectively. Since the combustion volume is not published by KingTech, it was decided to estimate the volume by measuring the dimensions of the combustion chamber since that component was available on hand. The total volume of the combustion chamber was then calculated to be .026 ft^3. Next, based on the definition of combustor loading parameter (CLP), as given in Eq. (2), CLP was calculated to be 3.3 $lbm/(s \cdot atm^2 \cdot ft^2)$. Given an equivalence ratio of 1.12 for Jet-A and a CLP of 3.3 $lbm/(s \cdot atm^2 \cdot ft^2)$, Fig. 6 on page 12 shows this engine should have stable burner characteristics when operating at full-throttle.

CHAPTER III

APPROACH AND METHODOLOGY

Static Test Stand Design

Concept of Operation

To be able to effectively test and analyze combustion characteristics of small-scale turbine engines while simulating operating conditions, a static test stand is needed for analytical and safety purposes. When the desired engine has been decided to test, it will need a secure mounting location and a way of measuring the thrust of the engine, all while being arranged in a safe configuration. Furthermore, these characteristics of the test stand need to stay consistent when other engines are being tested to reduce user error. General designs of test stands to measure thrust incorporates a bracket to mount the engine, a method of force balancing using instrumentation to capture thrust, and safety devices to prevent injuries if liberation of the engine occurs. The materials and parts that make up the test stand can be mounted to an optical board for ease of transportation and configuration. A simple moment arm thrust stand can be one of the most practical methods for analyzing thrust since there is only one rotation point, and the user can set the length scaling of the moment arms to reduce mathematical complexity. Essentially, the engine will be attached to a mounting bracket, and as thrust is produced, the moment arm pivots on a set of bearings, as illustrated in Fig. 12. The lower moment arm will be resting against a load cell that captures force through sampling signals. This load cell will have a specific range of force inputs that it can read with given values of sensitivity and error.

The load cell will be connected to a data acquisition instrument to covert the resulting samples into digital values that can be manipulated by a computer.

Figure 12: Static Thrust Test Stand

A platform like SENSIT includes software that collects, graphs, and interprets the inputted data. From there, a calibration factor can be applied to the data to model the thrust of the engine accurately. The engine control unit and other engine operating components are affixed to the outer cage. This prevents wires from entering the flow field, fuel spilling onto engine controls, and ease of interchangeability of batteries. Most of the materials throughout the test stand are made from non-conductive and non-corrosive metals to prevent further problems while operating the engines. T-slotted aluminum allows for adjustability throughout the apparatus to accompany many different engine manufacturers and models. During full-throttle operation, the rotating machinery of many of these small turbine engines can reach RPM values upwards of 150,000. If liberation were to occur at this operating speed, shrapnel from the turbine would surely cause serious injury. Therefore, a steel mesh cage is placed outside of the testing apparatus. The test stand and its optical board are then fixed to a testing cart for ease of transportability. These features outline a quick and easy method to test multiple engines, change out fuel types, and capture accurate thrust measurement data, all while maintaining safe operating procedures.

Moment Arm Analysis for Thrust Measurement

Again, due to simplicity and feasibility, a simple moment arm analysis design will be used to capture thrust data. The KingTech K-160 engine produces around 35 pounds of thrust, meaning a load cell with the appropriate range would need to be used. Other engine specifications for the K-160 are included in Table 1.

Table 1: KingTech K-160 Engine Specifications

Thrust	35 lbf
Weight	3 lb. 3.5 oz.
Diameter	4.06"
Total Length	10.23"
Max Shaft Speed	130000
Max EGT	700°C
Fuel Consumption	17.3 oz/min

To determine this range, a moment arm analysis should be used to calculate the force that the load cell would read. Figure 13 illustrates a free body diagram to show where the forces would be present. R_x would represent the thrust that the engine produces, while R_y would represent the opposing force that the load cell would counteract with.

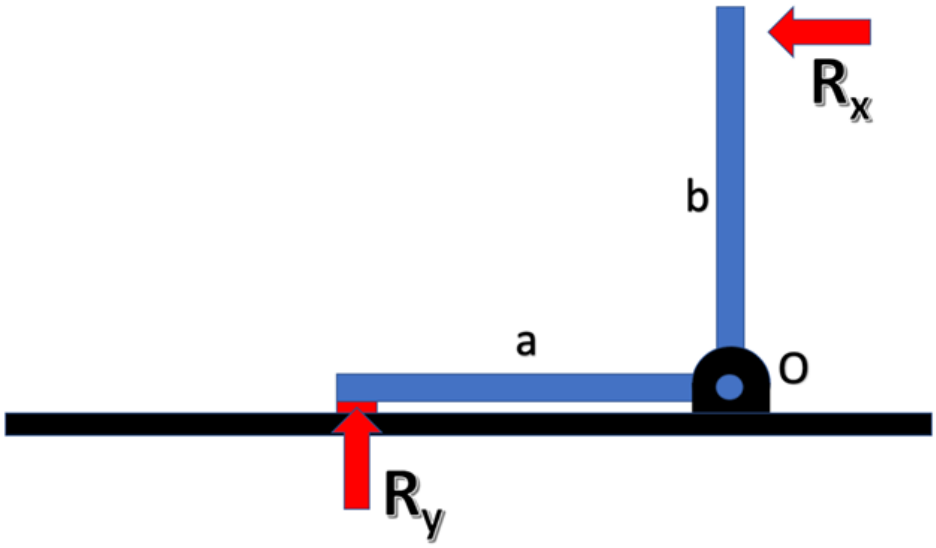

Figure 13: Freebody Diagram for Thrust Measurement

R_y can be calculated using Eq. (11) below. This value is found by summing the reaction forces in the y-direction and then taking a moment around point O.

$$\sum M_O = 0 = (-R_x \times b) + (R_y \times a) \tag{11}$$

If *a* and *b* are set equal to each other, R_x will also be equal to R_y. Therefore, the ideal design would incorporate moment arms of the same length, which means the load cell would need to have an effective range to encompass the predicted max thrust of the engine in operation. Before thrust measurements are recorded, the load cell will be tarred to zero. Furthermore, calibration techniques will be used to obtain a value to correct the thrust data. This value will account for friction within the bearings, flexing within the moment arms, and other suitable errors.

Pressure Chamber to Simulate Operating Conditions

Simulating Flight Conditions Analysis

To simulate operating conditions, the altitude that the aircraft is flying at and the flight speed of the aircraft need to be known. From the altitude, you can obtain the static or ambient pressure. Since total pressure is equal to the static pressure plus the dynamic pressure, one must calculate the dynamic pressure from the flight speed of the aircraft. Equation 12 shows how to calculate total pressure based on the ambient reference pressure and Mach number.

$$P_t = P_{ref}\left(1 + \frac{\gamma-1}{2}M^2\right)^{\gamma/\gamma-1} \tag{12}$$

Given a range of altitudes and flight speeds to simulate, this equation can be used to plot flight conditions and the total pressures resulting from them, as shown in Fig. 14 and Table 2.

Table 2: Total Pressure for a Given Flight Condition at Sea-Level

Mach Number	Dynamic Pressure (psi)	Total Pressure (psi)
0	0	14.7
0.1	0.1	14.8
0.2	0.42	15.11
0.3	0.95	15.64
0.4	1.71	16.41
0.5	2.74	17.43
0.6	4.05	18.74

Constant total pressure lines were also plotted to illustrate ambient pressures for certain altitudes that were of interest. As shown, Mach numbers of 0.0, 0.2, 0.4, 0.6, and 0.8 were plotted as a function of ambient pressure. These values were chosen because small turbine engines are not designed to function at flight velocities much higher than Mach 0.75 [5]. The resulting total pressure values are shown on the x-axis. The black line illustrates a static flight condition, or Mach 0.0. Anything to the left of this curve is not possible to test because it would require a system on the back of the engine to suck more air through the engine, further reducing the ambient pressure [1].

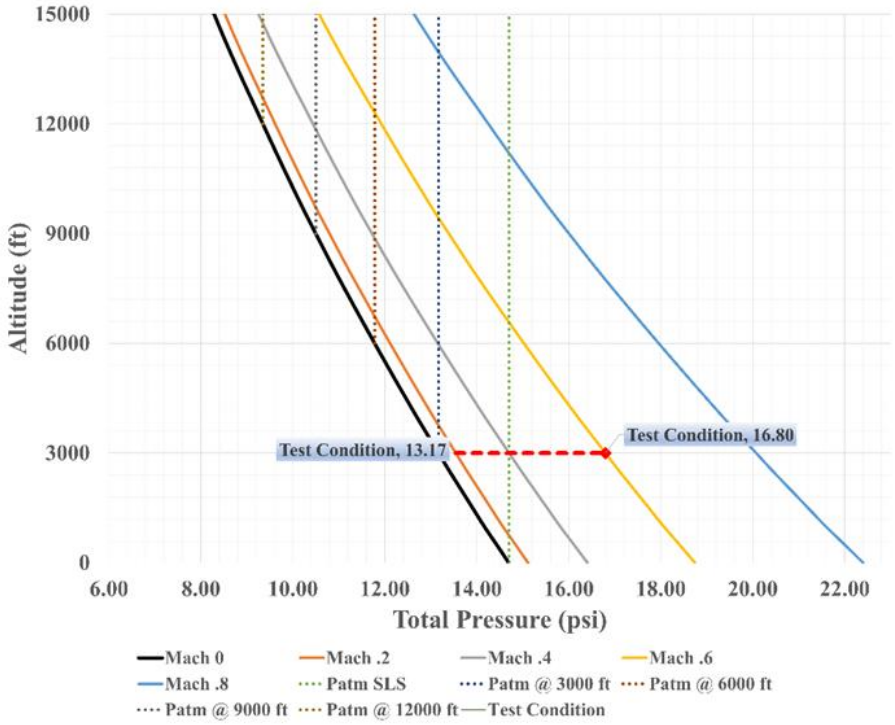

Figure 14: Simulating Flight Conditions Given Mach Number and Altitude

Moreover, given the location and its corresponding altitude where the engine would be tested, the graph shows the altitude's ambient pressure. Again, due to the limitation of altering the back pressure on the engine, anything left of the vertical ambient pressure line is not possible to test with this setup. Meaning, this test rig will solely be used for testing flight speeds for a given altitude while at that altitude. For example, say the test rig was at an altitude of 3000 ft, and the flight speed of interest was Mach 0.6; this graph is also set up to input that information and output

the test condition with the corresponding total pressures, as shown by the dashed red line. The left point on the line represents the ambient pressure for that altitude, and the point on the right represents the total pressure given a Mach value of 0.6. This value is important because it will directly relate to the total pressure that will be used to pressurize the chamber connecting to the front of the engine. The difference between the two points is the dynamic pressure, and this is also calculated automatically within the excel worksheet. Furthermore, an appropriate amount of mass flow of air is needed to sustain thrust throughout the testing. This mass flow can be calculated using the mass flow parameter (MFP), which is a function area of interest, total pressure, and total temperature. However, it is also a function of Mach number and gamma, the ratio of specific heats. Given Mach number and an assumption of gamma, MFP can be calculated. Then using AEDsys with Mach number as your input, a T_0/T_t value can be obtained. Using the ambient temperature, T_0, from altitude conditions, T_t can then be solved. Finally, Eq. (10) can be rearranged to solve for mass flow rate. This mass flow rate relates to the maximum amount of air the engine can intake for that Mach number and total pressure condition.

Overview and Experimental Procedure

Figure 15 shows the test rig and the equipment needed for the testing procedure. As stated before, the turbine engine will be mounted to a moment arm thrust stand, which is also mounted to an optical board for structural integrity and ease of adjustment. The figure also illustrates where the pressure chamber will be located, that is, attached directly to the leading edge of the turbine engine. This pressure chamber will be made from a high-pressure rated PVC pipe, sized to have approximately the same diameter as the engine, and will be attached using pipe ducting and hose clamps to seal air from escaping the chamber. This pipe ducting will have room to flex, preventing any restriction of the engine acting on the moment arm. Inserted into the end of the pressure chamber will be a quick disconnect valve, which will be used to connect to the pressure regulator and air compressor line.

Figure 15: Ground Test Rig Set-up

The excel worksheet also has an output for the dynamic pressure, which should also relate to the pressure the gauge on the air compressor tank indicates while testing since atmospheric pressure is already seen in the tank. However, depending on the value of total pressure that needs to enter the engine, there is a limit to the maximum amount of pressure drop through the system that can occur, and that limitation is due to the quick disconnect valve. In gas flow through an orifice, there is an occasion where the gas velocity reaches sonic conditions. This occurs for airflow when the absolute pressure ratio is around 0.528, i.e., when the downstream absolute pressure (P_2) is 52.8% of the upstream absolute pressure (P_1) [35]. This scenario is called the venturi effect and can be visualized using Fig. 16 below.

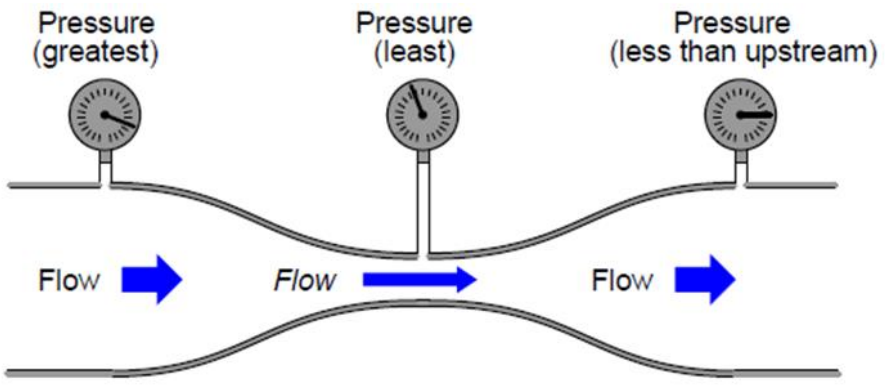

Figure 16: The Venturi Effect [36]

One major misconception about the mass flow rate through an orifice, once sonic velocity has been achieved by air, is that from that point on, mass flow rate also stays constant for all pressure ratios less than 0.528. However, it is important to note that mass flow rate is a function of three basic parameters, velocity, density, and area. As the air pressure (P_1) increases, the density of the air also increases; and since the mass flow rate is also a function of density, the mass flow rate increases linearly with pressure (P_1) [35]. The parameter that becomes "choked" or "limited" is the velocity of the air. Also, by maintaining a fixed inlet pressure to the orifice and allowing the outlet pressure (backpressure) to vary, there is a range of outlet pressures over which the mass flow rate is fixed. O'Keefe Controls Co. [35] provides a table to calculate the maximum standard cubic feet per hour (SCFH) of air flowing through a metal orifice based on the inlet pressure and orifice diameter in inches. The pressure line coming from the pressure chamber will be connected to an 80-gallon air compressor. This air compressor will have a pressure regulator, which will be set to the desired dynamic pressure that will govern the correct total pressure for the operating condition. The volume in this tank will essentially determine how long the testing can run since it will try to maintain that pressure by feeding more air through the line continuously. Furthermore, if the pressure in the pressure chamber is that of the required total pressure, the mass flow rate through the system can be read using a mass airflow meter to determine if sufficient airflow will be achieved.

Once the pressure chamber is pressurized to the desired total pressure, stage one in the engine start sequence will begin. The glow plug will then be powered on, and the starter will be engaged. When the rotor arrives at a value higher than the "ignition max RPM" programmed parameter, the starter will disconnect, and ignition fuel will be introduced. This step should produce an audible clicking sound, which is indicated by the burner fuel solenoid and the pulsating of the fuel pump. From this point on, it is a reasonable assumption that ignition has occurred, and a flame is present in the combustion chamber. If ignition does not occur, error messages such as "Glow Bad" and "Start Bad" will be displayed on the Ground Support Unit

(GSU). This method will be used to test the start reliability of the engine under different operating conditions, as discussed earlier.

Instrumentation to Validate Measurements

Although the pressure regulator will tell you the total pressure (in psig) entering the system, more instrumentation is needed to validate further the actual total pressures being achieved in the pressure chamber, most importantly near the leading edge of the engine. The instrumentation used in this study along with their included specifications is included in Table 3.

Table 3: Instrumentation and Corresponding Specifications

Instrument	Manufacturer	Range	Accuracy
Pressure Gauge	GAV	0 - 160 psi	± 0.01%
Pressure Regulator	Cash Acme	0 - 250 psi	± 0.02%
Load Cell	FUTEK	0 -500 lbf	± 0.5 %
Digital Scale	UltraShip	0 - 55 lbf	± 0.01%
Mass Flow Meter	Siargo	0 - 200 L/Min	± (2.5+0.5FS)%

A pitot tube, along with a differential pressure measuring device, generates a signal which represents the difference between the total or Pitot pressure (caused by the moving air stream plus the static air column) and the static pressure (pressure acting at all points in stationary air). The resultant pressure magnitude represents the true pressure caused by the movement of the air mass [36]. The minimum velocity should be high enough to provide a reliable reading from the pressure-sensing device at the minimum flow rate and low enough to maintain velocities in the subsonic range at the highest volumetric airflow rate. To obtain the most accurate readings, the sensing tip of the Pitot tube must be parallel to the direction of flow of the moving airstream. Furthermore, as air flows along a stationary solid boundary, such as a pipe wall, stresses are set up, which exerts a tangential force on the boundary as though the air were trying to adhere to it and drag it along. This is due to a property of a fluid or gas known as viscosity [37]. Essentially, the frictional drag reduces the velocity of the airstream near the pipe wall. Since the volumetric flow calculations are based on average airflow velocities, the ideal placement of the Pitot tube is

at the average velocity point in the velocity profile, shown by Fig. 17. Temperature probes, also known as thermocouples, can be used in conjunction with Pitot tubes to provide more accurate readings. However, through an analysis using AEDsys, the difference in total temperatures between the ambient condition and flight condition can be assumed to be negligible.

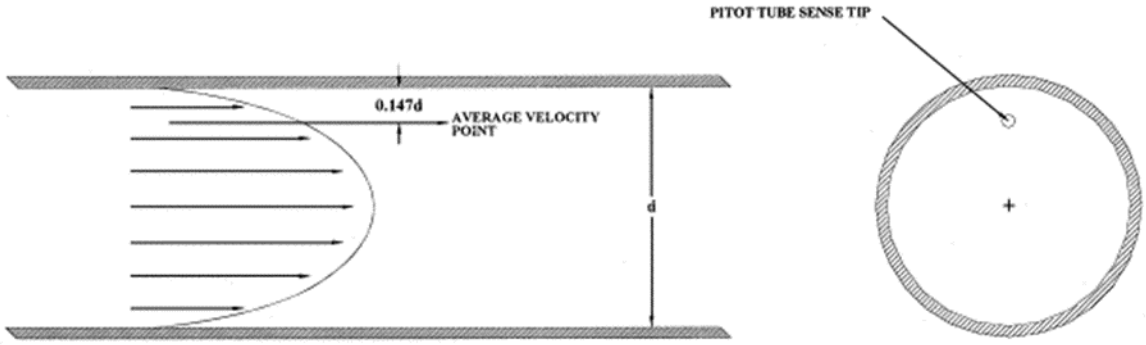

Figure 17: Ideal Placement of Pitot Tube Due to Viscosity [36]

Engine Control Unit Operation

Engine Operating Procedure

A specific series of events in the correct order needs to be followed to run a small-scale turbine engine properly. Before the operation begins, a checklist is typically used to verify safety precautions are in place. The next section, "FAR and OSHA Standards," will go into more detail on these safety precautions and the general codes and standards that govern them. The engine control unit (ECU) battery should be fully charged to initiate the startup sequence of the turbine successfully. Fuel lines and the fuel filter should also be checked, making sure they are clear with no restrictions. The fuel tank should be vented and unobstructed to allow for sufficient fuel flow through operation. The fuel tanks should be filled with the correct fuel for the turbine (manufacturer-specific recommended). Next, the fuel line should be purged to clear any air pockets in the system. The receiver switch can now be turned on, and the engine is ready for stage one of the startup sequence.

The KingTech Manual [38] provides a general guideline on how to operate their engines by taking you through the different stages in the engine startup sequence. Once the checklist has

been approved, the startup sequence begins with stage one. In this stage, the burner plug is powered and checked. Once hot, the starter is engaged at reduced power. The rotor will arrive at "ignition max RPM," and the starter will disconnect. Ignition fuel will begin to flow, and the preheat stage will commence. The temperature from this point on should steadily climb up to 72°C, which will then initiate stage two. This stage is known as the "switch over stage," where the main fuel opens, and a slightly yellow to bluish flame is expected. The starter motor continues to drive the rotor even faster in preparation for the fuel ramp. Some popping and flashes of yellowing blue flame will indicate stage three, fuel ramp, has begun. In this final stage, the burner valve is closed while the pump and start motor drive the engine up to idle temperature and RPM. Once achieved and operating, the transmitter takes over control of the engine, and the user can begin idling up the engine.

As mentioned previously, the process for recording thrust measurements during experimentation will commence from this point on. Just as important, small-scale turbines also have cooling sequences following the operation of the engine. After the user has finished gathering data or anytime throughout the testing, the trim stick can be set to "off" position to start the cooling sequence. If the engine were above idle RPM, cycling of the starter motor would begin until the exit gas temperature (EGT) is below the minimum programmed temperature, which is around 100°C. The receiver may then be powered off any time after the engine shuts down, and the ECU will continue to cool the turbine. In the event of the engine not going into the cool down mode after the turbine shuts down or flames out, the user can unplug and reconnect power to the ECU. This power cycle will enable the ECU to recognize that the engine temperature is still higher than normal and should engage auto cool down [38].

Engineering References, Codes, and Standards

The design of this test rig, as well as the operation of the turbine engine, will be functioning under multiple Federal Aviation Regulations (FARs) and Occupational Safety and Health Administrations (OSHA) codes. One of the most important regulations is FAR 25.303,

which requires a minimum factor of safety of 1.5 throughout a design. Even though the total pressures that will be seen in this experiment will be quite low, at the highest no more than 40 psi, it is still critical to know where the failure point could occur. The pneumatic hoses used in this experiment will be rated up to 300 psi, the pressure regulator at 125 psi, PVC tubing at 220 psi, and finally, the limiting factor, the hose ducting at 75 psi. This value is rated for pressures over twice that of the maximum pressure that will be encountered during experimentation, well above the required factor of safety of 1.5.

FAR 25.903e relates to one of the objectives in this study. The regulation relates to restart capability and says for turbine engine powered airplanes, if the minimum windmilling speed of the engines, following the inflight shutdown for all engines, is insufficient to provide the necessary electrical power for engine ignition, a power source independent of the engine-driven electrical power generating system must be provided to permit in-flight engine ignition for restarting [39]. The analysis conducted in this experiment will essentially outline an altitude and airspeed envelope for small-scale turbine engines for in-flight engine ignition and reignition.

FAR 25.939 covers turbine engine characteristics within the engines operating limitations, calling for no hazardous characteristics or vibrations causing flow distortion to occur at the inlet of the engine [40]. For the experimental setup, the only component that may shake violently will be the main air compressor. However, that should not be a concern because the vibrations should remain isolated from the other components. FAR 25.941a also states that if the design of an inlet is changed, proof that the engine still operates correctly for its designated purpose is required. Although the actual design of the inlet will not be altered, the engine cowling will have a hose duct clamped to the outside, slightly changing the form factor and geometry. This condition will be satisfied by operating the engine with the hose duct and PVC pipe alone, making sure the entire operating range of the engine is met, and no considerable problems that could affect the functionality of the turbine are presented.

In addition to following FARs, this study will also comply with OSHA codes and standards to provide sufficient safety precautions since combustion fuels will be used during experimentation. OSHA 1910.157 regulates that portable, approved fire extinguishers must be provided and easily accessible [41]. This will be met by keeping a CO_2 fire extinguisher (recommended for engine operation) within reaching distance while conducting engine tests. Finally, OSHA 1926.150 states that there must be a fire protection plan always installed throughout an experiment in preparation for any situation where a fire might be possible. Other than these standards, general personal protective gear like hearing protection and safety glasses will be used during testing.

Data Acquisition

One of the main objectives during this study is to determine a practical method to simulate in-flight and ground speed operating conditions for combustion research. Combustion characteristics would be tested with different fuels and fuel-air-ratios to show their effect on start reliability, fuel consumption, specific fuel consumption, exhaust gas temperature, and specific thrust. A great deal of data will be collected and analyzed throughout this process, so many forms of data acquisition will need to be implemented to distinguish between data sets and streamline the experiment. Luckily, most small-scale turbojet engines already incorporate several techniques coupled with instrumentation to provide useful information to the user.

For example, the KingTech engines can display the maximum, mean, and minimum values for the turbine RPM, exit gas temperature, and battery voltage. The most useful parameter of the three for this study will be the exit gas temperature. This value will be important when calculating the combustor loading parameter and the burner efficiency. Many factors govern this temperature, such as the fuel type, any additives, throttle condition, flight speed, altitude, and fuel-air-ratio. The turbine RPM value will be more useful in real-time during the experiment rather than having it outputted after the engine has been tested. The RPM value will essentially be used to operate a sweep of throttle conditions to analyze fuel consumption and specific thrust. As

for recording thrust measurements, as mentioned previously, a FUTEK load cell will be mounted under the moment arm to calculate the thrust of the engine. This load cell will include software from SENSIT to covert the resulting samples into digital numeric values that can be manipulated by a computer. Figure 18 shows the wiring diagram for the KingTech components and how the load cell data is received by the computer, with Table 4 describing the purpose of each component.

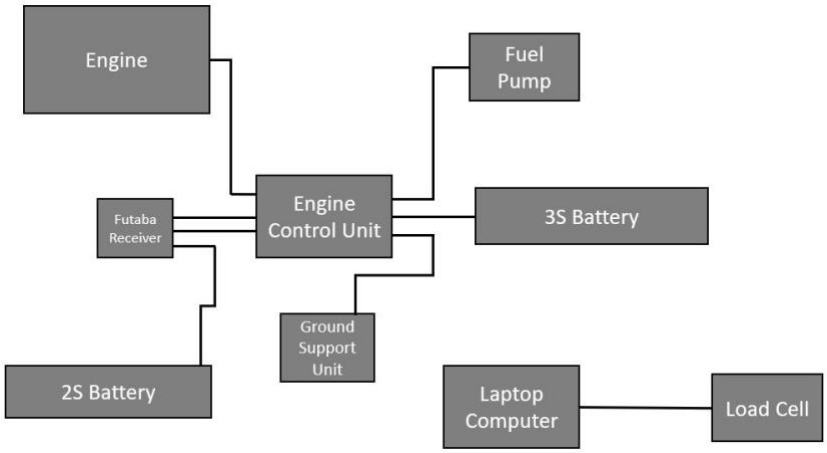

Figure 18: Wiring Diagram for KingTech Components

Table 4: Purpose and Description for Components in Wiring Diagram

Component	Purpose & Description
Engine Control Unit	Controls fuel supply, air management, fuel injection, and ignition
Ground Support Unit	Allows user to operate settings within the ECU and run engine
Futaba Receiver	Transmits wireless signals to controller or gives feedback to ECU
KingTech Engine	Turbojet used for testing and evaluation
3S Battery	Powers the ECU and fuel pump
2S Battery	Power the Futaba Receiver
Laptop Computer	Used to retreive thrust data from SENSIT software
Load Cell	Records and converts force data to be processed
Fuel Pump	Delivers appropriate fuel to combustor

Once this data is on the computer, it can be transferred into excel for proper data analysis. As for determining the ignition of the engine, again, through the software provided in KingTech ECU's, the turbine start sequence and its inner stages will be utilized for determining successful ignition attempts in the combustion chamber. All the necessary information to validate the

ignition will be displayed on the GSU, and several error messages will be made aware of indicating if this process has failed properly.

Fuel Distribution and Regulation

Overview of Small-Scale Turbine Fuel Distribution

Figure 19 shows the fuel system connection diagram for typical small-scale turbojet engines. KingTech highly recommends an ultimate air trap (UAM) for in-flight operations of their engines. This device will not be necessary for static testing since purging of the fuel lines will be done during the checklist phase. Shown in the diagram is also the main fuel tank, which can be of any size that the user chooses; it just needs to have a venting valve so fuel can flow freely. Bypassing the UAT would take the fuel directly to the fuel pump. This fuel pump will have a specific port for taking in fuel and delivering fuel. From there, the fuel will continue to the fuel filter. This filter is needed because the fuel pump may emit small particles that can block the solenoid valve in the turbine from completely closing. The fuel continues through a safety petcock after it exits the fuel filter. During the checklist process, this safety petcock should be flipped open, or fuel will not flow into the engine. Finally, the fuel is delivered to the turbine fuel connection port via push connection. It should also be noted that all the fuel lines will be 4mm in diameter except the few quarter-inch sections where adapters are needed. Once the fuel has entered the engine, it is distributed through a hollow diffuser to spread out evenly. This process splits the fuel into several fuel lines that span the length of the combustion chamber. As the fuel is pumped through these fuel lines, it is externally heated from any existing combustion apparent in the burner. Lastly, the fuel is dumped into annular cylinders; it travels along these cylinders, heating up even further, and then is finally splashed violently against the back of the burner wall to mix with air and initiate combustion.

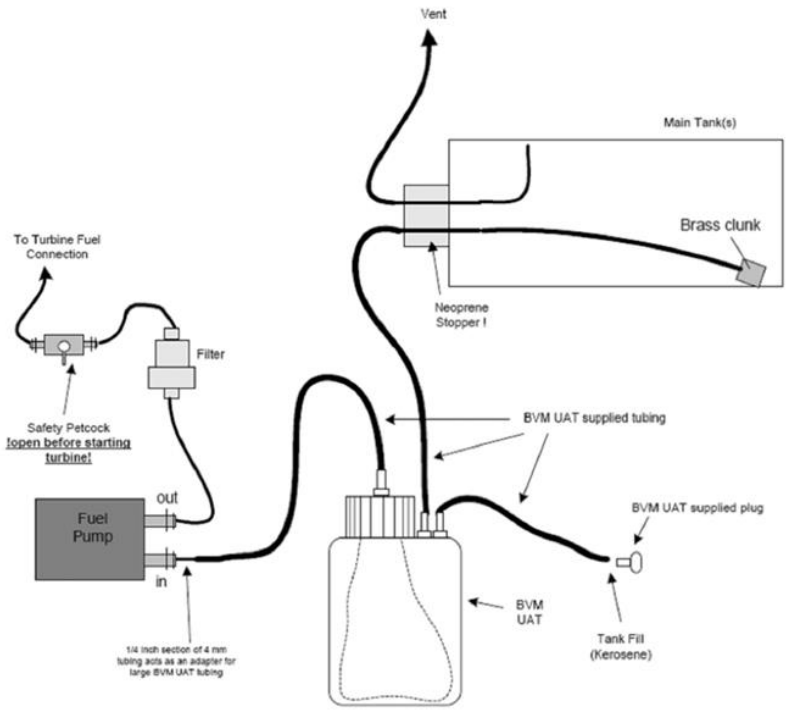

Figure 19: Fuel System Connection Diagram [38]

Determining the Effects of Fuel Type, Additives, and Fuel/Air Ratio

One big advantage of using small-scale turbojets for combustion research is that these engines are designed to function on several different types of fuels. KingTech engines can operate using Diesel, 1-K Kerosene, or Jet-A1 [38]. Among the three types of fuel, KingTech highly recommends using regular pump Diesel as it is readily available, inexpensive, has a higher energy density, and performs with up to 10-12% better fuel efficiency. It should also be noted that these fuels must be mixed with 5% KingTech Special Blend or synthetic turbine oil (Aeroshell 500 and 2-stroke oil are prohibited), or one quart of oil in every five gallons of fuel. To successfully maintain the engine and keep a full warranty, it is also recommended to use KingTech oil only since it provides the best lubrication properties for their engines. According to the European Biofuels Agency [42], the worldwide consumption of commercial aviation kerosene (Jet-A1) is about 200 Mt/y, and the projected annual growth rate is 4.5% by 2050 for this sector. The global airline transportation sector is among the largest contributors to all anthropogenic CO_2 released

into the atmosphere [43]. Any amount of fuel savings is worth considering to potentially decrease this number.

Quantifying the effects that fuel type has on burner characteristics can be done in several ways. The thrust specific fuel consumption (TSFC), or fuel mass flow rate per unit thrust, is one of the main parameters to analyze. By measuring the amount of thrust provided by the engine, knowing the weight of fuel before and after testing, and the fuel-to-air ratio, this performance parameter can be calculated. Since these parameters are all dependent on each other, the study needs to make sure that only one variable is not held constant while comparing fuels; this will be discussed further in the section "Fuel Regulation Sensitivity Study." Furthermore, these fuels each have a certain energy density or amount of energy stored in a given system or region of space per unit of volume. This characteristic will relate to how well the fuel combusts, produces energy, and delivers power to the turbine. Along with TSFC, the specific thrust will be the other main performance parameter to quantify the advantages of each fuel. Many of these characteristics can be combined to analyze the entire combustion process. Moreover, all these methods can be coupled with testing the start reliability to see which combinations produce the best results for engine ignition. Essentially, a plethora of information can be obtained to determine how to achieve optimal flight conditions.

General additives are included in aviation fuels to improve fuel performance or meet the requirements of aircraft or airline operators. Tetra-ethyl lead improves the anti-knock characteristics of aviation gas; however, due to concerns about lead emissions, there has been pressure to phase this additive out. Antioxidants are added to fuels to prevent the formation of gum and other antioxidation products. Metal deactivators can be included in improving the thermal stability of fuels. It has been designed to mitigate the effects of dissolved trace metals, especially copper, which can impair the thermal stability of jet fuels [48]. Corrosion inhibitors can also be used to reduce weathering in the fuel system. Fuel system icing inhibitors can be added to reduce the freezing point of any water that may be in the fuel system and prevent ice

crystal formation [48]. Lastly, static dissipater additives are sometimes added to minimize the hazardous effects of static charges that build up. Additionally, and less frequently, unusual additives are mixed into fuels for other specific reasons. Extensive use of ethanol in fuel increases the evaporation rate owing to a high cylinder temperature and high compression ratio, which typically leads to improved combustion [44]. The introduction of vegetable oil and hydrogen in the existing engine has been popular recently due to its sustainability without making any severe modification to the existing engine [45, 46]. Among different fuel blends, R20E (Jet-A 70% fuel, 20% Rapeseed, and 10% ethanol) has been shown to increase static thrust by 35% and decrease thrust specific fuel consumption by 41% [47]. Access to all these additives will be limited, but if accessible, they can be tested individually to analyze their effect on combustion.

Finally, the fuel-to-air ratio will also play a major role in analyzing combustion characteristics. Changing this ratio can be done by changing the voltage on the pump limit, corresponding to a change in the mass flow rate of fuel. KingTech claims this parameter can be increased from the original value by 15%-20% without causing too much wear on the pump [38]. The amount of fuel can be controlled even further by altering the settings in the start menu three of fourteen found in the KingTech software. This menu lets the user adjust the amount of fuel sent to the burner during the ignition phase of startup. This could be of particular interest when studying the effects of fuel type while simulating in-flight conditions to analyze engine start reliability. Likewise, menu eight of fourteen lets the user regulate the power sent to the starter motor controlling the amount of air injected into the burner that can occur during stage one of the start sequence. A wide variety of combinations can be tested with all these different parameters, some very dependent on others. So, several sensitivity studies will be used to incrementally adjust one parameter while keeping the others held constant to analyze their sole effect.

Fuel Regulation Sensitivity Study

As mentioned previously, many variables will be tested in this study. A sensitivity study determines how different values of an independent variable affect a particular dependent variable

under a given set of assumptions. This technique is used within specific boundaries that depend on one or more input variables. Two main studies will essentially be done in this experiment, one to analyze the start reliability given successful ignitions of the engine, and the other is analyzing performance parameters of the engine like specific thrust and thrust specific fuel consumption. Figure 20 outlines the specifics of these studies. There will be two major test groups, and each one will have its sensitivity study performed. “Major Constants” for both test groups include the two fuels that will be tested, Diesel and Jet-A. Meaning, each test group will perform a study holding either Jet-A or Diesel as the major constant. For test group “one,” once the fuel is chosen, the independent variable will be the fuel-to-air ratio. Several tests will be performed while incrementally changing this ratio while holding an operating condition or total pressure constant. This test group will focus on analyzing the start reliability and recording successful ignition attempts of the engine. Likewise, after the fuel has been chosen, test group “two” solely evaluates the performance parameters of the turbine engine like SFC, specific thrust, and EGT. Since the KingTech software does not allow the user to adjust the fuel-to-air ratio in the ECU for throttle conditions, the performance parameters will be evaluated at several different RPM conditions. At the end of this study, several graphs will be presented in unique ways to determine optimized combustion characteristics for a given in-flight operating condition. It should also be noted that these tests can be performed at different altitudes to gather more information.

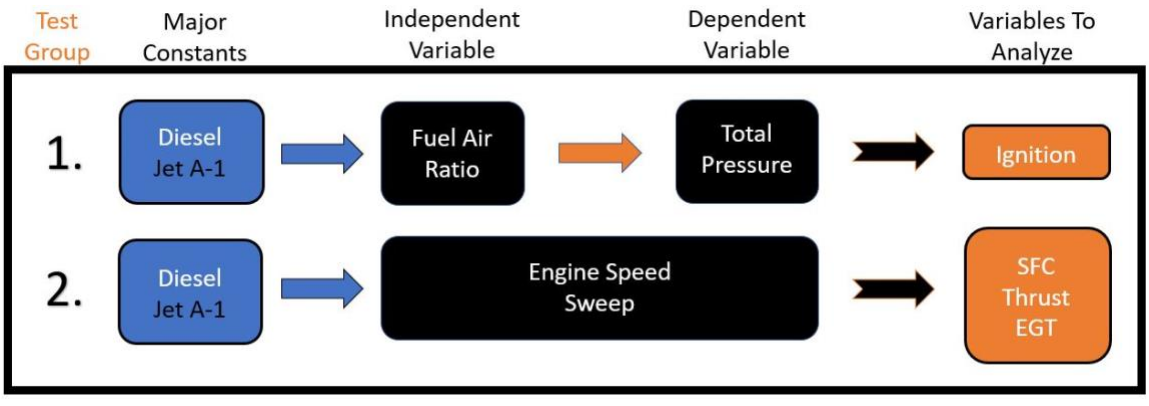

Figure 20: Test Matrix for Sensitivity Analyses

Advantages of a Small-Scale Turbine Engine Ground Test Rig

Affordability of Testing Apparatus

The specific test apparatus being used in this study will be comprised mostly of parts from previous projects, miscellaneous components found around the lab, and include a few pieces that needed to be purchased, which makes the study very affordable. However, the individual components of the apparatus are inexpensive in themselves. The KingTech K-160 turbojet engine is the most expensive component in the project at around $2500 [38]. The other considerable expense would be the air compressor, whose value changes based on many factors such as the model and manufacturer, rated power output, and volume of the tank. The other components like the PVC pipe, pressure relief valve, pressure regulator, pneumatic accessories, pitot tube, mass airflow sensor, and test stand brackets all total under $1000 [4]. Having a ground test rig that essentially costs under $6000 is very enticing to numerous aerospace industries. This low-cost rig allows university researchers to gain adequate experience with turbine combustion without needing multimillion-dollar facilities. This system is affordable to take to a given altitude to test operating conditions in those environments. This is highly attractive since once a system is added to the back of the engine to alter the back pressure, it becomes much more costly. Additionally, smaller commercial facilities can implement a design like this to test their fuel mixtures, additives, or other fuel characteristics that they develop for aviation fuel. Lastly, maintenance with this system is extremely inexpensive since the only component that should ever need maintenance will be the turbine engine. Additionally, these engines typically need an overhaul after twenty-five hours of operation [5]. Although this test rig utilizes a KingTech engine, the design of the test stand is configurable to incorporate many different manufacturers and models with a wide range of varying thrust values and physical engine size.

Interchangeability of Small-Scale Turbine Engines

Large test facilities are typically not capable of switching out engines very effectively, largely due to their size and weight. Most of the time, these facilities have designated test stands

for each and every engine that goes through testing. The design of this test apparatus allows the user to analyze several engines without heavily modifying the general stand. Each engine of this size should have engine clamps specific to its make and model. The design of the test stand allows these clamps to be bolted to the engine mount location very easily. Metal plates on each side of the mounts can be adjusted for various diameters by extending them inwards or outwards laterally. Furthermore, these mounting plates are fixed to t-slotted aluminum brackets that span the length of the engine. These brackets can be used to adjust the engines forward to backward position, making sure the center of gravity is located above the rotation point of the ball bearings. Since most of these small engine manufacturers include the fuel distribution system with the engine, interchanging the fuel system given a different make and model is quite simple as well. Most of these models will be able to utilize the same fuel tank and batteries to power the ECU, reducing the number of components to switch out. Lastly, the load cell to record thrust has an operating range of up to 500 pounds. This value allows the user to test magnitudes of small engine models. However, given the functionality of the rig, the engine can also be adjusted in its top to bottom position to change the moment arm length of the vertical distance to include an even larger range of thrust values. The test apparatus also has a major advantage in terms of size, making the rig very manageable to pack up and test at a location with a different altitude.

Mobility and Portability of Test Rig to Study Different Altitudes

An advantage of a test stand this size is the ability for the apparatus to be easily transported to different altitudes to conduct experiments. This design has the thrust test stand and the simulated operating condition system both attached to an optical table that sits on a wheelable cart. This optical table can easily be removed from the cart to place in transportation vehicles, wind tunnels, or other facilities. It is very efficient and practical to be able to wheel this cart system to an outdoor location when tested is needed. The entire system is reasonably lightweight and could easily be transported by two researchers. The most important specification of the air compressor is the capable pressure output, and since previous sections concluded that absolute

pressures would not surpass 40 psi, then the next important specification is the volume of the tank. This variable essentially determines the total time of testing or the total amount of time the system can be fed air without going below a designated total pressure value. Although larger air compressors would allow for longer testing times, the testing can still be done with air compressors of much smaller size. This means the 80-gallon tank could be replaced with a much smaller one to make the mobility even more advantageous. Furthermore, one desktop or mobile computer can be used to operate the entire system. The thrust being read from the load sensor feeds directly into a USB port, the engine ECU controls can be controlled through the computer via USB, and the air data computer that reads total and static pressure is powered through a USB port. So, if the computer has a power source (like a battery), the entire system is portable.

CHAPTER IV

ENGINE START RELIABILITY: EXPERIMENTATION, DATA ANALYSIS, AND RESULTS

Analyzing Combustion Ignition at a Flight Condition and Fuel/Air Ratio

Holding Flight Conditions Constant and Changing Fuel/Air Ratio

As mentioned in "Fuel Regulation Sensitivity Study," a multitude of ignition tests over a range of fuel to air ratios and flight conditions were tested to analyze the start reliability of the KingTech K-160 engine. Using a designated excel file in collaboration with Fig. 14 and given the desired flight speed, the total pressure for that condition can be found. As stated before, it important to note that these ignition tests are limited to simulating flight conditions at the location of testing. The test rig is only capable of simulating a total pressure on the inlet of the engine and not the exit. So, for example, if a flight condition of Mach 0.4 at an altitude of 3000 ft is desired, the test rig in this current design would have to be transported to a location where static pressure on the exit of the engine could simulate that altitude. Table 5 shows the test matrix for simulating a flight condition while adjusting the fuel-to-air ratio in the engine during the ignition phase. The KingTech software allows the user to adjust the pump voltage, which regulates how much fuel is being pumped into the combustion chamber, up to a max value of 440. A sensitivity study was performed by adjusting this value from -10.00% (a value of 12) to +10.00% (a value of 100) of the standard pump voltage, which is 56. This was done for a flight condition of Mach 0, 0.2, and 0.4 using their respective total pressures for sea-level. This procedure was done for Jet-A and Diesel. In total, seventy-eight ignition conditions were tested.

Table 5: Example of Test Matrix to Analyze Engine Ignition

Jet A1				
Total Pressure (psi)		Fuel/Air Ratio		Successful Ignition? (Yes=1, No=0)
		-10%		0
		-5%		0
		-4%		0
		-3%		0
		-2%		0
M=0, Pt = 14.7, Pg = 0		-1%		1
		Standard		1
		+1%		1
		+2%		1
		+3%		1
		+4%		1
		+5%		1
		+10%		1

If ignition was successful, a "1" was placed in the corresponding cell in the table. If ignition failed, a "0" was placed instead. Each individual test condition was performed twice to ensure the results remained consistent. So, if two successful ignitions occurred at that condition, a "1" one would be tabled. If out of the two ignition attempts, only one success occurred, a third attempt was made, and that outcome was then tabled. This table would then be used to illustrate the percentage of successful ignitions to the attempts made in various ways to create a map of ranges of fuel-to-air ratios for given flight conditions near sea-level. The tests were performed over two days with temperature conditions only changing ten degrees between the two days and five degrees within the testing period for that day.

Table 6: Fuel Pump Voltages for Testing

Pump Voltage for Ignition			
-10%	12	+1%	60
-5%	34	+2%	65
-4%	38	+3%	69
-3%	43	+4%	74
-2%	47	+5%	78
-1%	52	+10%	100
Standard	56		

Table 6 shows the pump voltages for testing. Once the pump voltage had been chosen, the start-up sequence of the engine was initiated, and stage one began. Under stage one, the

correct fuel amount based on the pump voltage would be regulated to the combustion chamber. The sequence then began the ignition phase, where the spark plug would attempt to ignite the fuel and air mixture within the chamber. A successful ignition occurred if the sequence moved to stage two, where the temperature would start to substantially increase. When switching from Jet-A to Diesel, residual fuel was assumed to be apparent in the fuel lines, pump, and fuel distribution system within the engine. The engine was operated at the idle RPM for roughly one minute to expel and burn the remaining Jet-A. Furthermore, the fuel pump battery was monitored and kept above a certain voltage to ensure a consistent voltage was supplied. Based on work from Armstrong [3], it was expected to find that higher air velocities through the combustor would possibly sweep the vaporized fuel from the combustor before an ignitable fuel-vapor and air mixture could be established. At sea-level static conditions, the lower air velocity in the combustion chamber at engine cranking speeds should allow the establishment of a combustible fuel-vapor and air mixture.

Verifying Total Pressures with Computational Fluid Dynamics

Determining the total pressure coming from the air compressor is dependent on many different factors. Equation 13, which illustrates a simplified formula for mass flow parameter (MFP), can be used in conjunction with Eq. (14) from compressible flow relationships to solve for unknown parameters within the two equations.

$$MFP(M) = \frac{\dot{m}}{A}\frac{\sqrt{T_t}}{P_t} \tag{13}$$

$$P_t = P_{ref}\left(1 + \frac{\gamma-1}{2}M^2\right)^{\gamma/\gamma-1} \tag{14}$$

Using Eq. (14), if the desired Mach number to be simulated and static pressure is known, the total pressure for that condition can be found. This is the total pressure that would need to be simulated at the leading face of the inlet to the engine. Using Eq. (13), "A" would be set to the area of the inlet of the engine, "P_t" would be the total pressure solved for previously, "T_t" would be equal to the total temperature for that condition, and mass flow rate would be equal to the appropriate

mass flow rate of air based on the RPM of the condition being tested. That would allow for MFP to be calculated at the entrance into the engine. To solve for the total pressure coming from the air compressor connection valve, since MFP is now known, Eq. (13) can be used once again to solve for "P_t," with "A" set to the area of the connection valve. For example, if the desired condition to simulate is Mach 0.6 at sea-level, Eq. (14) yields a total pressure of 18.74 psi with a dynamic pressure of 4.05 psi. For the ignition tests, based on the RPM for the ignition stage, a mass flow rate of .03 lbm/s was found. The area of the inlet into the KingTech K-160 is around 3.14 $in^{2,}$ and using a valve area of 0.5 in^2, utilizing the method described previously with Eq. (13), the total pressure being supplied by the air compressor was calculated to be 117 psi. This value will be used to compare the results to a computational fluid dynamics (CFD) solver.

For the CFD study, SOLIDWORKS 2021 built-in flow solver was used. Dimensions were taken of the pressure tube, engine length and diameter, engine nozzle inlet and exit area, and compressor inlet area to make a computer-aided design (CAD) model of the system. The dimensions on the engine were taken with dial calipers for their ability to output highly accurate digital values. The computational domain was set to internal and excluded cavities without flow conditions. The fluid type used was air, with options checked for laminar and turbulent flow type characteristics. For thermodynamic parameters within the initial conditions, ambient pressure was set as 14.7 $lbf/in^{2,}$ and the temperature was set to 68.1 ℉. "Lids" were placed at the inlet and exit to finalize the computational domain. In terms of boundary conditions, a total pressure of 117 psi was used at the connection valve exit, and an environment pressure was used for the exit of the engine. A pitot tube was modeled two inches in front of the engine and placed into the flow about 0.147 of the 4-inch diameter of the pressure tube. This pitot tube had an average total pressure surface goal applied to it that would be used to validate the test condition total pressure. For calculation control options, a refinement level of six was used. Under refinement settings, the approximate maximum cell count was 3,000,000, and the refinement strategy was set to periodic. A 16-core desktop with 32 GBs of RAM was utilized to run the simulation. The simulation would

come to a solution when all goals had converged and been satisfied. Finally, the initial global mesh was set to automatic at a level of seven. The total CPU time was a little more than three hours and converged after 541 iterations with 2.7 million cells. SOLIDWORKS converged on a value of 18.3 psi for the average total pressure surface goal on the leading face of the pitot tube. When comparing the solution to the analytical value of 18.74 psi, the percent difference was calculated to be 2.00%. Theoretically, this value is nearly identical to what the mass flow parameter equation calculated it to be. Figure 21 shows a cut plot with velocity streamlines of the simulation. Although CFD cannot be used to validate measurements, it can be used to illustrate the flow properties and recirculation of air as it travels through the duct. The hydraulic diameter is the "characteristic length" used to calculate the dimensionless Reynolds number to analyze if a flow is turbulent or laminar. A good rule of thumb is to have the inlet air properties five hydraulic diameters away from the engine to mitigate turbulent flow. As shown by the figure, the velocity streamlines become more smooth-running as they approach the inlet of the engine. Furthermore, the simulation seems to verify the mass flow parameter analysis when solving for a proper inlet total pressure to simulate the desired total pressure entering the engine for a given flight speed.

Figure 21: Simulating a Test Condition - CFD

Successful Engine Ignition Attempts

Ideally, an actual pitot tube connected to an absolute pressure transducer would have been used during testing to validate the analytical and computational fluid dynamic results. However, due to time and instrumentation availability, the devices were not able to be implemented into the design. Based on the mass flow parameter analysis (refer to Appendix), the CFD results, and the connection valve diameter, three inlet total pressure values were calculated

to use for the experimentation. For Mach 0, an inlet pressure of 23.47 psi was used. For Mach 0.2 and Mach 0.4, the inlet pressure values were 24 psi and 26 psi, respectively. The 80-gallon air compressor was then turned on and allowed to pressurize to around 120 psi. Once the tank reached that pressure, the pressure valve was opened and set to supply the pressure of the desired test condition. Before each start-up sequence was initiated, the total pressure from the compressor was examined on the pressure valve to verify the correct pressure was still being supplied. The pump value on the ECU was then changed to the desired test point, which finalized the steps leading up to the experiment. As previously mentioned, each ignition test was performed at least two times to verify successful ignition. The entire procedure for each ignition test took about two minutes. At lower supply pressures, the compressor could maintain the proper rate of air throughout that flight condition test group. However, for example, simulating Mach 0.4 resulted in the compressor emptying much quicker than the other flight conditions. Several times for this flight condition, the pressure valve had to be closed to allow the pressure in the tank to reach its proper pressure again. The air compressor outlet mass flow rate was essentially greater than the compressor pump inlet mass flow rate. At that flight condition, the volume in the tank dictated the number of tests that could be performed. If ignition failed, the combustor never ignited, which kept the combustion temperature low, and the next ignition test condition was performed almost immediately. If ignition were successful, the combustion chamber temperature would reach several hundred degrees before the engine was shut down. If that was the case, the next ignition test was performed once the combustion chamber has cooled and reached a steady-state condition. Figure 22 and Table 7 show successful ignitions for a flight condition over a range of fuel-to-air ratios.

Table 7: Successful Engine Ignition for Flight Condition at Sea-Level

Mach 0		Mach 0.2		Mach 0.4	
Jet-A	Diesel	Jet-A	Diesel	Jet-A	Diesel
62%	77%	54%	69%	46%	69%

Although only three flight conditions were tested, a clear trend became common throughout the experiment. For static conditions, in total, twenty-six ignition attempts were made using the two fuels. Jet-A was successful 62% of the time, while Diesel was successful 77% of the time. For Mach 0.2, Diesel performed better than Jet-A once again. Diesel had 69% successful ignitions when Jet-A only had 54%. Finally, for Mach 0.4, Diesel was successful 69% again, while Jet-A was only successful 46% of the attempts.

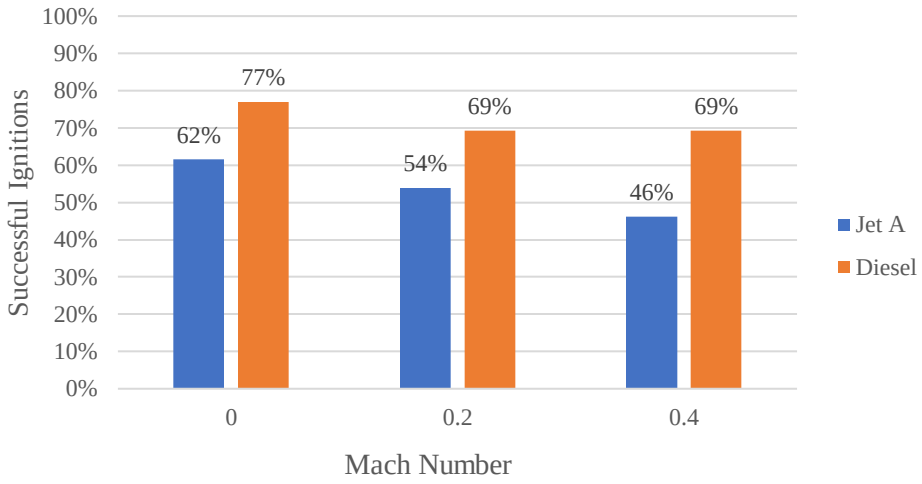

Figure 22: Successful Ignitions: Flight Condition over Range of Fuel/Air Ratios

The overall trend illustrates that an increase in flight speed reduces the percentage of successful ignitions. As the aircraft is flying faster, total pressure increases and the mass of air entering the engine also increases, basically causing the fuel-to-air ratio to decrease within the combustion chamber. This trend shows that either the combustible fuel-air mixture is being swept away by the incoming air or that the initial fuel-to-air ratio is too lean for the mixture to be ignited and properly combust. Additionally, the figure also shows that Diesel performed much better than Jet-A over the range of flight conditions. On average, Diesel had 72% successful ignitions over the 78 test conditions, while Jet-A had only 54% successful attempts, a difference of 18%. The flammability characteristics of the fuel type used are a function of the temperature in the combustor and the equivalence ratio. Although the flashpoint for Jet-A is lower than Diesel (126℉ and 100℉, respectively) [53], Diesel seemed to ignite much easier at the lower

temperatures, meaning the successful attempts were largely in part to the equivalence ratio needed for combustion. Another method of analyzing the data is by evaluating the percentage of successful ignitions for a fuel-to-air ratio over a sweep of flight conditions individually, as shown in Fig. 23.

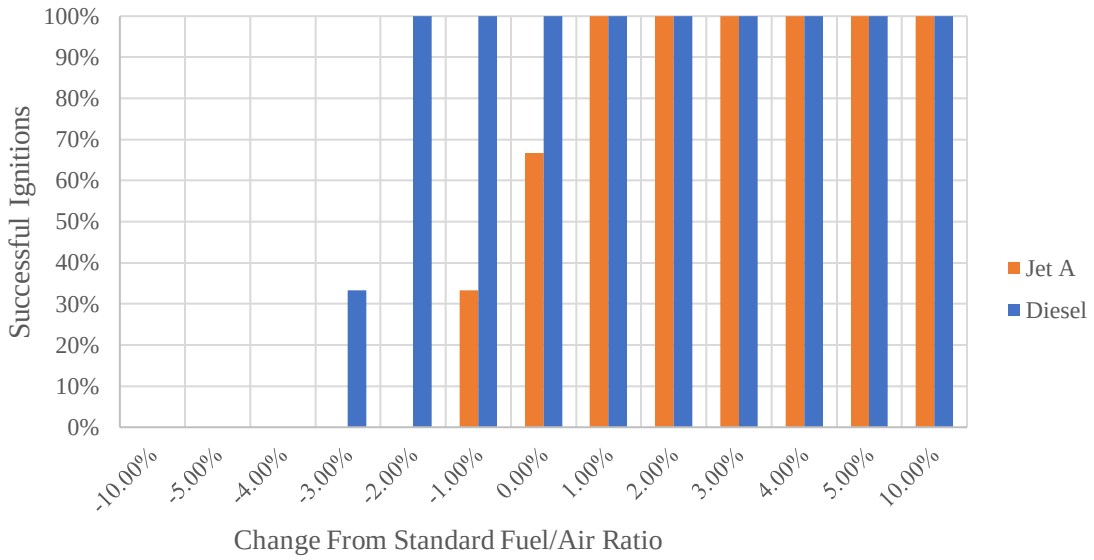

Figure 23: Successful Ignitions: Fuel/Air Ratios over Range of Flight Conditions

As explained in the experimental set-up, the pump voltage was changed from -10% to +10% of the max pump voltage from the standard recommended voltage of 56. Meaning, at -10%, the pump voltage was programmed to be 12, which is an extremely lean fuel-air mixture. On the other end, at +10%, the pump voltage was programmed to be 100, an extraordinarily rich fuel-air mixture. As shown by the figure, a pump voltage of -10% to -4.0% was too lean for either fuel to ignite, regardless of the flight condition. It was not until this value hit -3.0% until a successful ignition occurred, which was at Mach 0 using Diesel. The first successful ignition using Jet-A did not occur until this value reached -1.0%, which occurred at Mach 0. As the simulated flight speeds increased, the only way to initiate a successful ignition was to increase the fuel-to-air ratio. Simply put, the increased flight speeds decrease the fuel-to-air ratio within the combustion chamber but increasing the pump voltage mitigated that by increasing the amount of

fuel sent to the combustion chamber. From pump values of +1.0% to +10%, the amount of fuel sent to the burner completely offsets the influx of air given the extremely rich mixtures. The pump value could have been increased further past +10%, but the risk of flooding the engine increased.

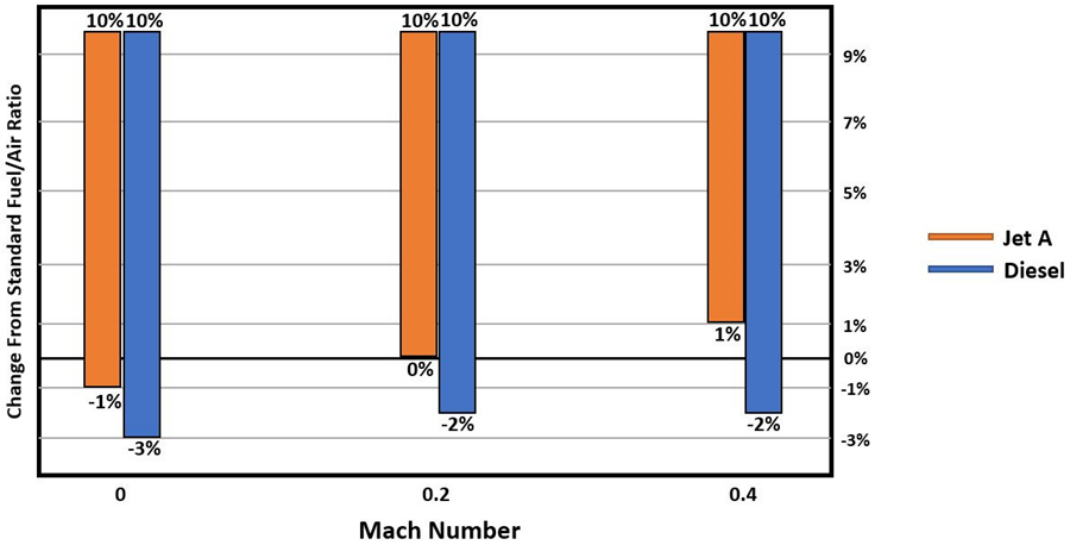

Figure 24: Successful Engine Ignition "Map"

Ultimately, a "map" of successful ignition attempts can be plotted to optimize the start reliability of the engine given the flight speed and fuel type used, as shown by Fig. 24 and Table 8.

Table 8: Results for Successful Engine Ignition "Map"

Mach 0		Mach 0.2		Mach 0.4	
Jet-A	Diesel	Jet-A	Diesel	Jet-A	Diesel
-1% to +10%	-3% to +10%	0% to +10%	-2% to +10%	+1% to +10%	-2% to +10%

For operating conditions at Mach 0, Jet-A best performs from pump voltages of -1.0% to +10% (51.6 and 100, respectively) from the standard value, and for Diesel, this range is -3.0% to +10% (42.8 and 100, respectively). For Mach 0.2 using Jet-A, the range is standard to +10% (56 and 100, respectively). For Diesel, this range would be -2.0% to +10% (47.2 and 100, respectively). Lastly, for Mach 0.4 with fuel type Jet-A, the range should be +1.0% to +10% (60.4 and 100, respectively). Interestingly, at Mach 0.4, for a successful ignition using Jet-A, an increase of 1.0% from the manufacturer's set pump voltage would be required.

Effect of Fuel Type and Ignition Characteristics on Start Reliability

It should be expected when fuel volatility is decreased, with a consequent decrease in evaporation rate, that a fuel-air mixture would be more difficult to ignite. Armstrong et al. [54] found that the altitude-ignition limit of an engine with the standard-engine-ignition system and fuel with 1 lbm/in^2 Reid vapor pressure in comparison with a fuel with a 6.2 lbm/in^2 vapor pressure, that the less volatile fuel reduced the altitude-ignition limit by 15,000 ft when testing at a flight speed of Mach 0.4. Ignition is aided by high pressure, high temperature, low gas velocity and turbulence, gaseous fuel-air mixture, proper mixture strength, and optimum spark duration. The simultaneous achievement of all these requirements is an actual turbojet engine combustor is nearly impossible, yet any attempt to satisfy as many requirements as possible will result in lower ignition energies, lower weight ignition systems, and greater reliability [55]. Foster et al. [56] found that a relationship between the minimum ignition-energy requirements and an empirical function of combustor-inlet air pressure and velocity V/sqrt(P) could be used to determine the relative ignition characteristics of the fuels at various combustor-inlet pressures and airflows. Based on the testing, the results indicated that the more volatile fuel (Jet-A) required more time for ignition than the less volatile fuel (Diesel). Since the more volatile fuel had a leaner fuel-air ratio at ignition, the temperature and, consequently, the pressure rise due to combustion would be less than for a less volatile fuel. Hence, the rate of flow of the burning gas through the combustion chamber would be lower, and the time required for the propagation of the flame throughout the rest of the combustor would be greater [57]. This could also be the reason Jet-A ignited less frequently than Diesel throughout the test groups. The KingTech software limits the amount of time the “ignition phase” takes place to limit damage to any of the components by “timing out” after a certain amount of time. It is a possibility that Jet-A could have ignited with more time, but that hypothesis cannot be tested with the current design.

Conclusion of Sensitivity Study

Significance of Results

Due to the limitations of the current design and given the testing location, the only operating conditions that were tested were different flight speeds at sea-level. The data gathered from the successful ignition attempts illustrate the optimal fuel-to-air ratio to use for flight speeds of Mach 0, 0.2, and 0.4 to maximize the start reliability of the small-scale turbojet. Since data was not obtained for any altitudes higher than sea-level, this "ignition map" should only be considered for aircraft operating at altitudes near sea-level. This reduces the number of applications this map could be used for. However, even at sea-level conditions, successful engine ignition can still be a concern for fast-moving aircraft, and knowing the proper fuel-to-air ratio is critical for performance. The Ryan Firebee was developed in 1951 and is the most widely used target aircraft ever. The plane was launched with the aid of a carrier or with the aid of the rocket-assisted take-off (RATO) on the launchpad [58]. These systems take off at extremely fast speeds with incredible acceleration. The rocket provides extra thrust to the aircraft to assist it in take-off when the turbojets cannot generate enough thrust. Once in flight, the rocket engine disengages, and the rest of the flight is conducted solely using the turbojet. Most times, the engines are running before the RATO device is initiated, but sometimes it can be beneficial to also ignite these engines after the vehicle has traveled a certain distance after launch, which can be problematic due to the high flight speeds. Based on the results of this analysis, running a rich fuel-to-air ratio enables the engine to have the highest chance of successful ignition.

This study also proves that with limited resources and budget, a ground test rig can be designed and assembled to sufficiently analyze the start reliability of different small-scale turbojet engines. Based on a mass flow parameter analysis, an altitude, and flight speed, a total pressure can be calculated to act as the simulated operating condition. Furthermore, once a connection valve size has been chosen for the pressure chamber, the required total pressure being supplied by the air compressor can be found. Figure 25 shows a graph that would enable the user to decide

connection valve size and based on the Mach number and area of that valve, the appropriate total pressure is established. It should be noted that this graph is specific to sea-level conditions in this configuration but can be adjusted to use the correct ambient static pressure for other altitudes.

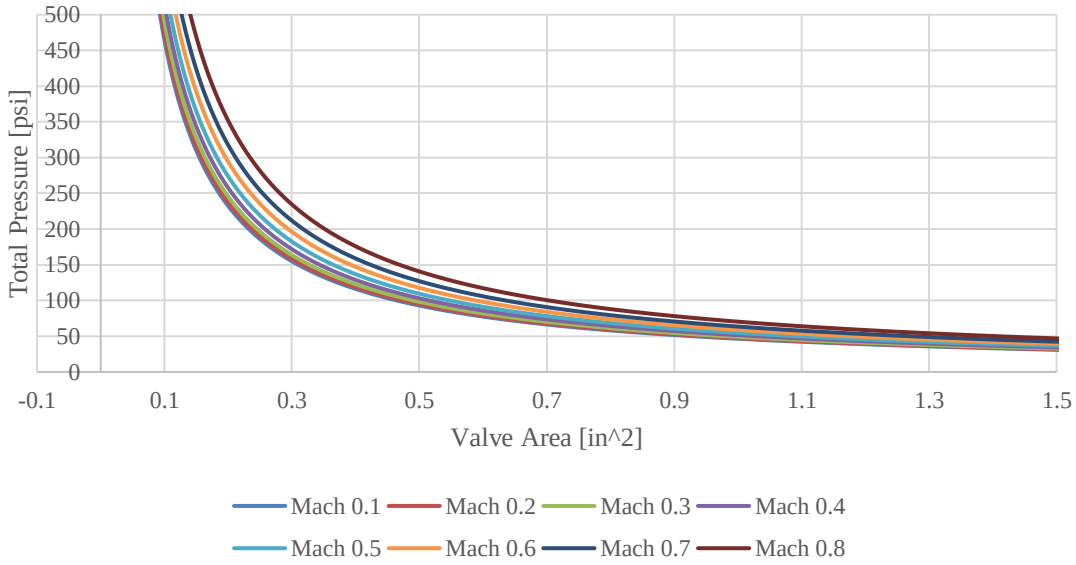

Figure 25: Determining Connection Valve Inlet Total Pressure

Figure 26 shows a close-up view of Fig. 25 to better illustrate the flight speed trends. For example, if a connection valve area of 1 in^2 was chosen and the desired flight condition to simulate was Mach 0.5 at sea-level, then the corresponding total pressure being supplied from the air compressor should yield a value of 55 psig.

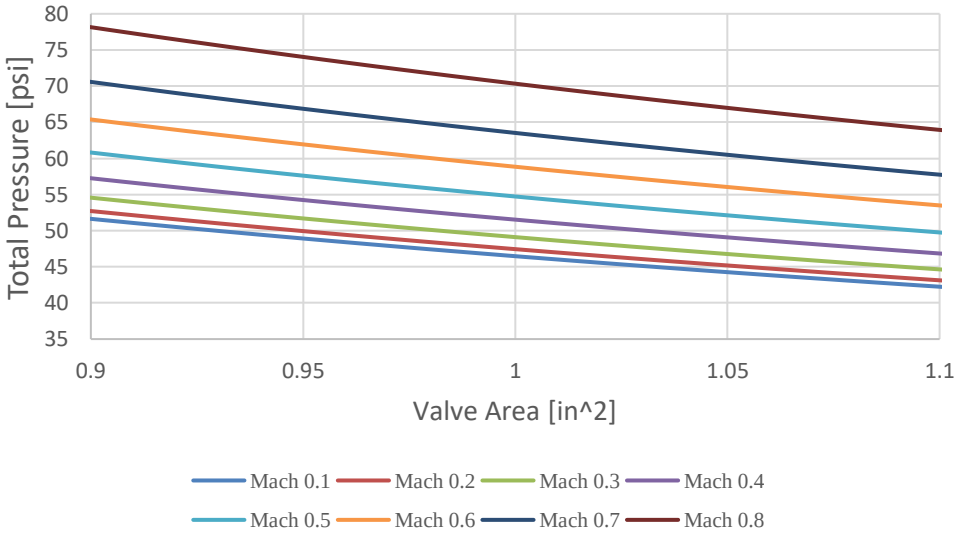

Figure 26: Inlet Valve Total Pressure for Valve Area of 1 in^2

Once again, it would be ideal to implement a pitot tube to measure the total pressure within the pressure chamber in real-time since each engine would have a different correction factor applied to it.

Prospect of Future Design and Experimentation

There are a few areas within the design that lack functionality and practicality, which could be improved on. For starters, the method for outfitting the connection valve to the pressure tank is not ideal since the connection valve is permanently attached in its current configuration. This could drastically be improved by designing a connection system that could be configured to many different value diameters. As mentioned previously, the mass flow rate becomes constrained at the minimum diameter in the system. So, if a connector valve has a diameter of 0.25 inches, then the pressure regulator valve and hose leading up to the air compressor also must contain a diameter no smaller than that 0.25 inches. Given a range of connection valve diameters, an excel file could be used to calculate the appropriate total pressures for the range of flight conditions. Also, regarding the air leakage, a 3D printed connection fitting could be made to precisely fit over the engine cowling to remain securely attached. The flexible duct would then connect the 3D printed piece to the PVC pipe with hose clamps. Ideally, when the engine manufacturer and model are decided, the 3D printed cowling for that engine would be secured and the hose ducting would connect to a PVC pipe of the same diameter as the engine compressor inlet. This would prevent some of the flow expansion occurring from the connection valve and reduce the amount of time to pressurize the pressure chamber, even though that effect would be minimal. Additionally, a pitot tube connected to an absolute pressure transducer with the correct range output would be installed near the leading edge of the engine. This pitot tube could measure total pressure to verify the mass flow parameter analysis and CFD simulation even further. More importantly, however, it could be used to receive real-time feedback from the pressure chamber.

Lastly, a data acquisition computer could be implemented to log and store the real-time pressure data to analyze for later purposes.

Even though this test rig is limited to testing flight speeds in its current configuration, there are methods to add additional components to be able to simulate altitudes as well. A scavenging system for altitude test stands is required to remove exhaust gasses from the test section, adjust the pressure at the test engine exit, and induce an airflow for the sub-ambient condition [1]. If a device like this is placed on the exit of the engine, the static pressure could be reduced to the desired altitude ambient condition. The total pressure being supplied from the connection valve would then be adjusted accordingly. Since the static pressure decreases with altitude, the largest total pressures for a range of operating conditions should be for flight speeds at sea-level. However, since the ambient temperature also decreases with altitude, it is quite possible that a heat exchanger to cool the incoming air would need to be incorporated. Nonetheless, the portability of the test rig allows the user to easily transport the system to a location where the desired altitude condition could be met.

CHAPTER V

ENGINE PERFORMANCE PARAMETERS: EXPERIMENTATION, DATA ANALYSIS, AND RESULTS

Analyzing Engine Performance Parameters at Sea-Level Static Conditions

Setting Throttle Conditions to Obtain Engine Speed Sweep

Evaluating a small-scale turbojet engine's performance parameter requires many conditions to be met to consistently perform tests, record data, and analyze the data obtained. One of the most practical ways of performing a throttle sweep to analyze RPM conditions is to manually change the max RPM value that the manufacturers initially regulate within the engine software. By doing so, as the engine is throttled up to maximum throttle, the software recognizes that the turbine is reaching the desired RPM and starts to reduce the amount of fuel being pumped into the combustion chamber automatically, which allows the turbine to settle at the appropriate RPM value steadily. This also removes the user's need to manually trim the throttle to reach the throttle condition more accurately. Additionally, the user can also adjust the acceleration delay in the software. This parameter corresponds to how quickly the engine throttles up to the condition that the stick position is in. During testing, this value was set near the upper limit for two main reasons. First, in terms of operability and sustainment, it is ideal for throttling the engine up slowly rather than have it produce large amounts of thrust instantaneously. This allows the engine to steadily heat up and provide an adequate fuel flow rate to properly lubricate the rotating machinery within the engine. Secondly, when this value is near the upper limit, the user can quickly throttle the controller or, in this case, a servo-tester to full position almost

instantaneously and permit the software to steadily reach the max throttle condition, reducing user error when duplicating the tests.

The maximum RPM value for the KingTech K-160 is about 128,000. Table 9 illustrates the test matrix used to analyze the different fuels and performance parameters of the turbine engine. The max throttle was reduced in increments of five percent down to negative twenty-five percent of the standard max RPM, which is a throttle condition of 96,000 RPM. Each throttle point was tested twice, and the average of the two values for each parameter was inserted into the table. Thrust data was recorded using the SENSIT software, as mentioned previously. Once the engine reached maximum throttle, this condition was held consistently for fifteen seconds. The thrust data was outputted into an excel file where it could be analyzed. Since the moment arm was set to a 2:1 ratio, the thrust value was then corrected for the length scaling. Furthermore, weather conditions regarding pressure and temperature were recorded by the hour to adjust the data by using corrected parameters.

Table 9: Test Matrix for Evaluating Engine Performance Parameters

Jet A1							
Total Pressure (psi)		Max RPM		Thrust (lbs)	Max EGT (C)	Average EGT (C)	FC (lbm/min)
		-25%		15.44	560	416	0.56
		-20%		18.22	552	408	0.64
M = 0, Pt = 14.7, Pg = 0		-15%		21.69	564	424	0.68
		-10%		25.61	576	424	0.78
		-5%		30.19	556	400	0.92
		Standard		35.7	604	416	0.96

Additionally, aside from thrust, the exit gas temperature (EGT), average exit gas temperature, and fuel consumption were recorded. KingTech also implements techniques in their software to measure and display several parameters on the GSU after each test has been performed, which is where the max EGT and average EGT values were taken from. Fuel consumption was recorded by placing the fuel tank on a scale and visually recording the amount of fuel the engine consumed during the fifteen-second period. The initial weight and end weight

of the fuel were recorded, and the fuel consumption was then calculated in lbs./min and inserted into the table. Based on these recorded parameters, data can be parsed to obtain other performance parameters like specific thrust, thrust specific fuel consumption, the fuel-to-air ratio, and thermal efficiency.

Thrust and Specific Thrust Results

Thrust is simply the reaction force applied on a surface in a direction perpendicular or normal to the surface, and it also represents the amount needed to accelerate one kilogram of mass at a rate of one meter per second squared. Figure 27 shows the corrected thrust graph for the KingTech K-160, which is stated by the manufacturer that it produces around thirty-five pounds of thrust at max throttle.

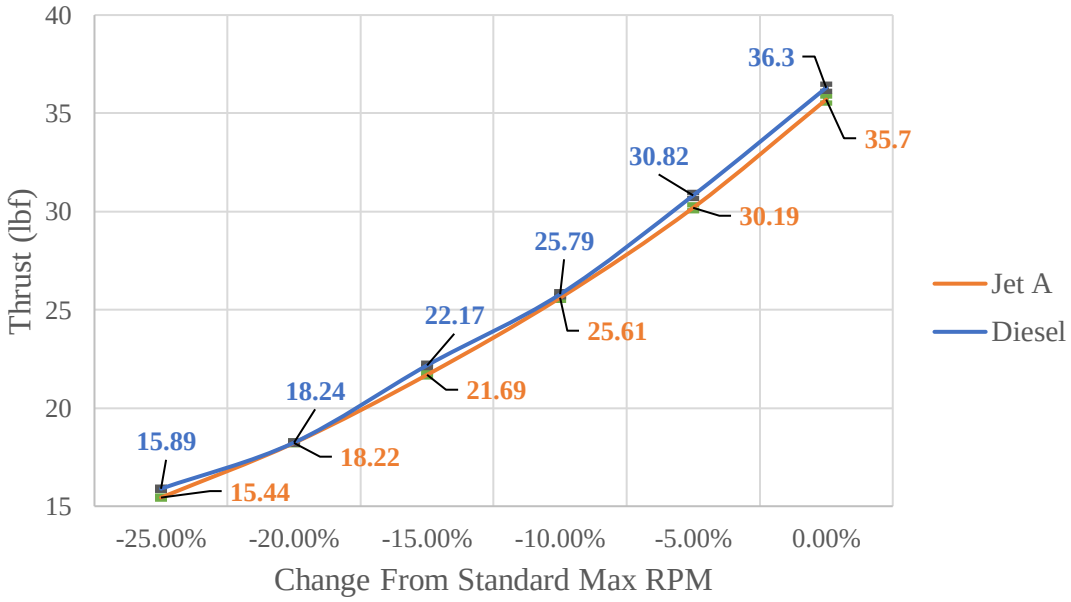

Figure 27: Corrected Thrust as a Function of Max RPM

As shown by the graph, when the test was performed at the standard 128,000 RPM condition, Jet-A produced 35.7 pounds of thrust, and Diesel produced about two percent more thrust at 36.3 pounds. As the max throttle conditions were scaled down in increments of five percent, Diesel consistently produced more thrust with an average of 1.60% greater thrust over the range of throttle conditions. Although the margin of performance is quite small for each

condition, the advantageous trend continued when evaluating the other parameters as well. Interestingly, the software from KingTech has the K-160 producing fifty percent of its overall thrust at seventy-five percent max throttle.

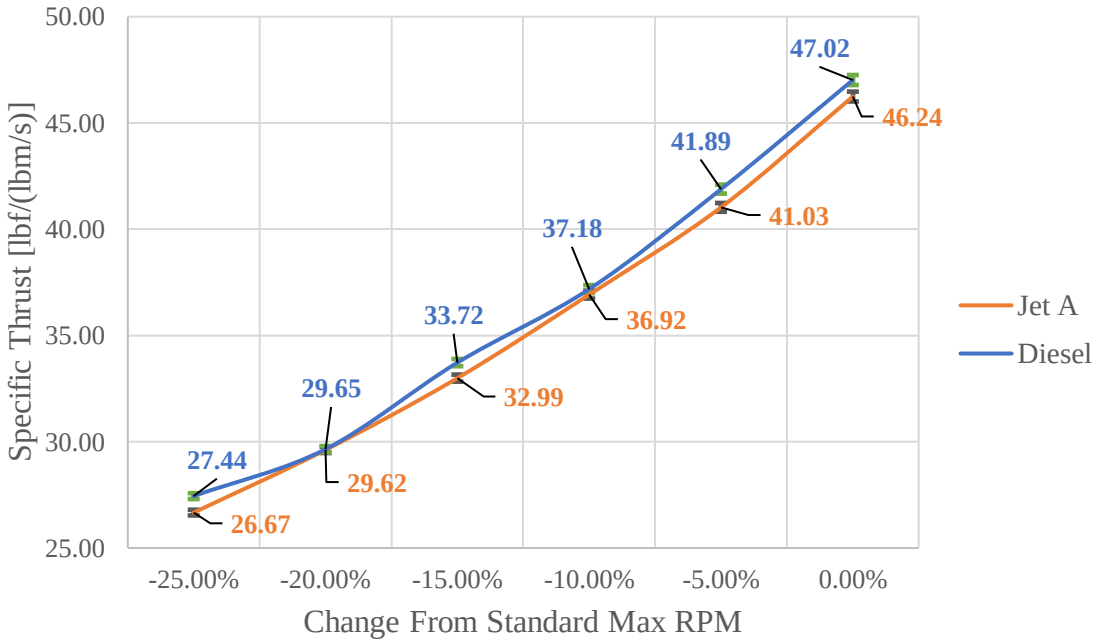

Figure 28: Specific Thrust as a Function of Max RPM

Specific thrust, as shown by Fig. 28, is the thrust per unit air mass flow rate and can be calculated by the ratio of net thrust/total intake airflow [49]. A higher specific thrust usually results in higher noise levels, which is typically not an important consideration for most military applications. Although the manufacturer lists the mass flow rate at full throttle condition, they do not list the mass flow rate for a throttle sweep. So, the mass flow rate of air was calculated by taking the ratio of mass flow rate produced at the full-throttle RPM to that of the desired throttle condition RPM. Likewise, with the thrust, Diesel again performed consistently better than Jet-A. This should be expected since the only parameter changing is the mass flow rate of air at the given throttle condition, which was the same for each fuel type. However, specific thrust is a unique way to determine how "thrusty" an engine is. At full throttle condition, the K-160 produced an average of 46.7 lbf for every pound mass of air each second. The largest variance in

specific thrust, which was 2.84%, came at an RPM value of 96,000, or -25.00% of the standard max RPM. The average percent difference for specific thrust across the throttle sweep was 1.59%; as for the overall trend of the graph, every 5% increment in RPM produced around a 10.00% increase in specific thrust.

Fuel Consumption and Thrust Specific Fuel Consumption Results

Another important parameter to evaluate is how much fuel the engine is consuming during operation. The rate of change of the aircraft weight dW/dt is due to the fuel consumption by the engines. The mass rate of fuel consumed is equal to the product of the installed thrust T and the installed thrust specific fuel consumption [6]. Fuel consumption is an important parameter to consider when evaluating the weight and endurance of an aircraft. Turbojets typically consume much larger amounts of fuel as compared to other engine cycle types. However, turbojets are usually more concerned with how much thrust they can produce per pound of fuel used, which is referred to as the thrust specific fuel consumption.

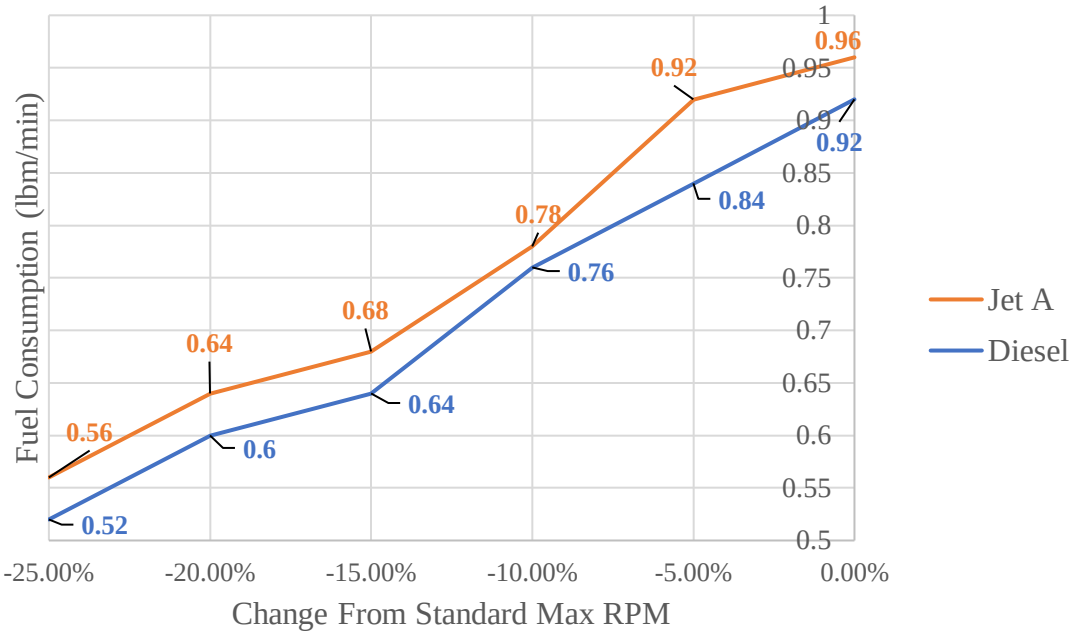

Figure 29: Fuel Consumption as a Function of Max RPM

For the general fuel consumption, Fig. 29 shows the measured values for each throttle condition. As mentioned previously, the fuel tank was placed on a scale to measure the fuel weight before and after the fifteen-second test period at the designated throttle condition. As expected, the most fuel was consumed at the standard max value of 128,000 RPM. Comparing the two fuels, Diesel was considerably more fuel-efficient than Jet-A. The mass flow rate of fuel being pumped into the combustion chamber is governed by the current RPM value of the rotating machinery. Essentially, the software in the ECU knows what RPM value the user has input, and it adjusts the fuel flow rate accordingly until the desired RPM value has been reached. Based on the figure, Diesel was able to produce the necessary amount of energy with less fuel as compared to Jet-A. On average, Diesel was 5.98% more fuel-efficient across the RPM sweep. It is also important to note that user error could have been introduced when visually recording the weight values from the scale; however, the results did remain consistent.

The thrust specific fuel consumption (SFC), designated by S for uninstalled conditions, can be calculated by first calculating the fuel/air ratio f and the thrust per unit of airflow, using Eq (15).

$$S = \frac{f}{F/\dot{m}_0} \tag{15}$$

TSFC is important to analyze how fuel-efficient an engine is when producing thrust. Lower SFC values represent better fuel efficiency and are typically achieved by using large turbofans or turboprops. Turbojets, on the other hand, produce large amounts of thrust at the cost of burning more fuel, resulting in larger values of SFC. Figure 30 demonstrates the SFC of the KingTech K-160 over a sweep of RPM values. Diesel, on average, resulted in a 7.64% lower SFC than Jet-A across the RPM sweep. Although higher RPM values resulted in more fuel consumption, based on the figure, it seems that the amount of thrust produced at full throttle is enough to result in a condition where SFC is the lowest.

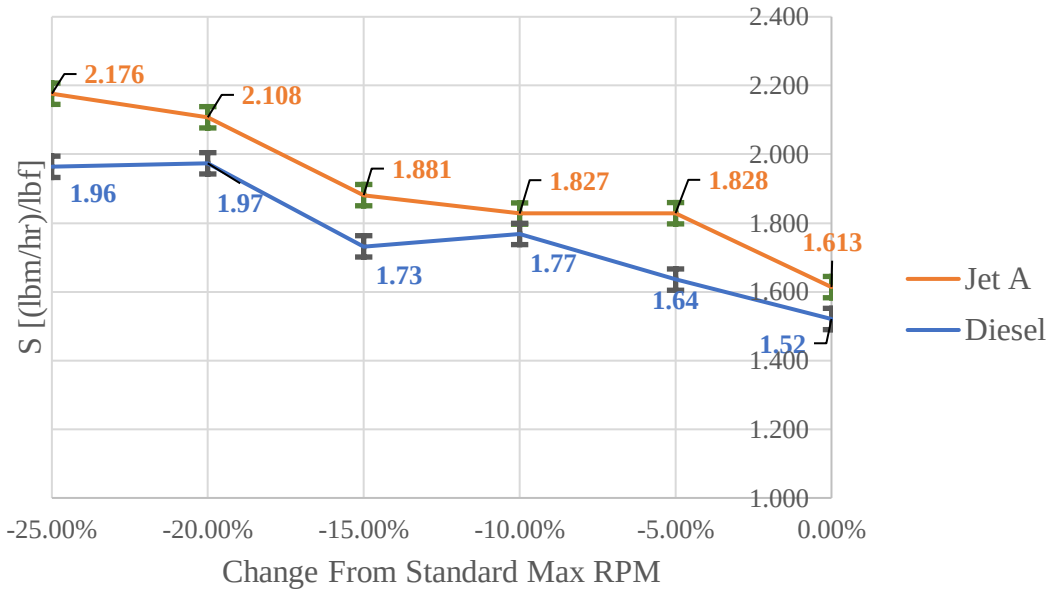

Figure 30: Thrust Specific Fuel Consumption as a Function of Max RPM

Max Exit Gas Temperature Results

In the event where jet engine technical details are unknown, or only a few of them are known from manufacturer's catalogs, the challenge becomes how to calculate and extrapolate critical performance parameters based on only fuel flow, jet exhaust temperature, and total thrust [50]. Once again, the same throttle sweep was used as in the previous sections, which ranged from 96,000 RPM to the standard 128,000 RPM. KingTech provides a "summary page" where it displays data from the previous four rounds of testing. The maximum exit gas temperature (EGT) and average EGT were recorded into an excel table from the GSU using this feature. Figure 31 shows the maximum EGT (°F) for the two fuels at the six different throttle conditions. Overall, Diesel produced values that were 3.92% hotter than Jet-A over that range of throttle conditions. For throttle conditions from -25% to -5% of the standard max RPM, the values remained fairly constant, increasing very slightly. The largest deviation came at the standard RPM value of 128,000, which resulted in a 6.9% difference between the values for the two fuels. Comparing the

two fuels altogether, since the EGT is directly related to the exit velocity of the engine, it should be no surprise that Diesel consistently produced higher EGT values.

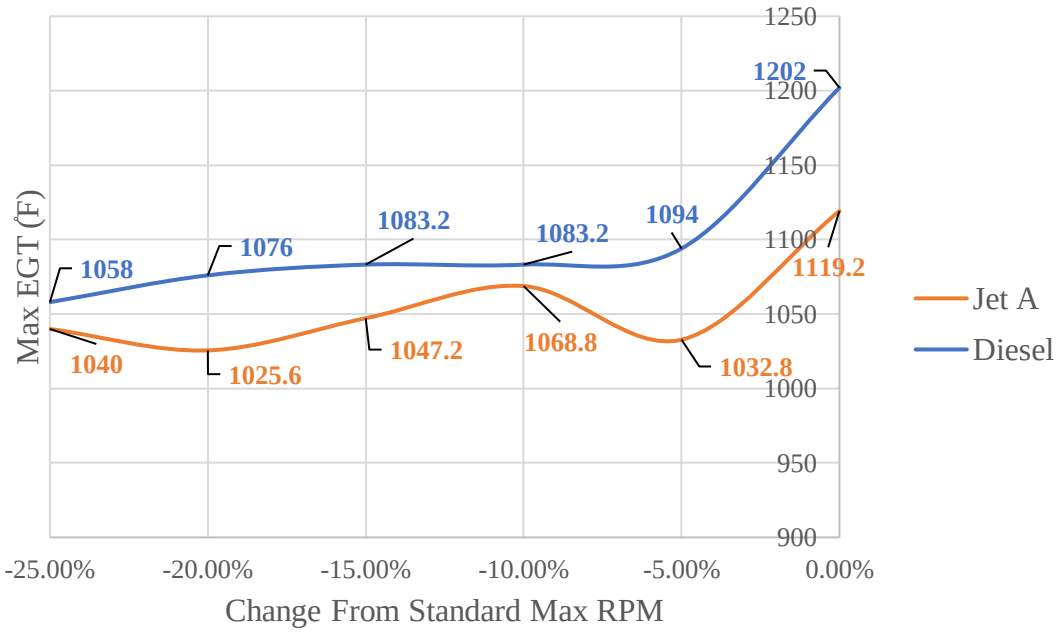

Figure 31: Maximum Exit Gas Temperature as a Function of Max RPM

It should also be noted that if the ambient temperature is low, less heating is needed for the same amount of thrust, reducing the EGT even further. The maximum temperature for a given engine (T_{t4}) is, however, independent of altitude and given by the materials used within the engine, typically the combustion chamber and turbine. In-flight, the continuous maximum temperature can be higher than on the ground when the cooling by the external flow is less effective.

Fuel-to-Air Ratio and Thermal Efficiency Results

The combustion chamber has the difficult task of burning large quantities of fuel, supplied through fuel spray nozzles, with extensive volumes of air, supplied by the compressor, and releasing the resulting heat in such a manner that the air is expanded and accelerated to give a smooth stream of uniformly heated gas. This task must be accomplished with the minimum loss in pressure and with the maximum heat release within the limited space available [51]. The fuel-

to-air ratio f, shown by Eq. (16), is simply how much fuel is being consumed per the same rate as the mass flow of air. Larger values of f indicate the engine is less efficient at producing thrust.

$$f = \frac{\dot{m}_{fuel}}{\dot{m}_{air}} \tag{16}$$

Jet-A produced an average f of 0.019 across the throttle sweep, and Diesel produced an average value of 0.017. Comparing the two fuels, Diesel performed 6.26% better than Jet-A over the range of throttle conditions. Similar to the thrust specific fuel consumption, both fuels produced larger values of f near the lower throttle RPMs, shown in Fig. 32. It seems that the KingTech engines inherently drive more fuel per pound of thrust produced at lower throttle conditions. This could be due to the lower EGT values occurring near, the lower RPM's, resulting in lower thermal efficiencies.

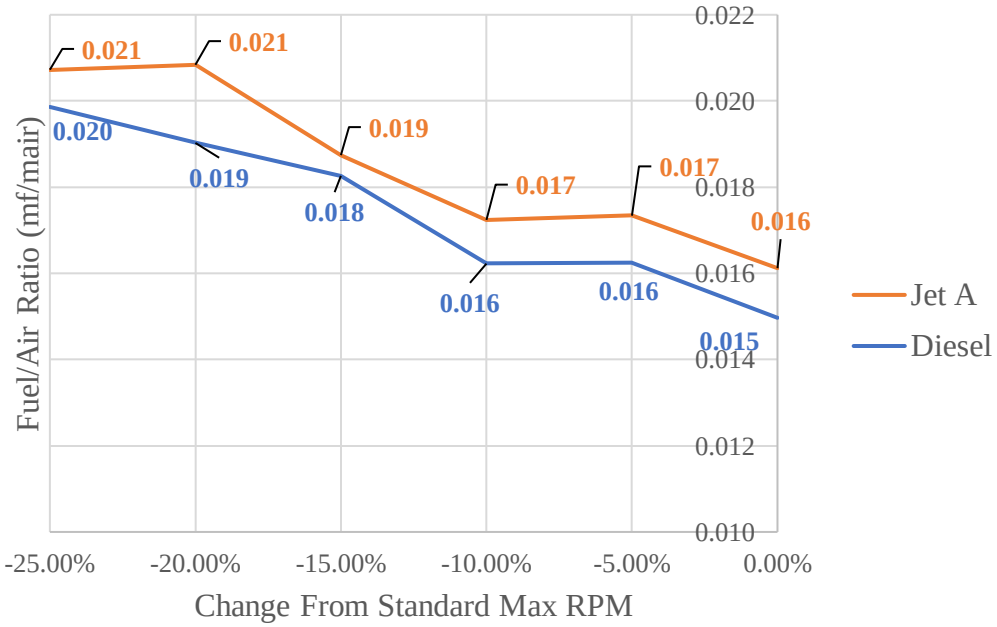

Figure 32: Fuel-to-Air Ratio as a Function of Max RPM

The thermal efficiency (η_{TH}) of an engine is another especially useful engine performance parameter. Thermal efficiency is defined as the net rate of organized energy (shaft power or kinetic energy) out of the engine divided by the rate of thermal energy available from the fuel in the engine. The fuel's available thermal energy is equal to the mass flow rate of the fuel

multiplied by the fuel lower-heating value h_{PR} [6]. Thermal efficiency, given by Eq. (17), is primarily a function of the fuel-to-air ratio, exit velocity, and lower-heating value.

$$\eta_{TH} = \frac{a_0^2[(1+f)(V_9/a_0)^2 - M_0^2]}{2g_c f h_{PR}} \tag{17}$$

When calculating $\eta_{TH,}$ since the engine tests were static, M_0 was equal to zero. For h_{PR}, a value of 43 MJ/kg for Diesel was used and 43.6 MJ/kg for Jet-A. Thermal efficiency for commercial aircraft engines has improved from about 30% to over 50% over the past fifty years [51]. However, as shown by Fig. 33, small-scale turbojets have much lower thermal efficiencies due to their limitations in material properties and increase in component losses. Jet-A had an average thermal efficiency of 8.00% over the throttle range, while Diesel's average thermal efficiency was 9%. Diesel was overall 10.5% more thermally efficient than Jet-A. The standard max full throttle value of 128,000 RPM resulted in the highest thermal efficiency over the throttle range, with lower RPM values resulting in lower efficiency.

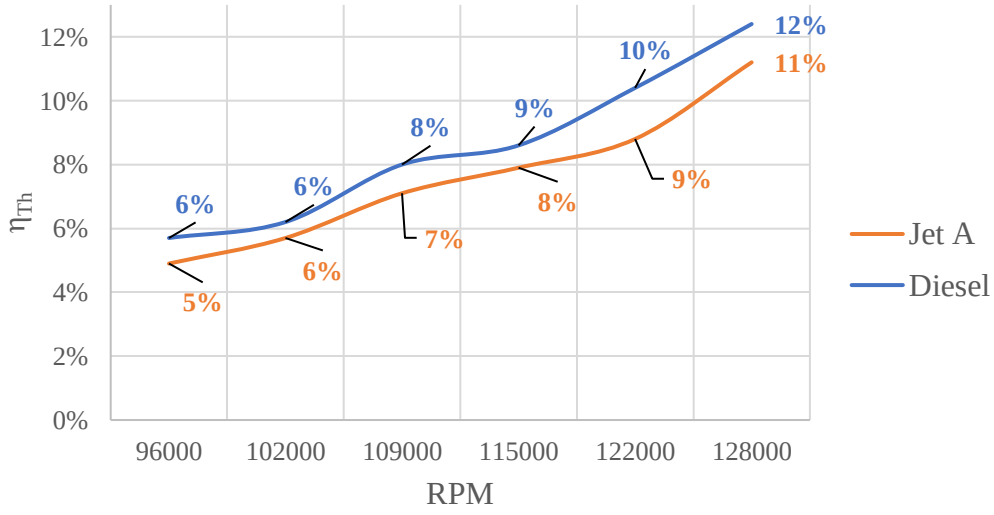

Figure 33: Thermal Efficiency vs. RPM

Conclusions of Sensitivity Study

Uncertainty Analysis

Kline and McClintock developed a useful method to estimate the measurement error using a root-sum-square technique. The overall uncertainty, shown by Eq. (18), is a function of

the precision and bias error. Not only that but a sum of both those errors for each measurement device used in the experiment.

$$U_X = \sqrt{{P_X}^2 + {B_X}^2} \tag{18}$$

$$U_R = f\left(U_{X_1}, U_{X_2}, U_{X_3}, \ldots U_{X_n}\right) \tag{18.1}$$

$$U_R = \pm\sqrt{\left(\frac{\partial R}{\partial X_1} U_{X_1}\right)^2 + \left(\frac{\partial R}{\partial X_2} U_{X_2}\right)^2 + \ldots + \left(\frac{\partial R}{\partial X_n} U_{X_n}\right)^2} \tag{18.2}$$

Knowing the equation for a given parameter, the partial derivative with respect to the other parameters within that equation can be taken. These are called the influence coefficients. This method was performed to determine the overall uncertainty contributing to the data evaluated in this study. Since the instrumentation in this study comprised of a load cell, digital scale to measure weight, and pressure gauge, a mixture of both precision and bias error will be incorporated into the overall uncertainty. Specifically, for specific fuel consumption, after the root sum of squares was taken and the partial derivatives were performed with respect to the mass flow rate of fuel and thrust, as shown by Equations 19.1 and 19.2, respectively. the overall uncertainty came out to be 1.65%.

$$SFC\left(\dot{m}_f, F\right) = \pm\sqrt{\left(\frac{\partial SFC}{\partial F} U_F\right)^2 + \left(\frac{\partial SFC}{\partial \dot{m}_f} U_{\dot{m}_f}\right)^2} \tag{19}$$

$$\frac{\partial SFC}{\partial \dot{m}_f} = \frac{\partial}{\partial \dot{m}_f}\left(\frac{\dot{m}_f}{F}\right) = \frac{-\dot{m}_f}{F^2} \tag{19.1}$$

$$\frac{\partial SFC}{\partial F} = \frac{\partial}{\partial F}\left(\frac{\dot{m}_f}{F}\right) = \frac{1}{F} \tag{19.2}$$

This uncertainty considered the precision errors resulting from the sampling data and the bias error given by the manufacturers. It was determined that the largest influencer came from

taking the partial with respect to F. This is due to the large range in the load cell. As the range for the load cell increases, the error while measuring a given value becomes more significant. So, choosing a load cell with a lower maximum force input could be more desirable to achieve higher accuracy and decrease the overall uncertainty. Table 10 shows the rest of the instrumentation uncertainty.

Table 10: Kline-McClintock Uncertainty Analysis

Parameter	Uncertainty
Thrust (lbf)	0.05%
SFC [(lbm/hr)lbf]	1.65%
Specific Thrust [lbf/(lbm/s)]	0.05%
Fuel Consumption (lbm/s)	0.01%
Fuel-to-Air Ratio	0.01%

Although flight speeds were not conducted while evaluating the performance parameters of the engine, once done, this same process would need to be applied for finding the uncertainty due to measuring the total pressure. Given a total and static pressure, the Mach number can be calculated using Eq. (20) and the uncertainty can be found by taking the partial derivatives as shown by Eq. (19.1).

$$M = \sqrt{\frac{2}{\gamma-1}\left[\left(\frac{P_{t_9}}{P_9}\right)^{(\gamma-1)/\gamma} - 1\right]} \tag{20}$$

$$M\left(P_{t_9}, P_9\right) = \pm\sqrt{\left(\frac{\partial M}{\partial P_{t_9}} U_{P_{t_9}}\right)^2 + \left(\frac{\partial M}{\partial P_9} U_{P_9}\right)^2} \tag{20.1}$$

$$\frac{\partial M}{\partial P_{t_9}} = \frac{\partial}{\partial P_{t_9}}\left(\sqrt{\frac{2}{\gamma-1}\left[\left(\frac{P_{t_9}}{P_9}\right)^{(\gamma-1)/\gamma} - 1\right]}\right) = \frac{P_{t_9}^{\frac{-1}{\gamma}} P_9^{\frac{-\gamma+1}{2\gamma}} (\gamma-1)^{\frac{1}{2}}}{2^{\frac{1}{2}}\gamma\left(P_{t_9}^{\frac{\gamma-1}{\gamma}} - P_9^{\frac{\gamma-1}{\gamma}}\right)^{\frac{1}{2}}} \tag{20.2}$$

$$\frac{\partial M}{\partial P_9} = \frac{\partial}{\partial P_9}\left(\sqrt{\frac{2}{\gamma-1}\left[\left(\frac{P_{t_9}}{P_9}\right)^{(\gamma-1)/\gamma} - 1\right]}\right) = \frac{-P_{t_9}^{\frac{\gamma-1}{\gamma}} P_9^{\frac{-3\gamma+1}{2\gamma}} (\gamma-1)^{\frac{1}{2}}}{2^{\frac{1}{2}}\gamma\left(P_{t_9}^{\frac{\gamma-1}{\gamma}} - P_9^{\frac{\gamma-1}{\gamma}}\right)^{\frac{1}{2}}} \tag{20.3}$$

After doing so, the influence coefficients are such, given by Eq. (20.2) and (20.3) The overall uncertainty can then be found given the accuracy of the gauges provided by the manufacturers, and accounting for the bias error, for each flight condition tested.

Overall Engine Performance

Figure 34 shows the variation of engine performance with both specific thrust and thrust specific fuel consumption for the KingTech K-160 turbojet engine. Analyzing both trends, if the fuel type being burned is unknown, a max throttle RPM from 119,000 to 122,000 should be considered to maximize the specific thrust while minimizing the thrust specific fuel consumption.

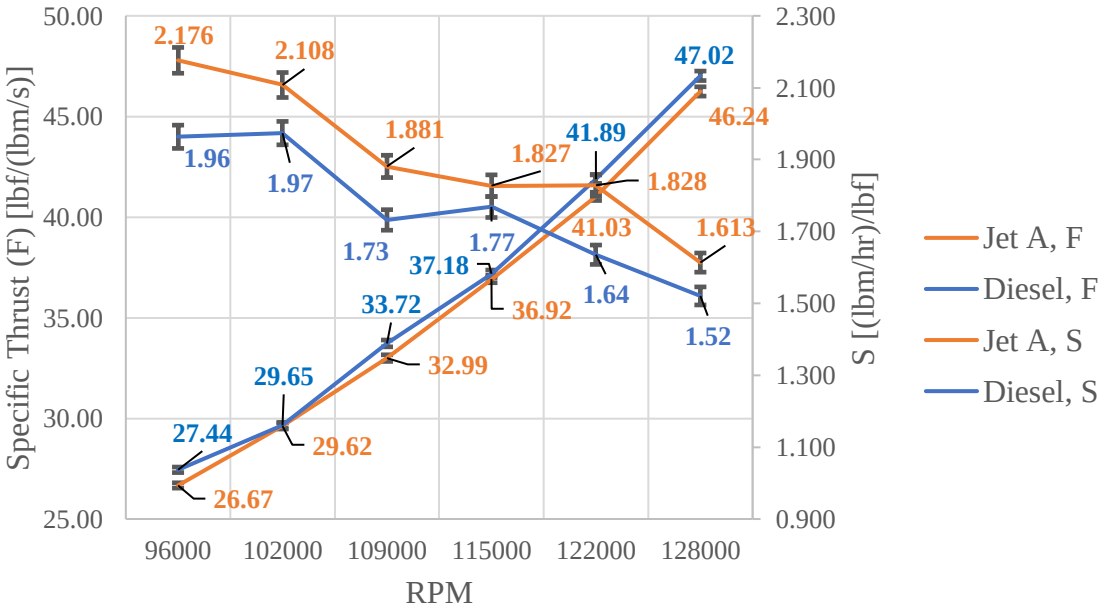

Figure 34: Engine Performance as a Function of Max RPM

For Jet-A specifically, the optimum point to balance the two variables is around 122,000 RPM. At that condition, the specific thrust is 42 lbf/(lbm/s) and the SFC is 1.8 (lbm/hr.)/lbf. Diesel, on the other hand, the optimized point occurs at 119,000 RPM. This condition yields a specific thrust of

39.5 lbf/(lbm/s) and SFC of 1.6 (lbm/hr.)/lbf. This performance graph should be analyzed over an entire range of flight values to concur which throttle conditions for this small turbine engine should be considered for optimized performance. Although it is like previous graphs, a partial-throttle performance graph for thrust specific fuel consumptions is another great method to use to demonstrate the performance of the engine at different thrust conditions. As mentioned previously, for the KingTech K-160, the SFC tends to decrease as more thrust is produced, as shown by Fig. 35.

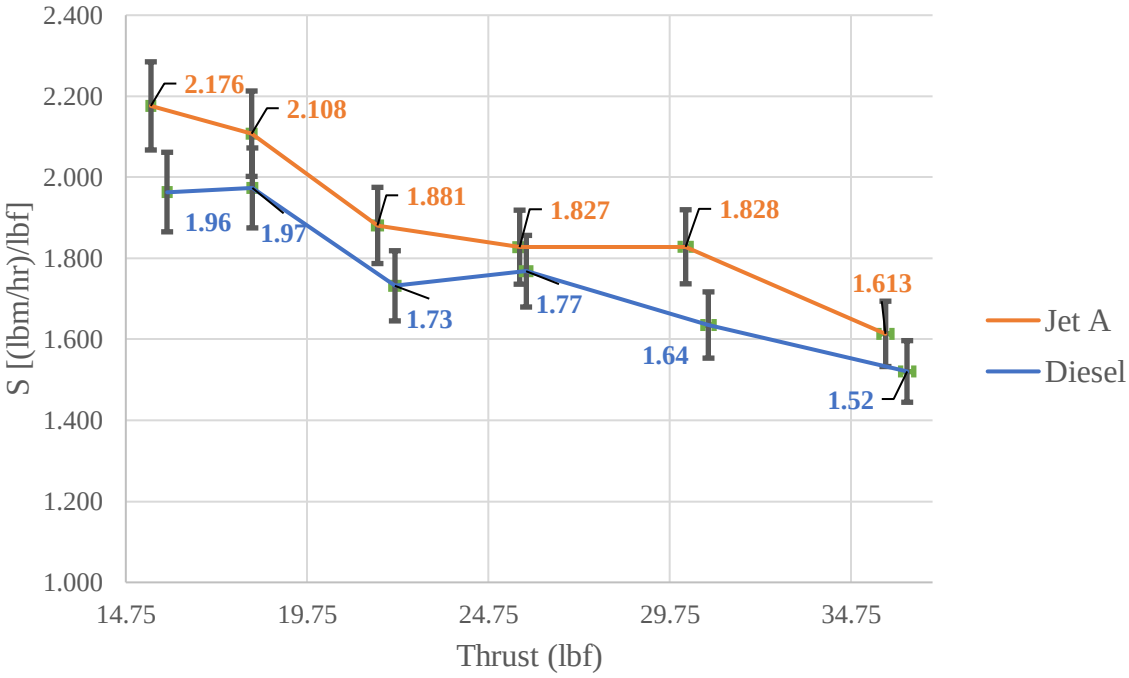

Figure 35: Partial-Throttle Performance, Thrust Specific Fuel Consumption

It may be tempting to assume small-scale turbojets are just miniaturized versions of larger gas turbine engines. However, these small-scaled engines are not simply a size reduction of the larger engines. They present unique characteristics such as simple designs with single-stage compressors and turbines, high rotational speeds, low-pressure ratios, and the ability to operate with a variety of fuels. They can and have been used by many researchers due to their ability to be operated within the confines of a laboratory [52]. Given the software integrated into many

small-scale turbines today, which output engine parameters like exit gas temperature and RPM and coupled with having a procedure to measure thrust and fuel consumption, important performance parameters can be evaluated to determine certain characteristics of the engine. As for these small engines, the viscous operating environment, and the loss mechanisms, which are proportionally more significant in the case of small turbomachines, lead to higher pressure losses and larger variations of the thermodynamic properties in each section of a small-scale turbine [52].

Limitations of Current Design and Future Considerations

It should be noted that all thrust measurements were tested at sea-level static conditions. This means that the pressure simulation rig was not used since the total pressure was that of ambient conditions, with a flight condition of Mach 0. Additionally, the small valve diameter on the pressure tank limits the mass flow rate of air being delivered into the tank by choking the flow, regardless of the total pressure being fed by the air compressor. A quick MFP calculation showed the maximum mass flow rate based on the current inlet connection valve area is 0.23 lbm/s, about that of which a K-70 ingests. Meaning, due to the significant RPM values, which require much larger amounts of mass air flow, the design would have to incorporate a valve of the appropriate diameter in addition to a larger compressor to provide the necessary flow rate. If the flow rate is not met, the turbine would essentially suck the air from the pressure chamber like a vacuum causing an adverse pressure gradient through the system. This would potentially cause the flame to propagate towards the compressor of the engine, causing a blowout rather than expel the exhaust through the nozzle. Furthermore, the method for recording fuel consumption is not ideal. Preferably, a weight scale that is capable of real-time logging data would give the user the ability to analyze and parse raw data as opposed to relying on visual feedback. Lastly, more software settings within the KingTech engine can be adjusted in future testing to finely tune certain characteristics of the fuel flow rate, idle RPM, deacceleration delay, pump power, etc.

CHAPTER VI

CONCLUSIONS, OUTCOMES, AND RECOMMENDATIONS

Conclusion and Major Observations

In conclusion, small-scale turbojets provide the necessary capabilities to adequately perform research to analyze combustion characteristics without needing substantial outside resources. These small engines typically already include instrumentation like pitot tubes and thermocouples to measure the air properties as they flow through the engine, which reduces the complexity and uncertainty of the test rig apparatus. The engine control units that control these engines have numerous settings that can be individually tuned by the user to optimize flight through a mission profile. The learning curve for operating these engines is prominent since they are simple, resilient, affordable, and can run on several types of fuels. Due to the simplicity, however, the performance parameters greatly suffer as compared to full-scale commercial and military turbojets.

Although the measured thrust obtained from the experiment was near identical to the manufacturer's specifications, the performance at each RPM value came with considerable fuel consumption. The larger amounts of thrust produced at the higher RPM values were enough to offset this drawback, thus, the engines' thrust specific fuel consumption decreased with an increase in RPM. For both Diesel and Jet-A, the fuel-to-air ratio decreased with an increase in RPM as well, which also related to the overall thermal efficiency of the engine. Again, at higher RPM values, the thermal efficiency was the greatest. At maximum throttle, the thermal efficiency

using Jet-A as the fuel type was 11.0%, and for Diesel, it was 12.0%, much lower than the 30% to 50% expected from full-scale turbojets today [51].

When the proper conditions are known, a mass flow parameter analysis can be greatly beneficial to relate total properties, area, and mass flow rate. This analysis coupled with compressible flow relationships can help predict the behavior of air as it flows through different environments with an increase in pressure and velocity. Simulating these operating conditions can be useful for analyzing the start reliability and performance parameters of the engine. However, these equations solve ideal scenarios through a constant area duct. Additional analysis using computational fluid dynamic simulations verifies the previous analyses.

Outcomes Attained from Research Objectives

Design of Test Apparatus to Simulate Operating Conditions

The first objective was to develop and demonstrate a design apparatus that could simulate in-flight and ground speed operating conditions. Figure 36 shows a close-up of the final design and how the apparatus was attached to the KingTech K-160 engine. Given the 35 lbs. of thrust that the engine produced, a test stand with stout components that could withstand the forces was designed and assembled. T-slot aluminum was utilized throughout the apparatus for its ability to secure components effectively while also retaining adjustability. The design of the test stand also allows for easy interchangeability of small-scale turbojets that produce up to 500 lbs. of thrust. The pressure chamber that mates to the face of the inlet can be done very quickly with the use of hose clamps. This means if static conditions were desired, removing the pressure chamber was simple and time efficient. Furthermore, thanks to the flexible ducting, the thrust measurement could still be obtained even with the pressure chamber affixed to the engine. Once all the components were assembled and ready for testing, the procedure remained simple for each test condition, reducing the amount of error between tests. Essentially, the only component that was even touched between each test was the pressure regulator valve to adjust the inlet pressure.

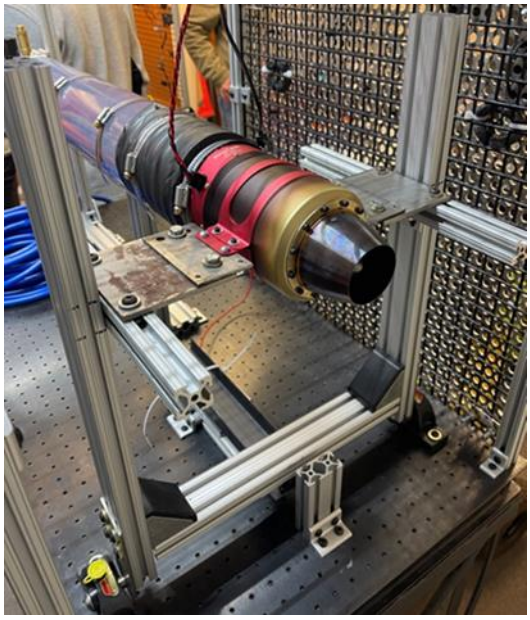

Figure 36: Final Ground Test Rig Apparatus

Identifying Combustion Parameters that Affect Start Reliability

The second objective was to determine which combustion parameters are superior in affecting the start reliability of a small-scale turbojet engine. Initially, it was sought out to analyze how different fuels, additives, and equivalence ratios affected this and the overall performance parameters of the engine. However, the testing procedure mostly focused on comparing Jet-A to Diesel when analyzing the start reliability, and this was done over a range of flight conditions while independently adjusting the fuel-to-air ratio. Figure 24 (page 25) shows the optimal fuel-to-air ratio for static conditions and flight speeds of Mach 0.2 and 0.4. The percentages shown reflect the variability from the standard pump voltage value of 56. At every flight condition, Diesel provided the necessary combustion characteristics to successfully ignite the fuel-air mixture in the combustion chamber. A clear trend was prominent and showed that with an increase in flight speed, the fuel-to-air ratio decreases, thus, negatively impacting the start reliability of the engine. At flight speeds ranging from static to Mach 0.2, both Jet-A and Diesel had successful ignition with the standard pump voltage. At Mach 0.4, Jet-A no longer ignited the fuel-air mixture, whereas, Diesel remained successful, even at a much leaner fuel-to-air ratio.

Based on the testing, the results indicated that the more volatile fuel (Jet-A) required more time for ignition than the less volatile fuel (Diesel). Since the more volatile fuel had a leaner fuel-air ratio at ignition, the temperature, and consequently, the pressure rise due to combustion would be less than for a less volatile fuel.

Ideally, this ground test rig would be taken to locations with different altitudes to perform the same ignition tests to effectively map out an entire operating envelope for a successful ignition. As mentioned previously, since the total temperature properties significantly change with an increase in altitude, additional components like a heat exchanger may be needed to cool the incoming air.

Advantages of a Small-Scale Turbine Engine Ground Test Rig

The final objective was to demonstrate the feasibility, mobility, and convenience of using a small-scale turbojet engine to analyze combustion characteristics. The ground rig used in this study was comprised mostly of parts from previous projects, miscellaneous components found around the lab, and a few parts that needed to be purchased. The KingTech K-160 turbojet engine itself costs around $2500 [38], however, the test components without the engine cost merely $3500. The total cost breakdown is given in Table 11.

Table 11: Ground Test Rig Component Cost Breakdown

Ground Test Rig Components	Quantity	Total Price
4in diameter PVC Pipe	1	$ 74.00
PVC Cap	1	$ 17.00
Optical Table	1	$ 200.00
Pressure Regulator	1	$ 43.00
Pressure Gauge	1	$ 13.00
Pneumatic Hose	1	$ 19.00
Quick-Disconnect Fittings	5	$ 80.00
Hose Clamps (pack of 10)	1	$ 15.00
T-Slot Aluminum	14	$ 100.00
Futek Load Cell	1	$ 600.00
Futek USB Connector	1	$ 1,000.0
Digital Scale	1	$ 45.00
Mass Flow Sensor	1	$ 200.00
Air Compressor	1	$ 1,000.0
KingTech K-160 Engine	1	$ 2,500.0
Total Cost		**$ 5,906.0**

Having a ground rig of this affordability is highly advantageous to test rigs that are magnitudes more expensive. Smaller commercial facilities can implement ground rig designs like this one to test their fuel mixture performances, additives, or other fuel characteristics. Military laboratories can use these rigs to optimize the in-flight performance of their aircraft by simulating the operating conditions. Maintenance with this system is extremely inexpensive since the only component that should ever need replacing is the turbine engine itself, which typically needs to be overhauled every twenty-five hours.

Facilities that are capable of testing larger engines typically are not able to easily switch out engines very effectively, due to the size and weight of the engine. The design of the test apparatus in this study allows the user to analyze several engines without heavily modifying the general stand. Metal plates on each side of the engine mounts can be adjusted for various diameters by extending them inwards or outwards laterally. Brackets are also present to adjust the engines forward to backward position, allowing the center of gravity to always be placed above the bearings of the moment arm. The t-slotted aluminum also gives the user the ability to adjust the moment arm length to account for thrust changes when interchanging different engines. Most of the fuel systems for these engines will also remain compatible since the fuel distribution systems comprise of the same components, such as the fuel tank, fuel pump, ECU, and batteries.

Lastly, a ground test rig of this size can be easily transported to different altitudes to conduct similar experiments. The design is affixed to an optical table that sets on a wheelable cart. This optical table can easily be removed from the cart to place in transportation vehicles, wind tunnels, or other facilities. Numerous times this cart containing the ground rig was wheeled to an outdoor location to be tested, which was quick and efficient each time. Previous research found that the maximum total pressure that would be supplied from the air compressor would be 40 psi, which means many air compressors could supply adequate pressure. However, the volume of the tank also became important during testing, especially when simulating higher total pressures since the mass flow rate of air was drastically increased. Finally, in larger facilities,

several computers may be required to operate the engine and the test rig itself. In this design, one desktop or mobile computer can be used to operate the engine and instrumentation.

Final Remarks and Recommendations

The data gathered from the successful ignition attempts illustrate the optimal fuel-to-air ratio to use for flight speeds of Mach 0, 0.2, and 0.4 to maximize the start reliability of a small-scale turbojet. Although no data were obtained for any altitudes higher than sea-level, the map of successful ignitions is still beneficial to fast-moving aircraft that rely on ignition near sea-level like with rocket-assisted take-off vehicles. Nonetheless, Fig. 14 (page 29) illustrates the expected total pressure due to flight speed and altitude. If flight speed remains under Mach 0.8, the simulated total pressure should never exceed 22 psi. It also demonstrates that with an increase in altitude, the dynamic pressure for a given Mach number decreases. Once the rig has been tested at several different altitudes, a flight envelope can be built for essentially any altitude and flight speed to optimize the engine performance using this figure to achieve the correct simulated conditions.

A proposed design to simulate an entire flight envelope of an aircraft would require several modifications to the current design. Since the total pressure that is supplied from the air compressor is highly dependent on the connection inlet valve diameter, a functional way to interchange these valve diameters would give the user several options to maximize the different types of air compressors that could be used. Furthermore, the correct inlet total pressure values being supplied by the air compressor are based on this connection valve area. The total pressure charts outlined in this study are specific to sea-level conditions and do will not function in their current state for different altitudes but can be adjusted to do so. Lastly, manufacturing a 3D printed inlet to fit over the cowling of the desired engine would mitigate much of the air leakage that occurs through the connection ports.

REFERENCES

[1] Lucido, N., et al. “A Modular Altitude Test Stand for a Small-Scale Turbojet.” *SciTech,* 2018.
[2] Cooper, Jonathon, and Lloyd Dingle. “Engineering an Afterburner for a Miniature Gas Turbine Engine.” *Aircraft Engineering and Aerospace Technology*, 2005.
[3] Armstrong, J., et al. “Investigation of Several Techniques for Improving Altitude-Starting Limits of Turbojet Engines.” *NACA Research Memorandum,* 1952.
[4] Elderidge, R., Stead, K. “Small Turbojet Windmill Prevention.” December 2019.
[5] Coulon, T., et al. “Thrust-to-Weight Improvement of Jetcat P100-RX Turbojet Engine.” May 2019.
[6] Mattingly, J. D., and Boyer, K. M., *Elements of Propulsion: Gas Turbines and Rockets*, VA: AIAA, 2016.
[7] Mattingly, J. D., Boyer, K.M., Haven, B. A., Heiser, W. H., and Pratt, D. T., *Aircraft Engine Design*, Reston, VA: AIAA, 2018.
[8 Kattchee, J., Merkel, I., Mena, D., Tucker, D., and Wilton, M., JetCat P100RX & Test Stand User Manual, Stillwater, OK: Oklahoma State University, 2018.
[9] Benini, E., and Giacometti, S., “Design, manufacturing, and operation of a small turbojet-engine for research purposes” Applied Energy, Volume 84, Issue 11, 2007.
[10] H.H. Chu, Hsiao-Wei Chiang, “Aerospace technology development – Small gas-turbine development” Aerospace Development Planning, National Science Council, Taiwan, ROC, 1996.
[11] El-Sayed, A. F., *Aircraft Propulsion and Gas Turbine Engines*, CRC Press, 2008.
[12] Coplin, J. F., Turbofan gas turbine engine, U.S. Patent 4827712A, 1986.
[13] Russel, J. B., *Performance and Stability of Aircraft*, Butterworth-Heinemann, 1996.
[14] Commaret, P., Desaulty, M., Hernandez, D., Laugeois, J., Mandet, G., and Martinez, R., Turbojet engine combustion chamber with a double wall converging zone, U.S. Patent 4901522A, 1990.
[15] Zheng, J., Wang, J., Zhao, Z., Wang, D., and Huang, Z., “Effect of equivalence ratio on combustion and emissions of a dual-fuel natural gas engine ignited with diesel”, Applied Thermal Engineering, Volume 146, 2019.
[16] Oates, G. C. (ed.), *Aerothermodynamics of Aircraft Engine Components*, AIAA Education Series, AIAA, Washington, DC, 1995.
[17] Oates, G. C. (ed.), *The Aerothermodynamics of Aircraft Gas Turbine Engines*, AFAPL-TR-7852, Air Force Aero Propulsion Laboratory, Wright-Patterson AFB, OH, July 1978.
[18] Lefebvre, A. H., *Gas Turbine Combustion*, Hemisphere, New York, 1983.
[19] Williams, F. A., *Combustion Theory*, Addison-Wesley, Reading, MA, 1965.
[20] Spalding, D. B., *Combustion and Mass Transfer*, Pergamon Press, Elmsford, NY, 1979.
[21] Grobman, J., Jones, R. E., and Marek, C. J., “Combustion,” *Aircraft Propulsion*, NASA SP-259, 1970.
[22] Yonezawa, Y., Toh, H., Goto, S., and Obata, M., “Development of the jet-swirl high loading combustor”, AIAA, Orlando, Florida, 1990
[23] Lefebvre, A. H., “Fuel Effects on Gas Turbine Combustion-Ignition, Stability, and Combustion Efficiency”, ASME. *J. Eng. Gas Turbine Power*, January 1985.
[24] Oates, G. G. (ed.), *Aircraft Propulsion Systems Technology and Design*, AIAA Education Series, AIAA, Washington, DC, 1989.

[25] John, J., and Keith, T., *Gas Dynamics*, Pearson, 3rd edition, 2006.
[26] Kim, C., Yoon, M., Yang, S., and Lee, D., "An Altitude Test Facility for Small Jet Engine," AIAA 2001-3680, 2001.
[27] NASA Glenn Research Center, "Propulsion Systems Laboratory," https://www1.grc.nasa.gov/facilities/psl/ Retrieved 2021-01-14
[28] Golladay, R. L., and Bloomer, H. E., "Investigation of altitude starting and acceleration characteristics of J47 turbojet engine", Lewis Flight Propulsion Laboratory, Cleveland, Ohio, 1951.
[29] Straight, D. M., and McCafferty, R. J., "Turbojet-Engine Starting and Acceleration", NACA, RM E55G28, 1950.
[30] Childs, J. H., "Preliminary Correlation of Efficiency of Aircraft Gas-Turbine Combustors for Different Operating Conditions", NACA, RM E50F15, 1950.
[31] "Gas Turbine Engine Performance Station Identification and Nomenclature", Aerospace Recommended Practice (ARP) 755A, Society of Automotive Engineers, Warrendale, PA, 1974.
[32] Liew, K. H., Urip, K., and Yang., S. L., "Parametric Cycle Analysis of a Turbofan Engine with an Interstage Turbine Burner", AIAA. *Journal of Propulsion and Power*, Vol. 21, No. 3, May-June 2005.
[33] Kumar, K., *Combustion Data for Jet-A, its Constituent Components, and Surrogate Mixtures*, Multi-Agency Coordination Committee for Combustion Research – 2009 Fuels Summit, 2009.
[34] JetCat USA. "Turbine Data Sheet", 2015.
[35] *Choked Flow of Gases* O'Keefe Controls Co., Trumbull, CT, 2003
[36] Klopfenstein, R., "Air velocity and flow measurement using a Pitot tube", ISA Transactions, Volume 37, Issue 4, 1998.
[37] Wecel, D., Chmielniak, T., and Kotowicz, J., "Experimental and numerical investigations of the averaging Pitot tube and analysis of installation effects on the flow coefficient", Flow Measurement and Instrumentation, Volume 19, Issue 5, 2008.
[38] KingTech Turbines. "KingTech Turbines – Engine Manual Series 2", 2016.
[39] Legal Information Institute. (n.d). *14 CFR 25.903 – Engines.* https://www.law.cornell.edu/cfr/text/14/25.903 Retrieved 2021-02-13
[40] Federal Aviation Administration. (March 19, 1986). *AC 25.939-1 – Evaluating Turbine Engine Operating Characteristics.*
[41] United States Department of Labor. (n.d). *Occupational Safety and Health Administration. 1910.157 – Portable fire extinguishers.*
[42] European Biofuels Agency. (2013). *2 million tons per year: A performing biofuels supply chain for E.U. aviation 1-37.*
[43] Ranucci, C., Alves, H., Monteiro, M., Kugelmeier, C., Bariccatti, R., Oliveira, C., and Silva, E., "Potential alternative aviation fuel from jatropha (Jatropha curcas L.), babassu (Orbignya phalerata) and palm kernel (Elaeis guineensis) as blends with Jet-A1 kerosene", Journal of Cleaner Production, Volume 185, 2018.
[44] Lee, C.H., Lee, K.H., "An experimental study on the combustion and emission characteristics of a stratified charge compression ignition (SCCT) engine", Energy Fuels, 21, 2007.
[45] Arenas, E.G., Palacio, M.C., Juantorena, A.U., Fernando, S.E. and Sebastian, P.J., "Microalgae as a potential source for biodiesel production: techniques, methods, and other challenges", Int J Energy Res, 2017.
[46] Bhosale, R.R., "Hydrogen production via thermochemical H_20 splitting using $CaSO_4$-CaO redox reactions", Int J Hydrogen Energy, 2019.
[47] Manigandan, S., Atabani, A.E., Ponnusamy, V., and Gunasekar, P., "Impact of additives in Jet-A fuel blends on combustion, emission and exergetic analysis using a micro-gas turbine engine", Fuel, Volume 276, 2019.

[48] Shell. (n.d). *Jet Fuel Additives.* https://www.shell.com/business-customers/aviation/aviation-fuel/aeroshell-performance-additive.html Retrieved 2021-03-01
[49] "Specific Thrust". www.grc.nasa.gov. Retrieved 2021-03-13.
[50] Novakovic, N., "Turbojet Engine Parameters Calculation on Fuel Flow and Exhaust Gas Temperature," SAE Technical Paper 2021-01-29, 2021.
[51] "How The Jet Engine Works". cs.standford.edu. Retrieved 2021-03-14
[52] Bakalis, A., and Stamatis, A., "Data analysis and performance model calibration of a small turbojet engine," Journal of Aerospace Engineering, 2011.
[53] "Flash Point – Fuels". Engineeringtoolbox.com. Retrieved 2021-03-17
[54] Wilsted, H., and Armstrong, J., "Preliminary results of a turbojet-engine altitude-starting investigation," NACA, 1951.
[55] Straight, D., and McCafferty, R., "Turbojet-Engine Starting and Acceleration," NACA RM E55G28, 1956.
[56] Foster, H., and Straight, D., "Effect of Fuel Volatility Characteristics on Ignition-Energy Requirements in a Turbojet Combustor," NACA RM E52J21, 1953.
[57] Braithwaite, W., and Sivo, J., "Evaluation of Altitude-Ignition Characteristics of Three Fuels of Different Volatility," NACA RM E53L11, 1954.
[58] Turkay, M., et al. "Research on Applications of Mini-Turbojet and Turbojet Engined Military UAVs," Scientific Research and Education in the Air Force, 2019.

APPENDICES

Mass Flow Rate Parameter Analysis

Constants

$\gamma_t := 1.4$

Inputs

$P_{ref} := 14.69\ psi$ $M_{.1} := .1$ $M_{.2} := .2$ $M_{.4} := .4$

From AEDsys

$T := 59\ °F$ $T\_T_T := .998$ $T_T := \frac{T}{T\_T_T} = 60.039\ °F$

Solving for Total Pressures

$$P_{t.1} := P_{ref} \cdot \left(1 + \frac{\gamma_t - 1}{2} \cdot M_{.1}^2\right)^{\frac{\gamma_t}{\gamma_t - 1}} = 14.793\ psi$$

$$P_{t.2} := P_{ref} \cdot \left(1 + \frac{\gamma_t - 1}{2} \cdot M_{.2}^2\right)^{\frac{\gamma_t}{\gamma_t - 1}} = 15.105\ psi$$

$$P_{t.4} := P_{ref} \cdot \left(1 + \frac{\gamma_t - 1}{2} \cdot M_{.4}^2\right)^{\frac{\gamma_t}{\gamma_t - 1}} = 16.402\ psi$$

Flight Speed of Mach 0.1

$m_{dotig} := \frac{.03 \cdot lbm}{s}$ $A_{comp} := 3.14\ in^2$ $P_{t.1} := 14.8\ \frac{lbf}{in^2}$ $T_T = 519.7094\ R$

$$MFP_{comp} := \frac{m_{dotig} \cdot \sqrt{T_T}}{A_{comp} \cdot P_{t.1}} = 0.0147\ \frac{lbm \cdot R^{\frac{1}{2}}}{s \cdot lbf}$$

$d := .65 \cdot in$ $r := \frac{d}{2} = 0.325\ in$ $A := \pi \cdot r^2 = 0.332\ in^2$ $A_{valve} := A = 0.332\ in^2$

$$P_{tvalve} := \frac{m_{dotig} \cdot \sqrt{T_T}}{A_{valve} \cdot MFP_{comp}} = 140\ psi$$

$P_{tcorr} := .1676 \cdot P_{tvalve} = 23.472\ psi$

Flight Speed of Mach 0.2

$$m_{dotig} := \frac{.03 \cdot lbm}{s} \qquad A_{comp} := 3.14\ in^2 \qquad P_{t.2} := 15.11\ \frac{lbf}{in^2} \qquad T_T = 519.7094\ R$$

$$MFP_{comp} := \frac{m_{dotig} \cdot \sqrt{T_T}}{A_{comp} \cdot P_{t.2}} = 0.0144\ \frac{lbm \cdot R^{\frac{1}{2}}}{s \cdot lbf}$$

$$d := .65 \cdot in \qquad r := \frac{d}{2} = 0.325\ in \qquad A := \pi \cdot r^2 = 0.332\ in^2 \qquad A_{valve} := A = 0.332\ in^2$$

$$P_{tvalve} := \frac{m_{dotig} \cdot \sqrt{T_T}}{A_{valve} \cdot MFP_{comp}} = 143\ psi \qquad P_{tcorr} := .1676 \cdot P_{tvalve} = 23.964\ psi$$

Flight Speed of Mach 0.4

$$m_{dotig} := \frac{.03 \cdot lbm}{s} \qquad A_{comp} := 3.14\ in^2 \qquad P_{t.4} := 16.41\ \frac{lbf}{in^2} \qquad T_T = 519.7094\ R$$

$$MFP_{comp} := \frac{m_{dotig} \cdot \sqrt{T_T}}{A_{comp} \cdot P_{t.4}} = 0.0133\ \frac{lbm \cdot R^{\frac{1}{2}}}{s \cdot lbf}$$

$$d := .65 \cdot in \qquad r := \frac{d}{2} = 0.325\ in \qquad A := \pi \cdot r^2 = 0.332\ in^2 \qquad A_{valve} := A = 0.332\ in^2$$

$$P_{tvalve} := \frac{m_{dotig} \cdot \sqrt{T_T}}{A_{valve} \cdot MFP_{comp}} = 155.3\ psi \qquad P_{tcorr} := .1676 \cdot P_{tvalve} = 26.025\ psi$$

Jet A1				
Total Pressure (psi)		Fuel/Air Ratio		Successful Ignition? (Yes=1, No=0)
		-10%		0
		-5%		0
		-4%		0
		-3%		0
		-2%		0
M=0, Pt = 14.7, Pg = 0		-1%		1
		Standard		1
		+1%		1
		+2%		1
		+3%		1
		+4%		1
		+5%		1
		+10%		1
		-10%		0
		-5%		0
		-4%		0
		-3%		0
		-2%		0
M=0.2, Pt = 15.11, Pg = 0.42		-1%		0
		Standard		1
		+1%		1
		+2%		1
		+3%		1
		+4%		1
		+5%		1
		+10%		1
		-10%		0
		-5%		0
		-4%		0
		-3%		0
		-2%		0
M=0.4, Pt = 16.41, Pg = 1.71		-1%		0
		Standard		0
		+1%		1
		+2%		1
		+3%		1
		+4%		1
		+5%		1
		+10%		1

Diesel				
Total Pressure (psi)		Fuel/Air Ratio		Successful Ignition? (Yes=1, No=0)
		-10%		0
		-5%		0
		-4%		0
		-3%		1
		-2%		1
M=0, Pt = 14.7, Pg = 0		-1%		1
		Standard		1
		+1%		1
		+2%		1
		+3%		1
		+4%		1
		+5%		1
		+10%		1
		-10%		0
		-5%		0
		-4%		0
		-3%		0
		-2%		1
M=0.2, Pt = 15.11, Pg = 0.42		-1%		1
		Standard		1
		+1%		1
		+2%		1
		+3%		1
		+4%		1
		+5%		1
		+10%		1
		-10%		0
		-5%		0
		-4%		0
		-3%		0
		-2%		1
M=0.4, Pt = 16.41, Pg = 1.71		-1%		1
		Standard		1
		+1%		1
		+2%		1
		+3%		1
		+4%		1
		+5%		1
		+10%		1

Jet A1							
Total Pressure (psi)		Max RPM		Thrust (lbs)	Max EGT (C)	Average EGT (C)	FC (lbm/min)
		-25%		15.44	560	416	0.56
		-20%		18.22	552	408	0.64
M = 0, Pt = 14.7, Pg = 0		-15%		21.69	564	424	0.68
		-10%		25.61	576	424	0.78
		-5%		30.19	556	400	0.92
		Standard		35.7	604	416	0.96

Diesel							
Total Pressure (psi)		Max RPM		Thrust (lbs)	Max EGT (C)	Average EGT (C)	FC (lbm/min)
		-25%		15.89	570	424	0.52
		-20%		18.24	580	404	0.6
M = 0, Pt = 14.7, Pg = 0		-15%		22.17	584	400	0.64
		-10%		25.79	584	412	0.76
		-5%		30.82	590	416	0.84
		Standard		36.3	650	400	0.92

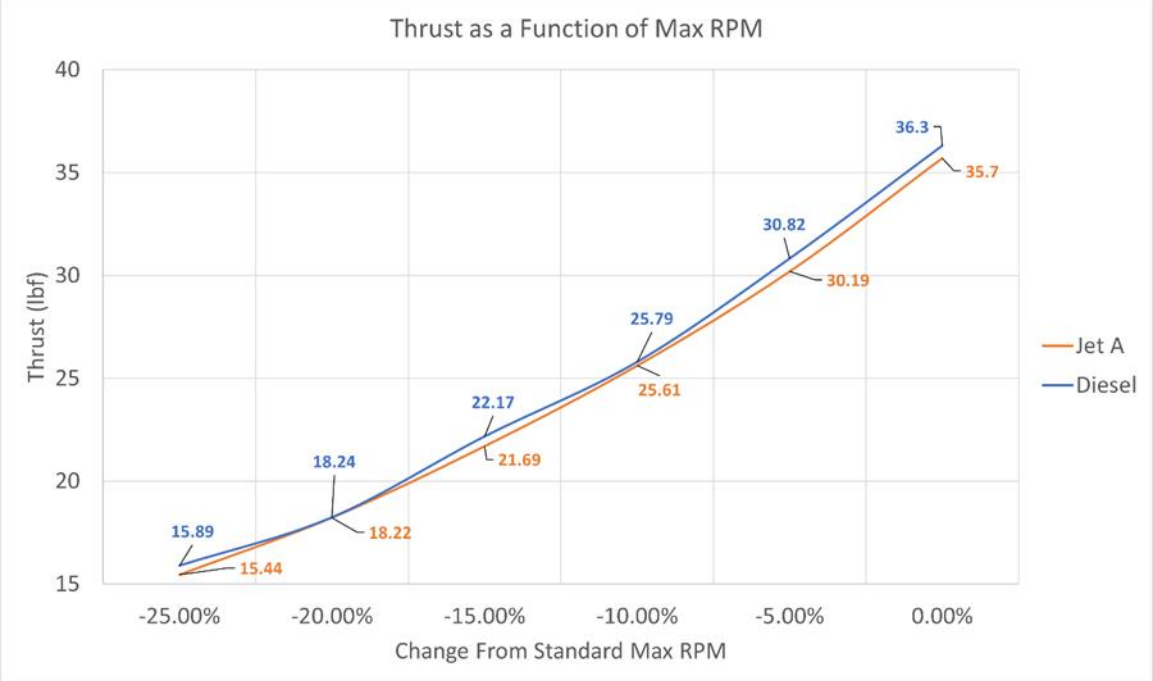

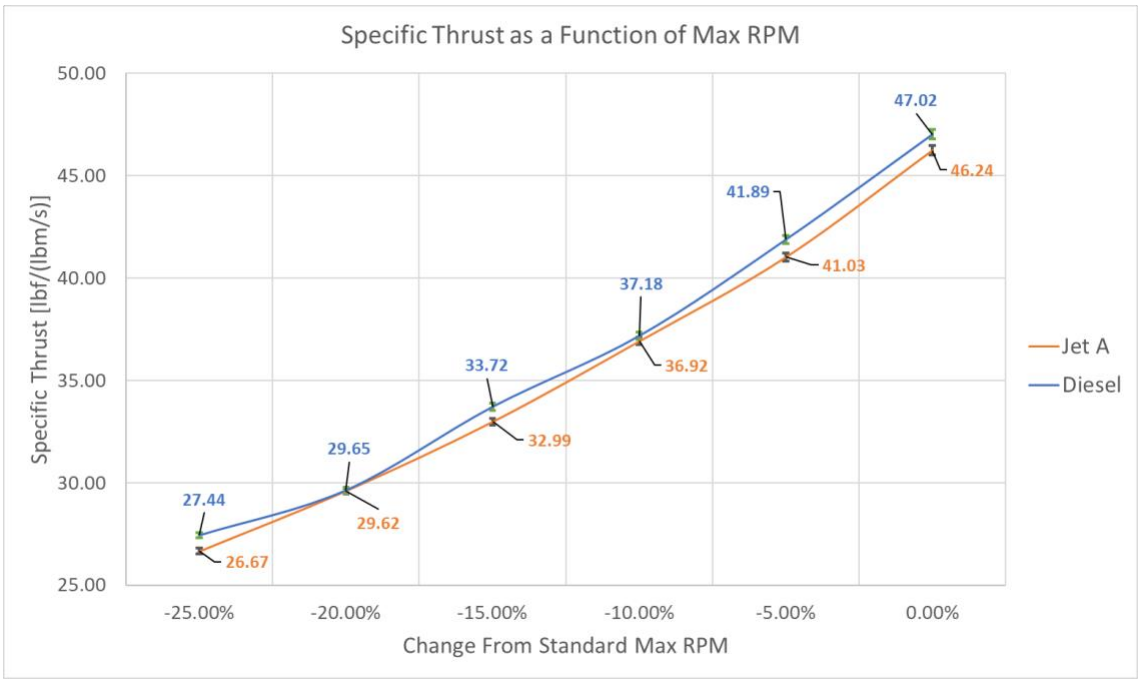
Specific Thrust as a Function of Max RPM
Specific Thrust [lbf/(lbm/s)]
50.00
45.00
40.00
35.00
30.00
25.00
-25.00%
-20.00%
-15.00%
-10.00%
-5.00%
0.00%
Change From Standard Max RPM
47.02
46.24
41.89
41.03
37.18
36.92
33.72
32.99
29.65
29.62
27.44
26.67
Jet A
Diesel

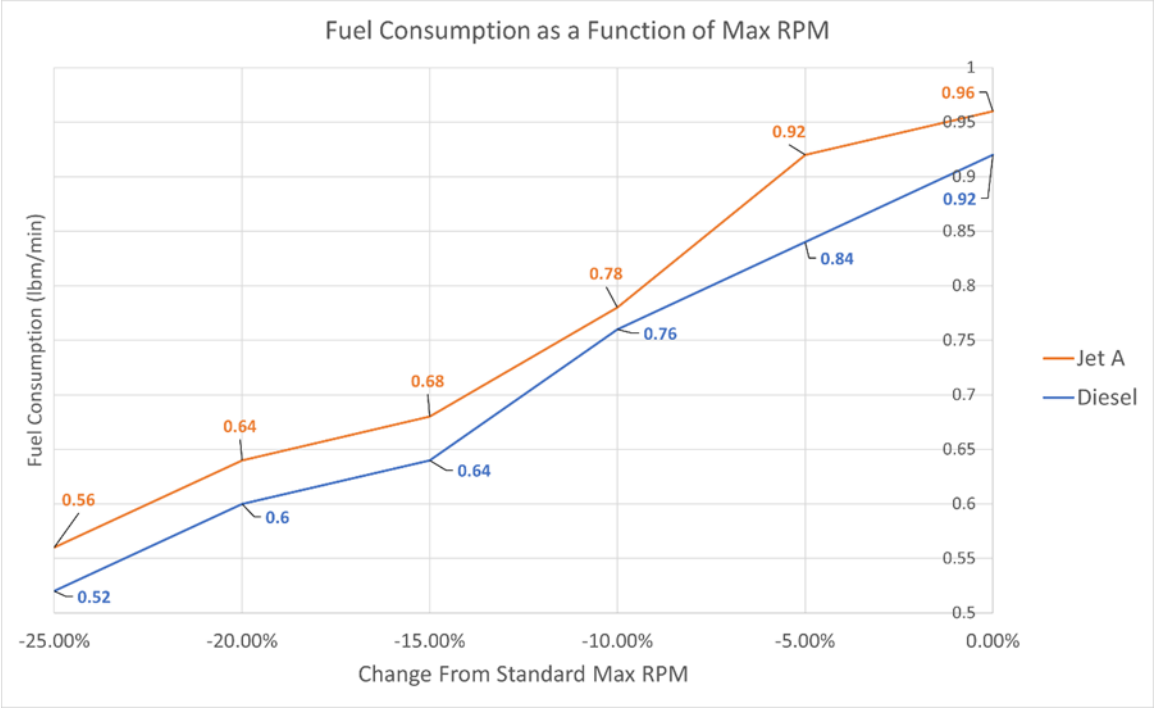
Fuel Consumption as a Function of Max RPM
Fuel Consumption (lbm/min)
1
0.95
0.9
0.85
0.8
0.75
0.7
0.65
0.6
0.55
0.5
-25.00%
-20.00%
-15.00%
-10.00%
-5.00%
0.00%
Change From Standard Max RPM
0.96
0.92
0.92
0.84
0.78
0.76
0.68
0.64
0.64
0.56
0.6
0.52
Jet A
Diesel

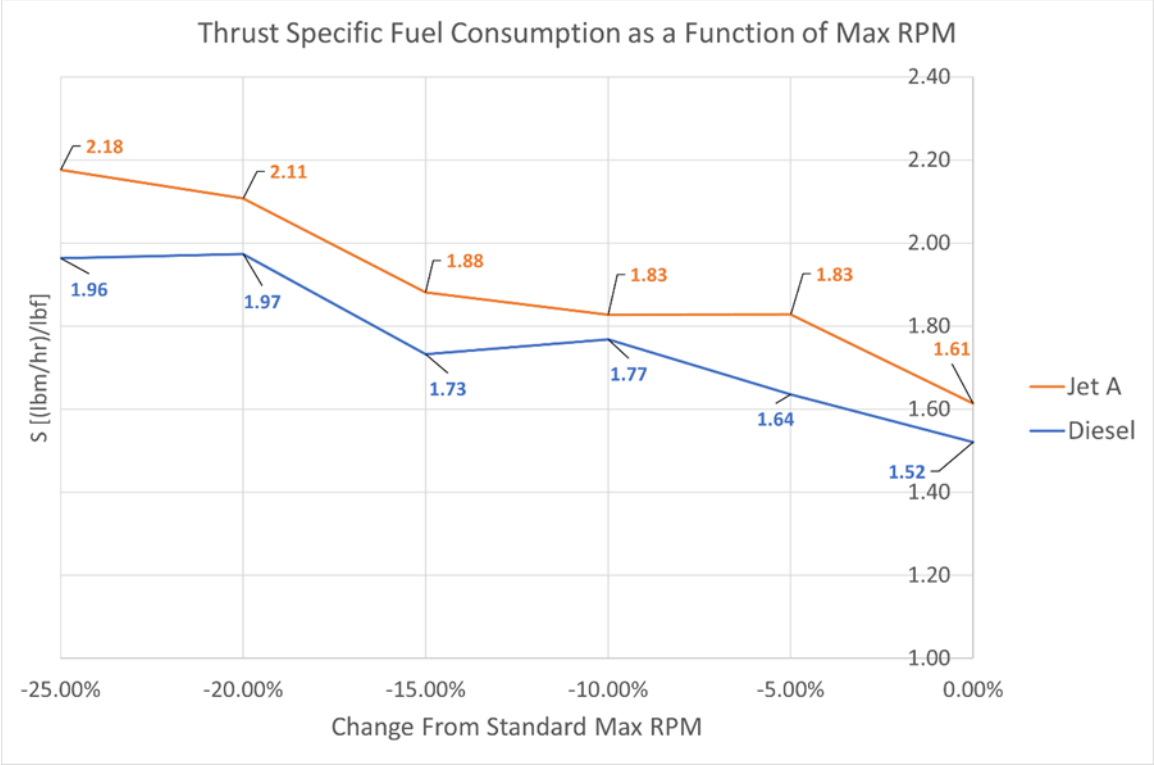
Thrust Specific Fuel Consumption as a Function of Max RPM
S [(lbm/hr)/lbf]
2.40
2.20
2.00
1.80
1.60
1.40
1.20
1.00
2.18
2.11
1.88
1.83
1.83
1.61
1.96
1.97
1.73
1.77
1.64
1.52
-25.00%
-20.00%
-15.00%
-10.00%
-5.00%
0.00%
Change From Standard Max RPM
Jet A
Diesel

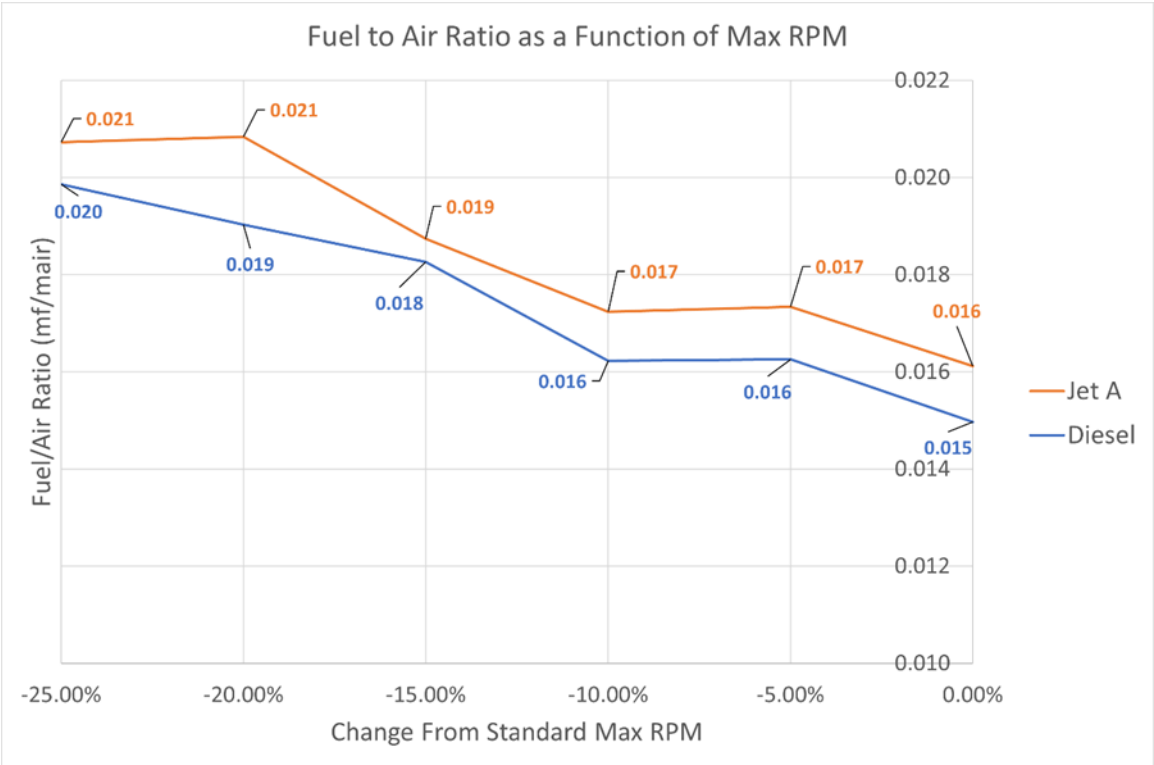
Fuel to Air Ratio as a Function of Max RPM
Fuel/Air Ratio (mf/mair)
0.022
0.020
0.018
0.016
0.014
0.012
0.010
0.021
0.021
0.019
0.017
0.017
0.016
0.020
0.019
0.018
0.016
0.016
0.015
-25.00%
-20.00%
-15.00%
-10.00%
-5.00%
0.00%
Change From Standard Max RPM
Jet A
Diesel

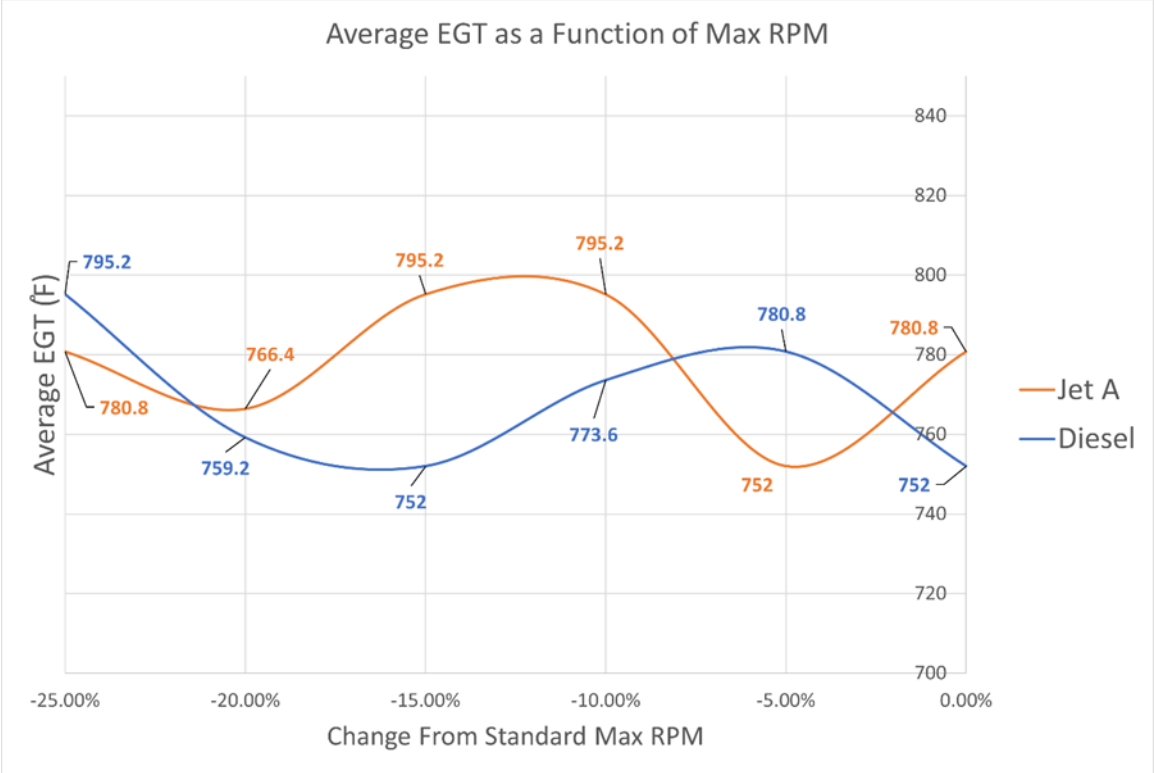
Average EGT as a Function of Max RPM
Average EGT (F)
840
820
800
780
760
740
720
700
795.2
795.2
795.2
780.8
780.8
766.4
780.8
759.2
773.6
752
752
752
-25.00%
-20.00%
-15.00%
-10.00%
-5.00%
0.00%
Change From Standard Max RPM
Jet A
Diesel

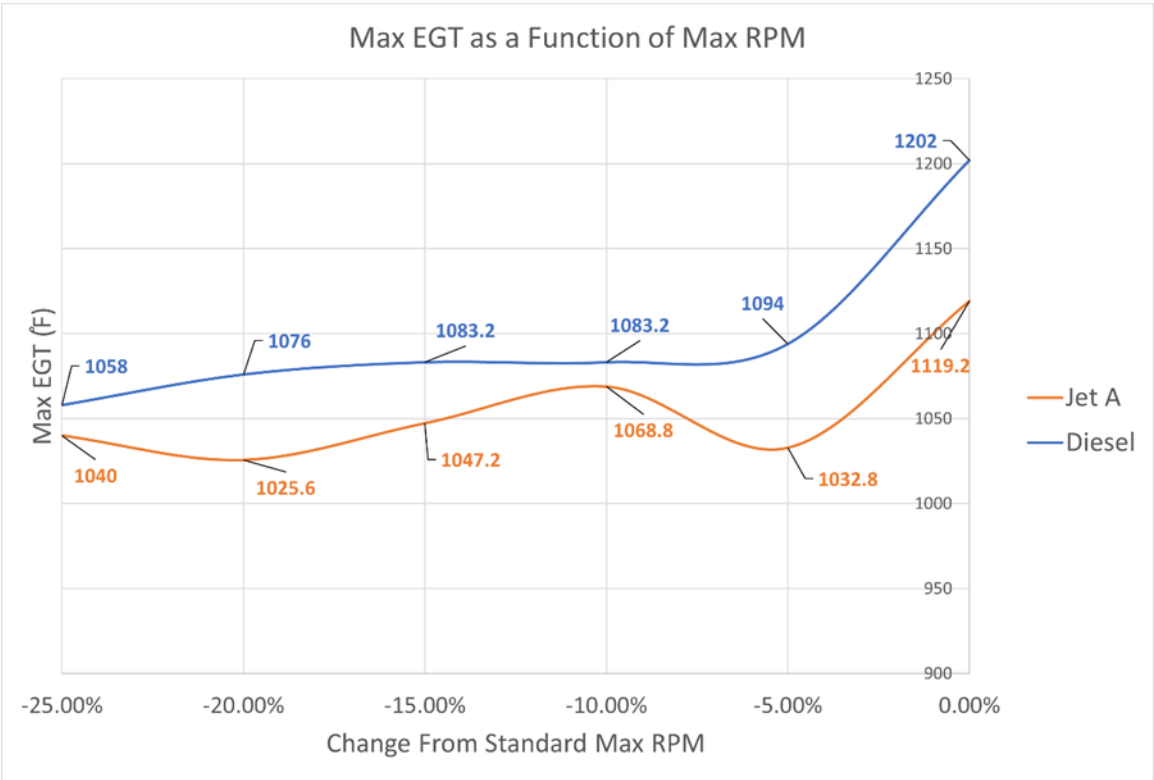
Max EGT as a Function of Max RPM
Max EGT (F)
1250
1200
1150
1100
1050
1000
950
900
1202
1094
1083.2
1083.2
1076
1058
1119.2
1068.8
1047.2
1040
1025.6
1032.8
-25.00%
-20.00%
-15.00%
-10.00%
-5.00%
0.00%
Change From Standard Max RPM
Jet A
Diesel

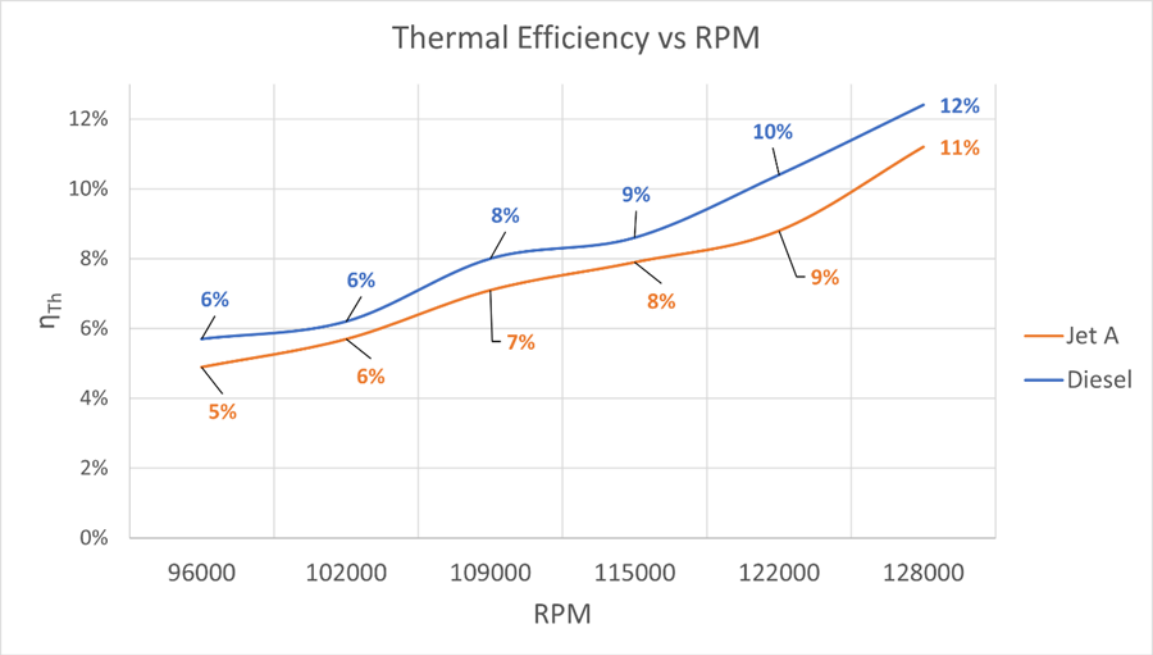
Thermal Efficiency vs RPM
12%
10%
8%
6%
4%
2%
0%
η_{Th}
96000
102000
109000
115000
122000
128000
RPM
6%
6%
8%
9%
10%
12%
5%
6%
7%
8%
9%
11%
Jet A
Diesel

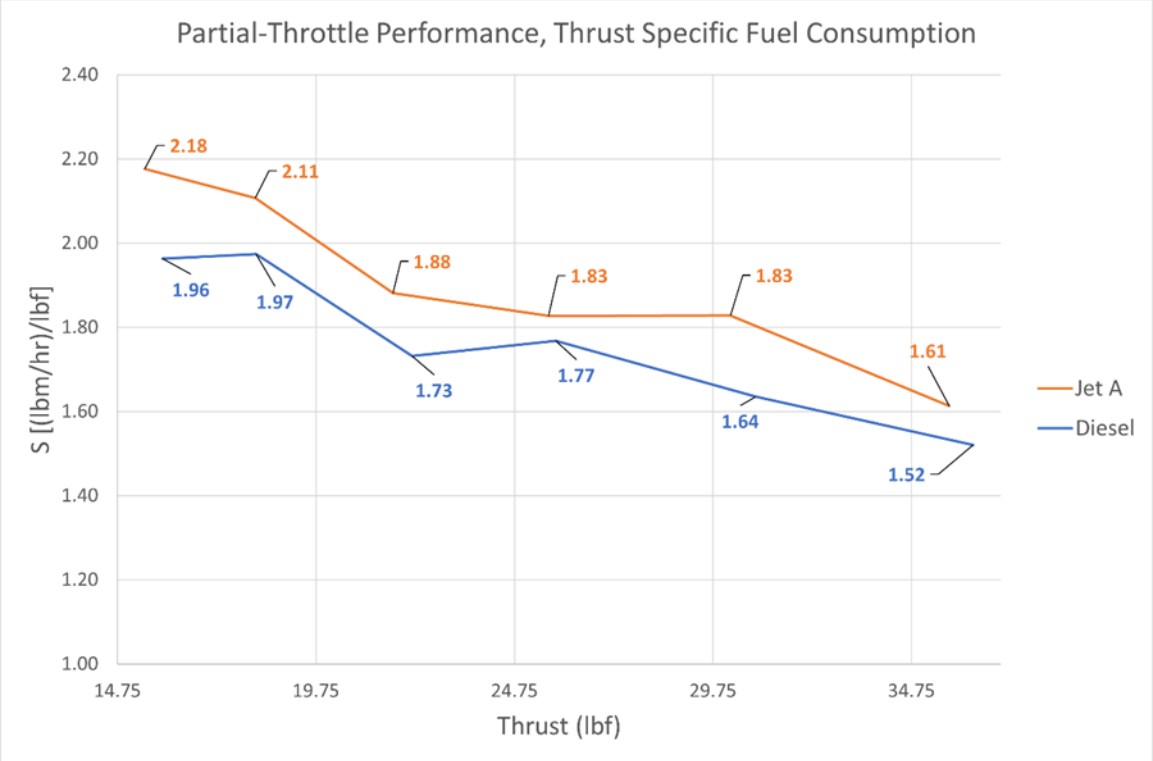
Partial-Throttle Performance, Thrust Specific Fuel Consumption
2.40
2.20
2.00
1.80
1.60
1.40
1.20
1.00
S [(lbm/hr)/lbf]
14.75
19.75
24.75
29.75
34.75
Thrust (lbf)
2.18
2.11
1.88
1.83
1.83
1.61
1.96
1.97
1.73
1.77
1.64
1.52
Jet A
Diesel

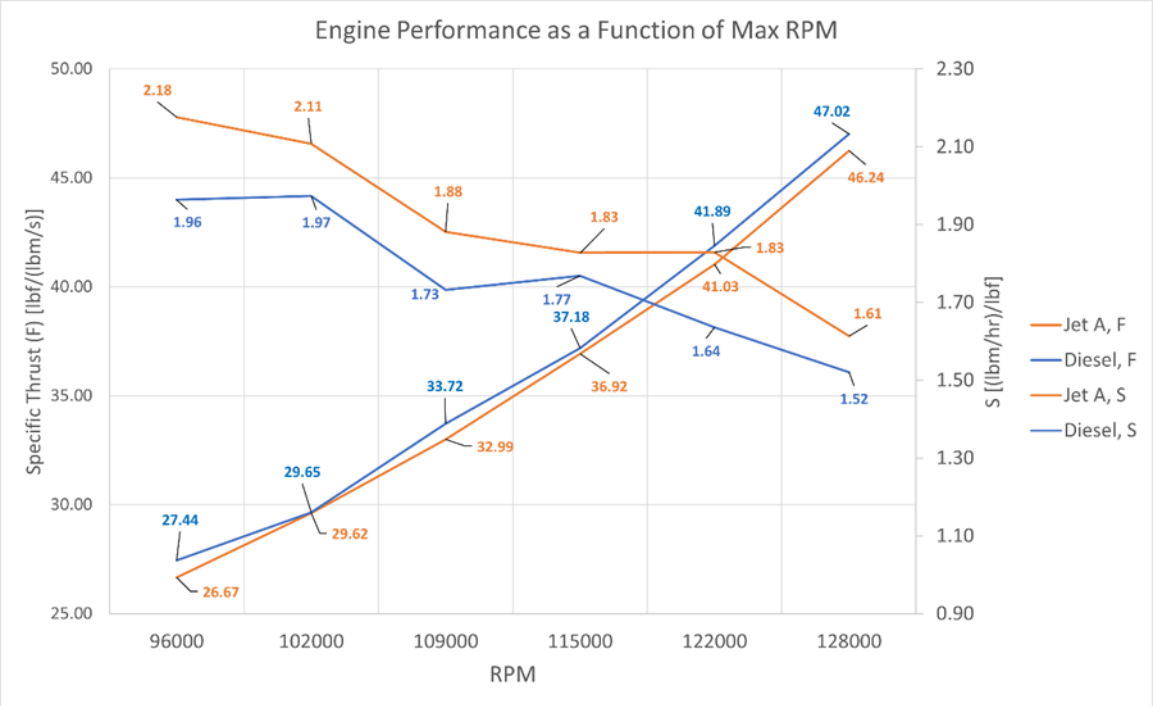
Engine Performance as a Function of Max RPM
Specific Thrust (F) [lbf/(lbm/s)]
S [(lbm/hr)/lbf]
RPM
50.00
45.00
40.00
35.00
30.00
25.00
2.30
2.10
1.90
1.70
1.50
1.30
1.10
0.90
96000
102000
109000
115000
122000
128000
2.18
2.11
1.88
1.83
1.83
1.61
46.24
41.03
1.96
1.97
1.73
1.77
1.64
1.52
47.02
41.89
37.18
36.92
33.72
32.99
29.65
29.62
27.44
26.67
Jet A, F
Diesel, F
Jet A, S
Diesel, S

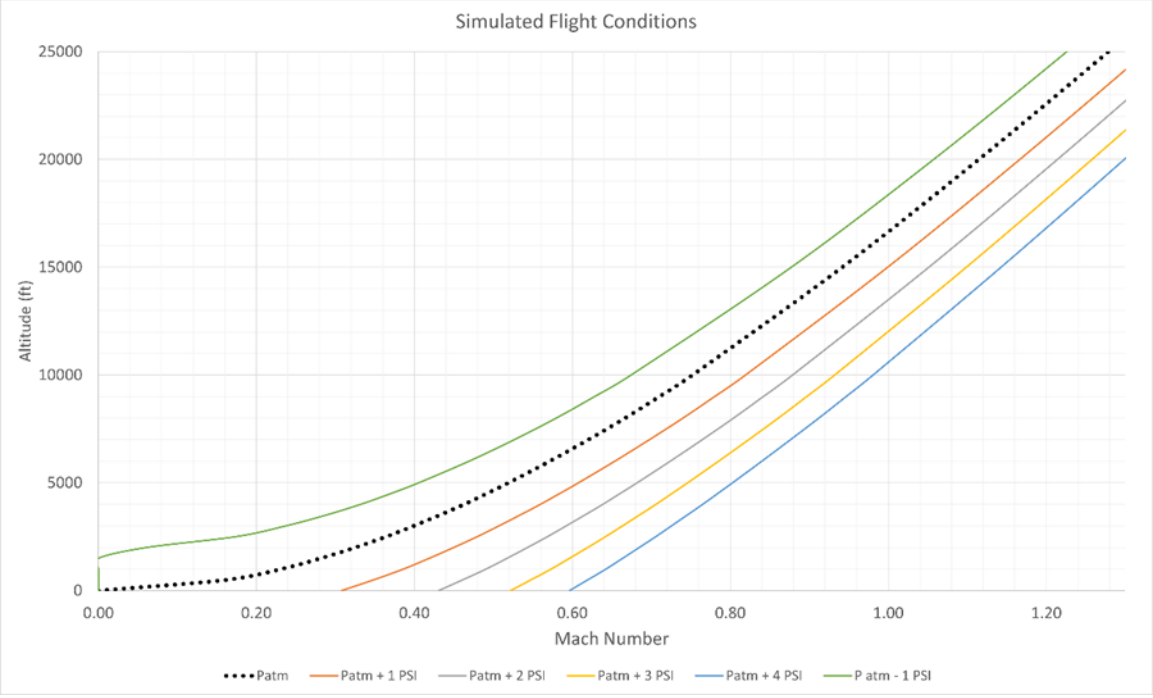
Simulated Flight Conditions
Altitude (ft)
Mach Number
25000
20000
15000
10000
5000
0
0.00
0.20
0.40
0.60
0.80
1.00
1.20
Patm
Patm + 1 PSI
Patm + 2 PSI
Patm + 3 PSI
Patm + 4 PSI
P atm - 1 PSI

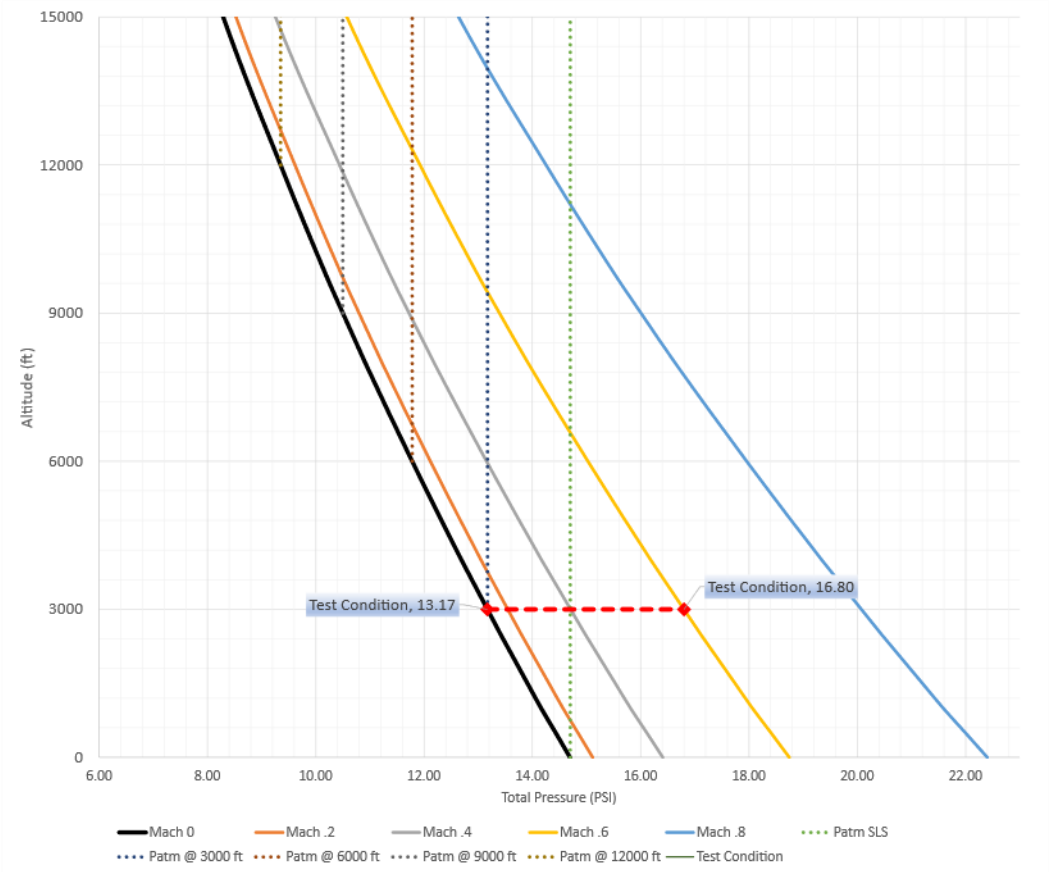
15000
12000
9000
6000
3000
0
Altitude (ft)
6.00
8.00
10.00
12.00
14.00
16.00
18.00
20.00
22.00
Total Pressure (PSI)
Test Condition, 13.17
Test Condition, 16.80
Mach 0
Mach .2
Mach .4
Mach .6
Mach .8
Patm SLS
Patm @ 3000 ft
Patm @ 6000 ft
Patm @ 9000 ft
Patm @ 12000 ft
Test Condition

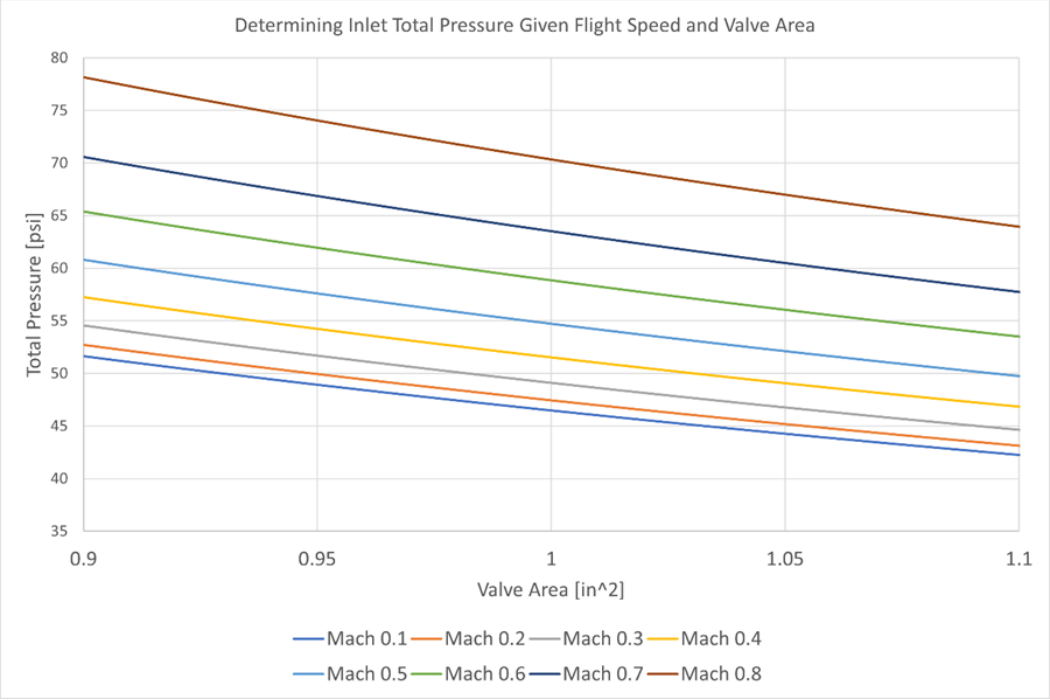
Determining Inlet Total Pressure Given Flight Speed and Valve Area
80
75
70
65
60
55
50
45
40
35
Total Pressure [psi]
0.9
0.95
1
1.05
1.1
Valve Area [in^2]
Mach 0.1
Mach 0.2
Mach 0.3
Mach 0.4
Mach 0.5
Mach 0.6
Mach 0.7
Mach 0.8

VITA

Colton Ray Swart

Candidate for the Degree of

Master of Science

Thesis: A MOBILE GROUND TEST RIG FOR EVALUATING SMALL-SCALE TUROBJET IN-FLIGHT PERFORMANCE AND START RELIABILITY

Major Field: Mechanical and Aerospace Engineering

Biographical:

Education:

Completed the requirements for the Master of Science in Mechanical and Aerospace at Oklahoma State University, Stillwater, Oklahoma in May 2021.

Completed the requirements for the Bachelor of Science in Mechanical and Aerospace Engineering at Oklahoma State University, Stillwater, Oklahoma in May 2019.